GROUNDWATER FLOW OF A PROPOSED URANIUM IN-SITU RECOVERY MINE SITE AND SURROUNDING AREAS, WELD COUNTY, COLORADO

MIORI YOSHINO

B.A., University of Colorado at Boulder, 2006

A thesis submitted to the

Faculty of the Graduate School of the

University of Colorado in partial fulfillment

Of the requirement for the degree of

Master of Science

Department of Geological Sciences

2011

This thesis entitled:
Groundwater Flow of a Proposed Uranium In-Situ Recovery Mine Site
and Surrounding Areas, Weld County, Colorado
written by Miori Yoshino
has been approved for the Department of Geological Sciences

____
Shemin Ge

____
Raymond Johnson

____
Alexis Templeton

Date________________________

The final copy of the thesis has been examined by the signatories, and we find that both the content and the form meet acceptable presentation standards of scholarly work in the above mentioned discipline.

Yoshino, Miori (M.S., Geological Sciences)

Groundwater Flow of a Proposed Uranium In-Situ Recovery Mine Site and Surrounding Areas, Weld County, Colorado

Thesis directed by Professor Shemin Ge

ABSTRACT

With continued proposals for uranium in-situ recovery in northeastern Colorado, it is necessary to acquire a detailed understanding of background groundwater flow in order to estimate potential mining impacts. Groundwater studies for northern Denver Basin aquifers are limited. This study focuses on discerning in-situ recovery influences on groundwater flow in the Laramie-Fox Hills aquifer by using a steady state, regional scale groundwater flow model and a local scale model in the proposed mining zone. General stratigraphy of the study area includes, in ascending order, the Pierre Shale, the Fox Hills Formation, and the Laramie Formation. Data from public well records were used for hydraulic head mapping and calibrating the groundwater model. Slug and bail tests conducted in the Lower Laramie Formation yielded a hydraulic conductivity range between 9.2×10^{-7} m/s and 1.8×10^{-6} m/s. The Pierre Shale is considered less permeable with an assumed hydraulic conductivity of 1.0×10^{-8} m/s or less. MODFLOW, a finite-difference numerical model, was used to simulate the background steady state groundwater conditions. Groundwater generally flows south and slightly east. Model calibration achieved a correlation coefficient of 0.86 between model hydraulic head and observed water level data. The local scale model used two 7-spot pumping and injection well configurations to examine water level drawdown in response to long term pumping. For a given rate of pumping at 275.22 m^3/d and injection at 54.5 m^3/d at the pumping and injection wells respectively, drawdown effects

were limited to a ~80 meter radius surrounding the well field in the proposed sandstone. MT3D, a three-dimensional solute transport model, was used for simulating solute transport in groundwater around the well field. Modeling results suggest that solute concentrations are generally confined by low-permeability shale layers under the given groundwater flow and pumping and injection scenarios. Lateral transport was limited to the radial extent of drawdown. Impacts of in-situ recovery on groundwater flow in areas overlying, underlying and downgradient of the Upper Fox Hills Formation can be minimized given an adequate understanding of the hydrogeologic conditions surrounding the recovery site.

ACKNOWLEDGEMENTS

I would like to thank first and foremost my advisor, Shemin Ge, for taking a chance on me by accepting me into the program, for guiding me as I struggled through it, and for always encouraging me to answer my own questions. I am grateful to have trained under her instruction and received her advice, honesty, and support throughout this project. I am also grateful for her tolerance of my novice questions, for her patience as I came into a world unknown to me, and for always keeping her expectations of me just a little too high.

I would like to extend my appreciation to researchers of the U.S. Geological Survey Uranium Energy Resources Team for providing me with unique training opportunities and for exposing me to broader research topics and new perspectives. I am especially thankful of my supervisor Raymond Johnson for not only offering guidance, but also for allowing me to make my own mistakes and making himself available when my efforts fell apart. Andrew Manning also provided much appreciated advice and support throughtout my time at the Denver Federal Center. Fellow students in the hydrogeology research group at the University of Colorado, Brent Aigler, Lyndsay Ball, Matthew Weingarten, Kali Abel, and Jessica King, provided valuable field assistance, support, advice, and friendship. I would like to extend many, many thanks to In Wook Yeo, whose timely visit to our research group helped me overcome large hurdles in the last months of the project, and whose constructive support and positive encouragement kept me going on my most challenging days. I would also like to thank my late-night comrades, Jeremy Ring and Gabriela Keeton for making nights in the office easier to endure. I am thankful of Alexis Templeton for her constant encouragement in geochemisty and for opening my eyes to new and exciting research in the field. My work in ArcGIS was greatly assisted by several peers and colleagues at various stages of my research—Kevin Befus, Evan

Pugh, Lyndsay Ball, Matt Granitto and Stuart Giles. Valuable assistance with fossils was greatly appreciated; shell preparation was undertaken by Amanda Yoshino, and identification was generously provided by Talia Karim. I would like to thank my family and friends for their constant support throughout my graduate study. My most heart-felt gratitude is for Kelly Fenson-Hood for her companionship as a fellow graduate student, for her loving criticism when I was frustrated, and when I needed it, for convincing me there was always a reason to celebrate. I am thankful for William, who kindheartedly took care of me and offered generosity, wisdom, and compassion at a time when I had little to give in return. I would like to thank Matt Silverman for introducing me to geology so long ago, and for being a consistent source of wisdom and support throughout my graduate career. Similarly, I would like to extend my thanks to John Gustavson for offering his perspectives and for giving me truth when I needed to hear it. Finally, I would like to extend my appreciation to Powertech Uranium Corporation for both granting me access to two wells I used to conduct slug tests and for making their geologic and water level data publicly available. This research was supported by the Department of Geological Sciences, University of Colorado at Boulder and by the U.S. Geological Survey Energy Resources Program.

CONTENTS

TABLES

FIGURES

CHAPTER 1:
INTRODUCTION

Demands for uranium resources have increased in recent years as nuclear power is an alternative fuel that can reduce fossil fuel consumption and atmospheric CO_2 emissions. Mining and milling of uranium ore has taken place in the United States since the 1900s through various methods, depending on the geology and lithology of the deposit. For relatively deep, low-grade deposits uranium is often extracted by a mining technique known as in-situ recovery. This method involves the addition of a uranium-mobilizing solution (such as water with oxygen and bicarbonate additions) into sandstone-hosted ore zones through a multi-well injection and extraction system to produce a uranium-rich fluid at the surface. This solution is subsequently processed to concentrate uranium into a uranium oxide powder known as yellowcake. Figure 1-1 depicts the in-situ recovery process, in which both mining (by solution) and milling occur (ion-exchange columns).

The benefits of in-situ recovery include recycling groundwater and reducing surface disturbance and related effects, as compared to traditional techniques of open pit or underground mining. The influence of in-situ recovery on the groundwater during and after mining is a valid concern. This study thus seeks to understand the existing groundwater system using groundwater flow modeling. Conditions set forth in regional modeling serve as a hydrogeological reference for the local scale simulation of pumping activity. Groundwater quality is not examined in this study. Instead, the focus of this study is on physical flow parameters.

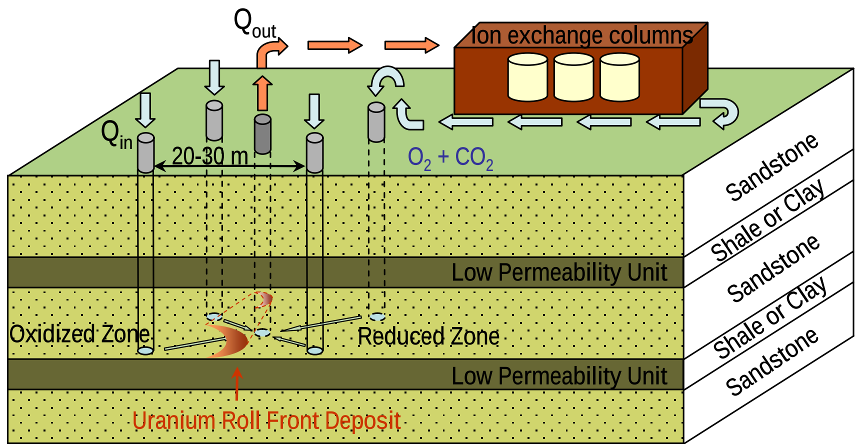

Figure 1-1. In-situ recovery process using a 5-spot well configuration to mine subsurface uranium ore. Four injection wells surround one pumping well. Water is re-injected into sandstone after uranium-bearing groundwater is pumped and processed through ion-exchange columns at the surface. Extraction rate is typically greater than total injection by 1-3% in order to maintain a cone of depression around the pumping well. Uranium ore bodies typically range 1-5 meters in thickness.

The Centennial Project is a proposed in-situ recovery mine site about fifteen miles northeast of Fort Collins, CO (Fig. 1-2), and is situated among private farmlands. Private wells used for irrigation, drinking and stock water are completed in the Laramie-Fox Hills aquifer, the same aquifer as the proposed mining zone. This aquifer has interbedded, relatively thick shale units (3 meters to 15 meters) which limit hydraulic connection between sandstones. The stratigraphy of the area includes the Pierre Shale overlain by the Fox Hills Formation and Laramie Formation near the surface (Fig. 1-3). These three formations regionally dip east and slightly north as a result of Laramide Uplift, and are unconformably overlain by the Tertiary Ogallala and White River Formations, and Quaternary glacial till and alluvium (Fig. 1-4). The Tertiary formations are significant to uranium deposits due to chemical weathering of the uranium-bearing minerals at the surface concentrating mobilized uranium in porous rocks below.

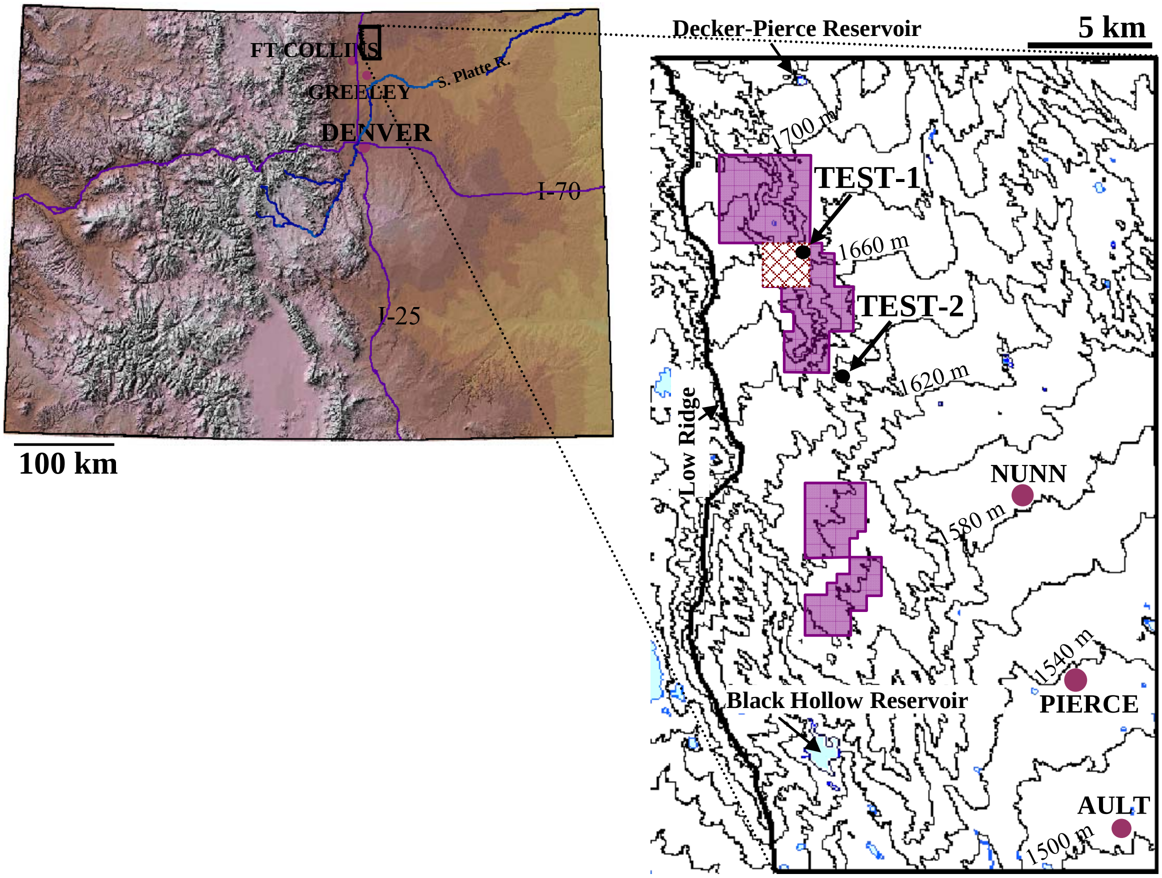

Figure 1-2. Digital elevation, major highways and cities in Colorado. Inset shows study area boundary, topography and surface water features, slug test locations (black dots), proposed mining permit boundary (shaded purple), and approximate area of aquifer pumping test (cross-hatch) (Powertech, 2008). Shaded relief map is the courtesy of the Colorado Geological Survey.

PERIOD	ROCK TYPE	FORMATION
Quaternary	Glacial debris, Alluvium	Undifferentiated
Tertiary	Alluvium	Ogallala
	Conglomerate	White River
Upper Cretaceous	Shale, sandstone, mudstone, coal	Laramie
	Sandstone, shale/mudstone	Fox Hills
	Shale	Pierre Shale

Figure 1-3. Stratigraphic column of geologic formations in the study area, in ascending age order: The Pierre Shale, Fox Hills Formation, Laramie Formation, White River Formation, Ogallala Formation, and undifferentiated Quaternary deposits.

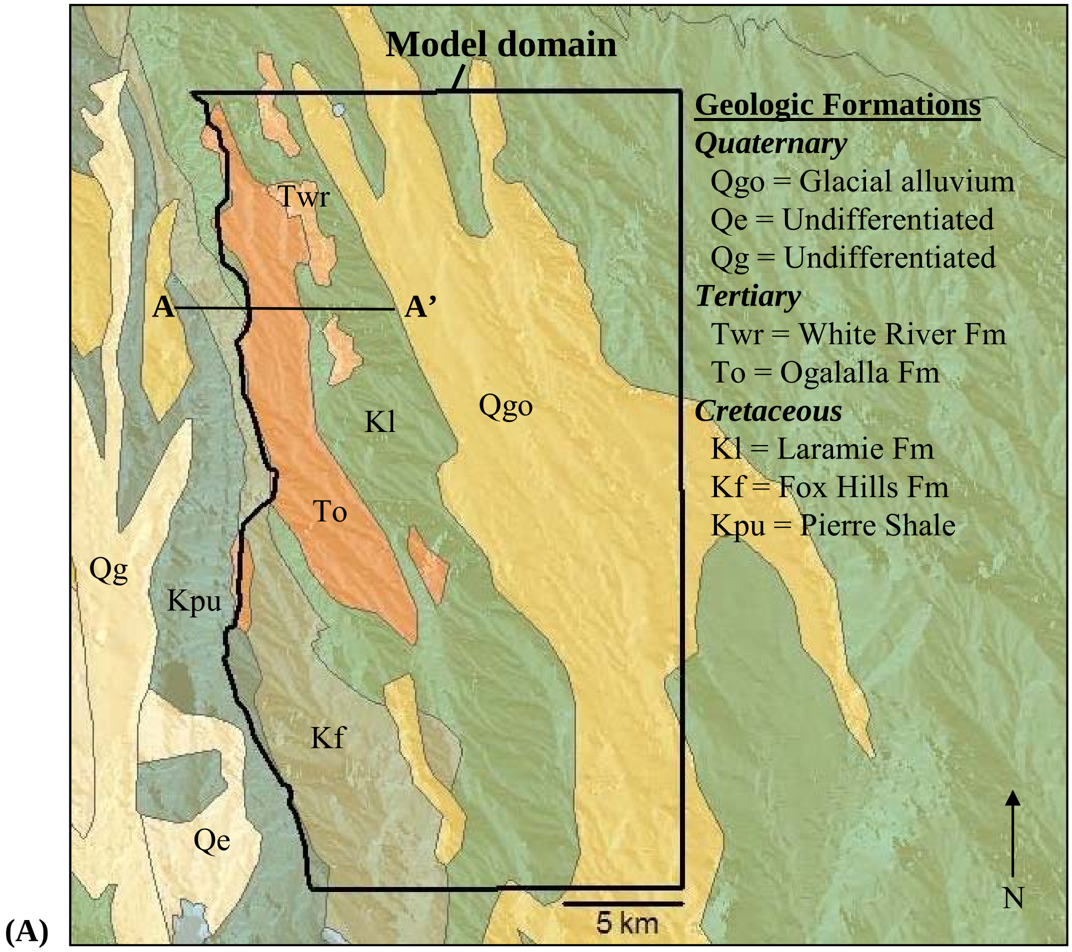

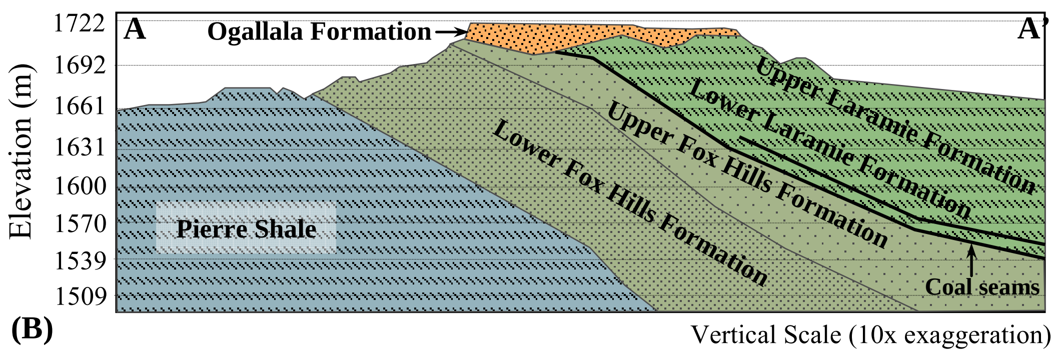

Figure 1-4. Geologic map of the study area (Green, 1992) (A). Cross section from west to east shows the east dip of strata due to past Laramide Uplift, (adapted from Powertech Uranium Corporation, 2009) (B).

1.1 Background: Uranium Roll-Front Deposits

Figure 1-5 depicts the conceptual setting of uranium roll-front deposition in sedimentary units. Dissolution of uranium occurs by oxygen and carbon dioxide-bearing groundwater. Subsequently uranium is transported downgradient into underlying, tilted sandstones. Multiple roll-front deposits may form if sandstone layers are separated by low permeability shale units. Precipitation, or mineralization, of uranium ore typically occurs at the redox boundary between oxidized and reduced groundwaters.

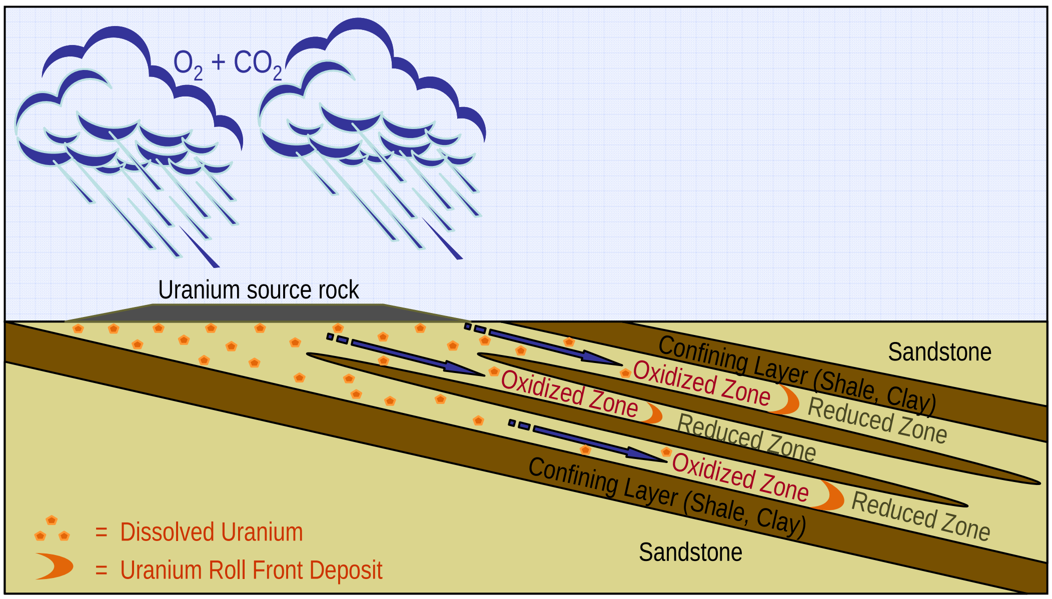

Figure 1-5. Conceptual setting of regional uranium ore deposits emplaced over thousands to millions of years. Oxygen-bearing groundwater mobilizes uranium through oxidation reactions, and atmospheric carbon dioxide may form carbonates, bicarbonates, or carbonic acids which complex with oxidized uranium species in groundwater and allow for transport downgradient.

A roll-front formation is a secondary deposit, deriving from a primary uranium source. Primary sources include magmatic intrusions, volcanic ash, or mineralizing fluids in hydrothermal vents that may produce elevated uranium concentrations at depth (Min et al., 2005). Five factors are needed for a roll-front uranium deposit to develop: a source of uranium, a transporting media, a host rock, a trapping mechanism, and a preservation mechanism (Charbeneau, 1984). Rhyolitic volcanic ash is the most common primary uranium source because it is the most readily weathered and contains higher concentrations of uranium than mafic rocks (Zielinski, 1975). The transporting medium for uraniferous material is groundwater. The common host rock is sandstone, usually interbedded between fine-grained material such as shale, mudstone or siltstone. The interfingering of coarse and fine-grained material helps trap to uranium in distinct roll-front deposits. Finally, uranium is preserved by precipitating out of groundwater to form relatively insoluble uranium minerals. This formation of roll-front deposits can take anywhere from thousands to millions of years.

Uranium can exist in several oxidation states—from U(III) to U(VI)—but it only occurs naturally as U(IV) and U(VI) in the form of stable $UO_{2(am,s)}$, $UO_2{}^{2+}{}_{(aq)}$, and other uraniferous minerals. Depending on aquifer characteristics, the uranous [U(IV)] and uranyl [U(VI)] forms may either precipitate as distinct minerals, adsorb to sediment surfaces, or complex with various ligands. These behaviors thus affect where uranium is found and how it can be recovered from an aquifer. Generally, U(IV) is solid and immobile, and U(VI) is aqueous and mobile in groundwater.

The upgradient side of the roll-front formation is host to an oxidizing zone created by meteoric waters entering from an outcrop. This allows for chemical dissolution of uraniferous material from the original source rock and transport of uranium into underlying tilted sandstones. The oxidizing groundwater can cause uranium to go into solution, where it may aqueously complex with carbonates. More specifically, the oxidizing water reacts with uranous minerals and diagenetically converts uranium into the uranyl form that is able to bind with carbonates and other dissolved ligands in groundwater. Uranium is transported by groundwater until it reaches the reducing zone often caused by the presence of organic matter, pyrite, or anoxic groundwater. While these are the most reactive reductants, other components in water, such as Fe(II), or rock are able to reduce uranium as well. The geochemical changes in groundwater near roll-front deposits can be characterized broadly by the major reactions of uranium, iron, sulfur, oxygen, and carbon dioxide (Davis and Curtis, 2006).

The roll-front deposit may appear in a C-shape when viewed in cross section, but in plan view it typically appears in a sinuous trend, forming at the redox boundary. The location and form of the redox boundary is often a product of the paleoenvironment. Roll-front deposits may occur in multiple sandstone layers as a result of interbedded shale or mudstone layers. Lithologic changes in the stratigraphic column reflect changes in the depositional environment.

Roll-front deposits may not always appear in a symmetrical C-shape. In fact, uranium precipitates may concentrate along the contact between the sandstone and shale, elongating the C-shape. Incongruities or heterogeneities in the material composition in the sandstone layer may cause distortion of the C-shape as well (Davis, 1969).

1.2 Background: In-Situ Recovery

In-situ recovery involves two processes: oxidation that dissolves uranous minerals into solution and aqueous complexation that inhibits precipitation or adsorption to minerals. The most commonly used lixiviant (mining fluid) is a solution saturated with oxygen gas (O_2) and a carbonate (CO_3^{2-}) species. Oxygen is used as the oxidizing agent to solubilize uranous minerals such as coffinite ($USiO_4$) and uraninite (UO_2). Dissolved carbonate species are employed for aqueous complexation of U(VI) which allows uranium to be transported by groundwater during mining because uranium remains in groundwater rather than precipitating out of solution.

More specifically, bicarbonate anions (HCO_3^-) are able to complex with the U(VI) produced where O_2 reacts with uranyl minerals. Produced $UO_2(CO_3)_2^{2-}$ in groundwater is shown in Reaction 1.1 below.

$$UO_{2(s)} + 2HCO_3^- + 0.5O_2 \longleftrightarrow UO_2(CO_3)_2^{2-}{}_{(aq)} + H_2O \tag{1.1}$$

In the oxidation and reduction reactions that occur during mining, oxygen is reduced as uranium is oxidized from a uranous mineral to a uranyl ion. In Reaction 1.1 the reduced uranous mineral is shown on the left and the oxidized aqueous uranyl ion is shown on the right.

Half reactions for the reduction of oxygen (Reaction 1.2) and the oxidation of uranium (Reaction 1.3) are shown below. The addition of the two half reactions represents uranium oxidation in water, where two electrons are transferred from uranium to oxygen. The rate at which these reactions occur primarily depends on the oxidation potential and acidity of groundwater.

$$0.5O_2 + 2H^+ + 2e^- \longleftrightarrow H_2O \tag{1.2}$$

$$U^{4+} + 2H_2O \longleftrightarrow UO_2^{2+} + 4H + 2e^- \tag{1.3}$$

In-situ recovery depends on the suspension of uranyl ions in groundwater because pumping regimes control groundwater flow direction. Groundwater can transport uranium from injection wells to extraction wells once uranium is complexed with colloids or ligands such as a carbonates, as shown in Reaction 1.1. More specific geochemical processes during mining depend on characteristics of the natural aquifer system such as mineralogy and water chemistry. Substrate speciation, existing colloids, pH, oxidation potential, reaction kinetics, microbial processes, and aqueous complexation with organic and non-organic ligands affect uranium precipitation and dissolution. These parameters and processes may change with time due to either natural groundwater flow or mining solutions used during in-situ recovery.

1.3 Purpose and Scope

The governing question of this study is how in-situ recovery of uranium at the Centennial Project might affect the groundwater environment in the Laramie-Fox Hills aquifer. Groundwater issues regarding in-situ recovery are centered around groundwater geochemistry and physical groundwater flow. Uranium geochemistry depends on groundwater acidity, oxidation potential, mineralogy, and microbiology of the aquifer. These factors are all interrelated and finding a comprehensive understanding of the dynamics between them can be arduous. Studying the physical flow system helps to define areas most likely to be affected by mining. The focus of this thesis is to study the potential impacts to the Laramie Formation and Lower Fox Hills Formation that bound the proposed mining zone (Upper Fox Hills Formation). The Centennial Project has been proposed by Powertech Uranium Corporation, hereafter referred to as Powertech.

Perceived as a safe and economical method of uranium mining, there is a paucity of literature on the long-term effects of in-situ recovery on aquifers, particularly with regard to the notion that less permeable layers constrain groundwater from leaving the mining zone. Regionally, natural flows ultimately lead to groundwater moving out of the mining zone, but it is not clear if mining will exacerbate this process or cause mining-related constituents to be transported beyond mine site boundaries. An initial understanding of groundwater flow is fundamental for planning and interpreting groundwater flow and geochemical simulations of the mining process. This study presents a pre-mining condition, steady-state regional scale groundwater flow model as well a local scale flow model within the proposed mining zone (Fig. 1-2).

The groundwater data used in this study are gathered from literature, field tests, a Powertech aquifer pumping test, and various online government databases. Organizations reporting information used in this study include the Colorado Division of Reclamation Mining and Safety, the Colorado Division of Water Resources, the Colorado Department of Public Health and Environment, and the Environmental Protection Agency. First, attributes of principal geologic formations are discussed on a regional scale within the study domain utilizing existing geologic maps. A structure contour map of the Pierre Shale-Fox Hills Formation contact and an isopach map of the Laramie-Fox Hills aquifer have been reported by others (Robson and Banta, 1987) and are used in this study to infer relationships between the major geologic formations. Groundwater levels in the study area are illustrated with hydraulic head contour maps derived from well construction report data found in the Colorado Division of Water Resources online database. To obtain values for hydraulic conductivity in the Lower Laramie Formation, two slug tests were conducted. A 2008 multi-well aquifer pumping test by Powertech provides a larger-scale measurement of hydraulic conductivity through a sandstone within the proposed mining zone. All of the above data and related information were utilized in modeling natural groundwater flow in the region.

A local scale model that included mining activity was developed to examine potential impact on groundwater in the vicinity of mining well fields. One section within the northern proposed mining zone was modeled based on hydraulic head information from regional modeling as well as geophysical logs and water levels reported by Powertech to governing organizations (Colorado Division of Reclamation Mining and Safety, Colorado Division of Water Resources). A steady state simulation of in-situ recovery using two 7-spot well configurations was examined to approximate water level drawdown and mining fluid transport during pumping processes. In-situ recovery was simulated by the addition of water and a solute tracer at injection wells. Injection wells created relatively high pressure zones and surround central extraction wells that created low pressure zones. The addition of a tracer at injection wells was simulated to infer advection and dispersion processes related to the transport of mining fluids. Hydraulic head changes to the overlying and underlying strata are analyzed.

This study is limited to physical flow processes and excludes likely scenarios in which uranium and other related constituents react with groundwater and dissolved constituents. Furthermore, advection and dispersion were defined using typical values, and therefore they were not specific to the Centennial Project. Resulting horizontal and vertical solute transport calculations were reasonable for the site based on other available information. Initial solute concentration was assigned a value high enough to be easily tracked for the duration of the simulation, but does not represent a real world value (such as a solute concentration that may be used in an actual tracer study). The observed concentration distribution illustrates flow direction and velocity of mining fluids in one area of the proposed mining zone under generic in-situ recovery practices.

CHAPTER 2:
REGIONAL HYDROGEOLOGY

Understanding hydrogeology requires knowledge of both the geologic system, such as structure and lithologic composition, and the spatial distribution of water levels. In this chapter, regional and local geology is described first. Existing information on the regional geology includes basin-scale structure and isopach contour maps of the Laramie-Fox Hills aquifer (Robson and Banta, 1987), digital geologic maps (Green, 1992), and well logs from Powertech wells and other literature. The natural groundwater system has been characterized by Robson and Banta (1987) using a state-scale hydraulic head contour map. In addition to previous mapping, this study presents a regional composite hydraulic head contour map of the Laramie-Fox Hills aquifer which was assembled from water level data from the Colorado Office of the State Engineer.

2.1 Regional Geology

In the area of interest within the Denver Basin there are three principal geologic formations. They are, in descending order, the Laramie Formation, the Fox Hills Formation, and the Pierre Shale (Figure 1-4). The Upper Laramie Formation consists of thick beds of shale and is considered a less permeable aquitard with the exception of two thin sandstone aquifers (Sherman and others, 1978). The Lower Laramie Formation contains beds of calcareous shale and clay, coal, and sandstone (Babcock and Bjorklund, 1956). A more detailed cross section showing these lithologies within each formation in the northern portion of the study area is available from Powertech through the Colorado Division of Reclamation Mining and Safety website (*http://mining.state.co.us*) and is provided in Appendix I. The Laramie-Fox Hills aquifer consists of the Lower Laramie Formation and underlying Upper Fox Hills Formation, interbedded with less permeable mudstone and shale layers.

The lower member of the Fox Hills Formation exhibits a coarsening-upward grain size sequence. The upper member is a more permeable sand deposited in a barrier-island bar system (Ethridge and others, 1979). The Fox Hills Formation outcrop within the study domain strikes generally north-south (Fig. 1-4a) or approximately S 20º E depending on the area within the basin, and dips northeast at an angle between 1.6 and 10 degrees (Hershey and Schneider, 1972).

The Pierre Shale was deposited in a marine setting and the Fox Hills and Laramie Formations were deposited in marginal marine environments subject to transgression and regression of the Western Interior Cretaceous Seaway shoreline. The transition between the Fox Hills Formation and Laramie Formation is often inconsistent due to interfingering of sandstones and shale. Within the study domain, however, the division between the two is marked by thin but laterally consistent coal seams (Spencer, 1986), two of which are shown in Figure 1-4b. Similarly, the transition between the Pierre Shale and the overlying Lower Fox Hills Formation is indistinct because the upper part of the Pierre Shale contains two thick sandstones. In fact, in some areas these sandstones are porous enough to be used as a water resource, although depth and low water quality diminish their significance (Kirkham and others, 1980). Figure 2-1 shows a structure contour map of the base of the Laramie-Fox Hills aquifer (roughly the Pierre Shale-Fox Hills Formation contact) in the study area.

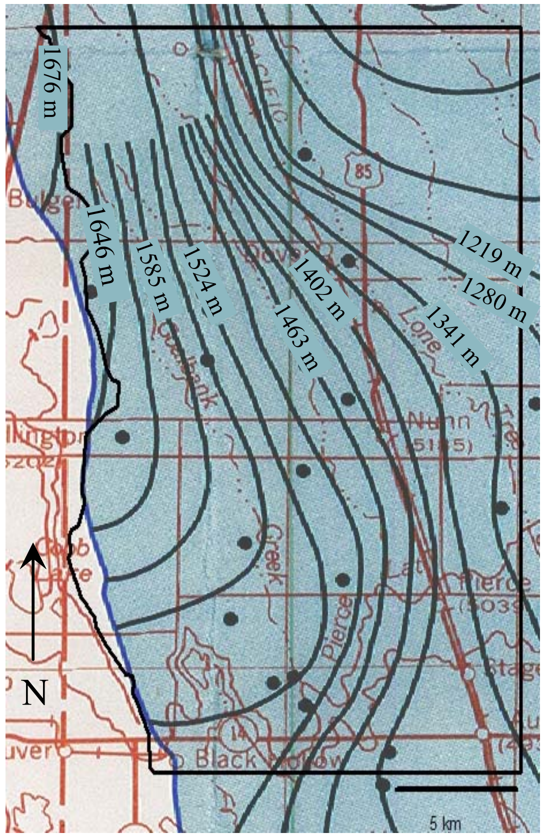

Figure 2-1. Contour of the base structure of the Laramie-Fox Hills aquifer. Elevation is shown in meters above sea level. (Adapted from Robson and Banta, 1987).

Uranium mineralization occurs along the aforementioned paleo-marine shoreline where barrier-island sands contain organic matter from continental or marine origin. Fossils found at Laramie and Fox Hills Formation outcrops indicate a shallow marine depositional environment. Samples taken from a road-cut outcrop expose fragments of oyster and clam fossils in the Lower Laramie Formation where it contacts the Upper Fox Hills Formation (Fig. 2-2). These fossils indicate high productivity in the region, and suggest the presence of organic matter content in these layers. This is significant because organic matter may increase reducing conditions in the aquifer, which are needed to precipitate uranium out of groundwater in the sand and shale units. Although the calcareous shells of oysters and clams themselves may not contain much organic matter, they are comprised of calcium carbonate, which may contribute to the buffering capacity of the rock and/or the transportation of uranium in groundwater by aqueous complexation. This only occurs if the shells dissolve into groundwater. Regardless, the presence of oyster and clam fossils in the area support the notion that facies changes of the Laramie and Fox Hills Formations are a result of a migrating marine shoreline during the Upper Cretaceous time period.

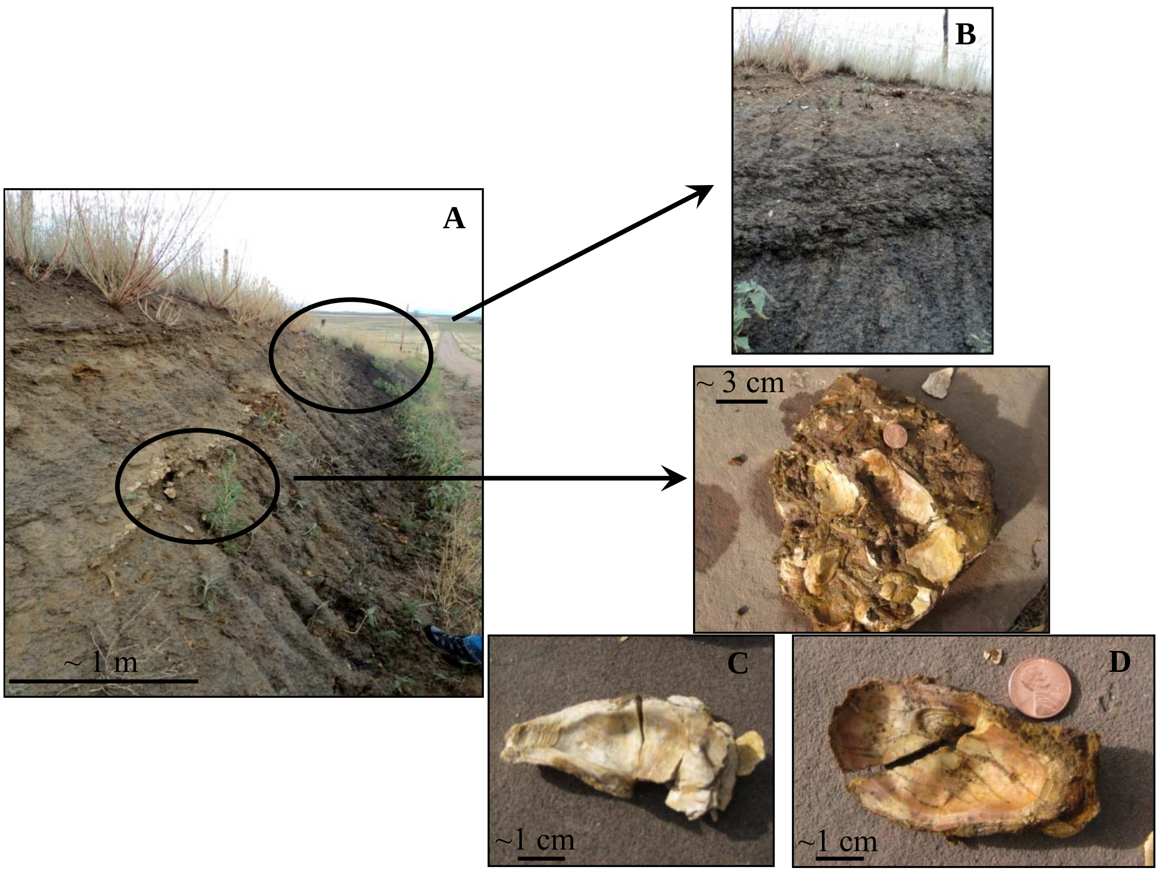

Figure 2-2. The contact between the Lower Laramie and Upper Fox Hills Formation crops out at a road-cut within the study boundary. Subhorizontal seams of layered black shale (B), mudstone, and sandstone are host to fossil shells (A). Large fragments of *Ostrea* sp. have been separated from a rock sample (C) and (D).

The contact between the tilted Laramie Formation and overlying flat-lying deposits of the Ogallala Formation, White River Formation, and Quaternary alluvium exhibits angular unconformity due to Laramide Uplift of the basement sedimentary rocks and a gap in time between depositions (nonconformity). The Oligocene White River Formation consists of tuffaceous siltstone and loosely to moderately cemented sandstone, with conglomerates in paleochannels. The Miocene Ogallala Formation consists of uncemented to well-cemented gravel, sand, silt, and minor clays. Quaternary deposits which cover much of the eastern half of the study domain are made up of gravel and alluvium from the Slocum, Verdos, and Rocky Flats Alluviums (Braddock and Cole, 1978). These Tertiary and Quaternary deposits have higher hydraulic conductivity than the underlying sedimentary formations by roughly one to two orders of magnitude (Arnold, 2010), as discussed later in this thesis. However, because they are primarily surficial deposits, they have minimal impact on groundwater flow in the deeper Laramie-Fox Hills aquifer.

2.2 Groundwater Flow

The section of the Laramie-Fox Hills aquifer pertinent to this study lies in west-central Weld County, Colorado, to the northeast of Fort Collins and north of Greeley. It lies north of the Greeley Arch anticline within the greater Denver Basin (Topper, 2003) (Fig. 2-3). Partially overlain with alluvial material discussed above, the Laramie and Fox Hills Formations crop out on both sides of the Greeley Arch near the South Platte River. North of the Greeley Arch these outcrops trend northeast and northwest into Wyoming.

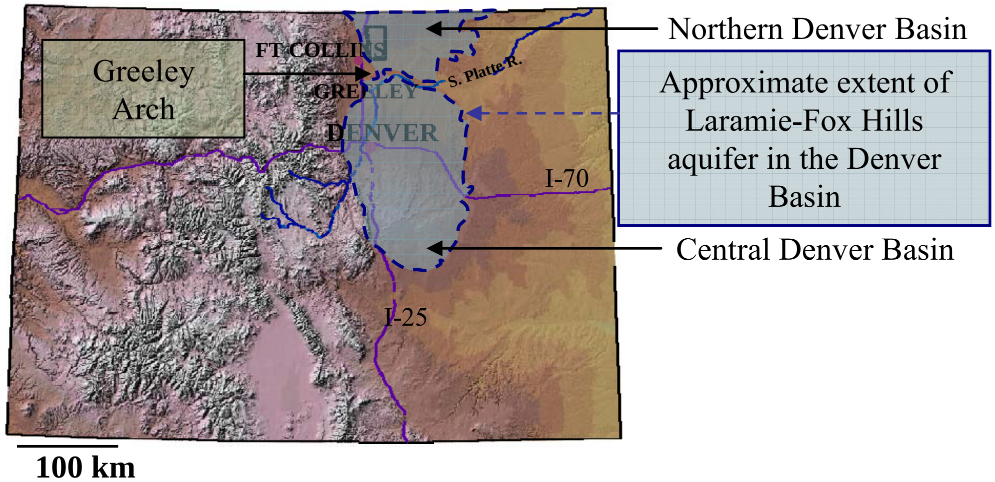

Figure 2-3. Colorado map showing approximate boundaries of the northern and central portions of the Denver Basin separated by the Greeley Arch anticline. The Laramie-Fox Hills aquifer lies in both basins. The study area is outlined in black in the Northern Denver Basin.

The Laramie-Fox Hills aquifer consists of the Upper Fox Hills Formation and two thick sandstone units (9 meters to 15 meters) in the Lower Laramie Formation. In some areas, sandstones in the lower part of the Fox Hills Formation are considered part of the aquifer as well (Robson and Banta, 1987). At a regional scale, this study assumes that the base of the Laramie-Fox Hills aquifer is the same as the contact between the Pierre Shale and the Fox Hills Formation.

Groundwater flow is commonly discussed in terms of distribution of hydraulic head that is defined as the sum of elevation head and pressure head (Fetter, 2001):

$$h = Z + \frac{P}{\rho g} \tag{2.1}$$

Where h is hydraulic head (m), Z is elevation head (m), P is pressure [kg/(s^{2}m)], ρ is density (kg/m^3), and g is gravity (m/s^2). Hydraulic head is determined in the field by measuring water level in a well. The measured water level will reflect the hydraulic head for the unit in which the well screen exists. In unconfined aquifers, where groundwater levels may fluctuate due to the lack of a confining unit, hydraulic head is equal to the water level elevation. A confining unit is defined as a geologic unit with little or no intrinsic permeability. In an aquifer that is bound by a confining unit (a confined aquifer), hydraulic head is equal to the water level that may rise above the elevation of the aquifer. In this study hydraulic head is expressed as meters above mean sea level.

Hydraulic heads may be measured or calculated over a given region and a contour map can be created to show spatial head distributions, gradient patterns, and flow directions within a system. Groundwater flows from high hydraulic head areas to low hydraulic head areas, and therefore head contour maps may be used to infer groundwater flow direction. Groundwater flow paths are roughly perpendicular to hydraulic head contours, although heterogeneity and anisotropy within the aquifer may disrupt this relationship.

Robson and Banta (1987) presented a hydraulic head contour map of the Laramie-Fox Hills aquifer which confirms a general flow pattern trending south (Fig. 2-4). Caution must be taken, however, with the simplified rendering of the map because it was generated relying on sparse well data, has not been updated recently, and only represents a portion of the original larger basin-scale map. As such, it provides only a generalized illustration of regional groundwater flow relevant to this study area.

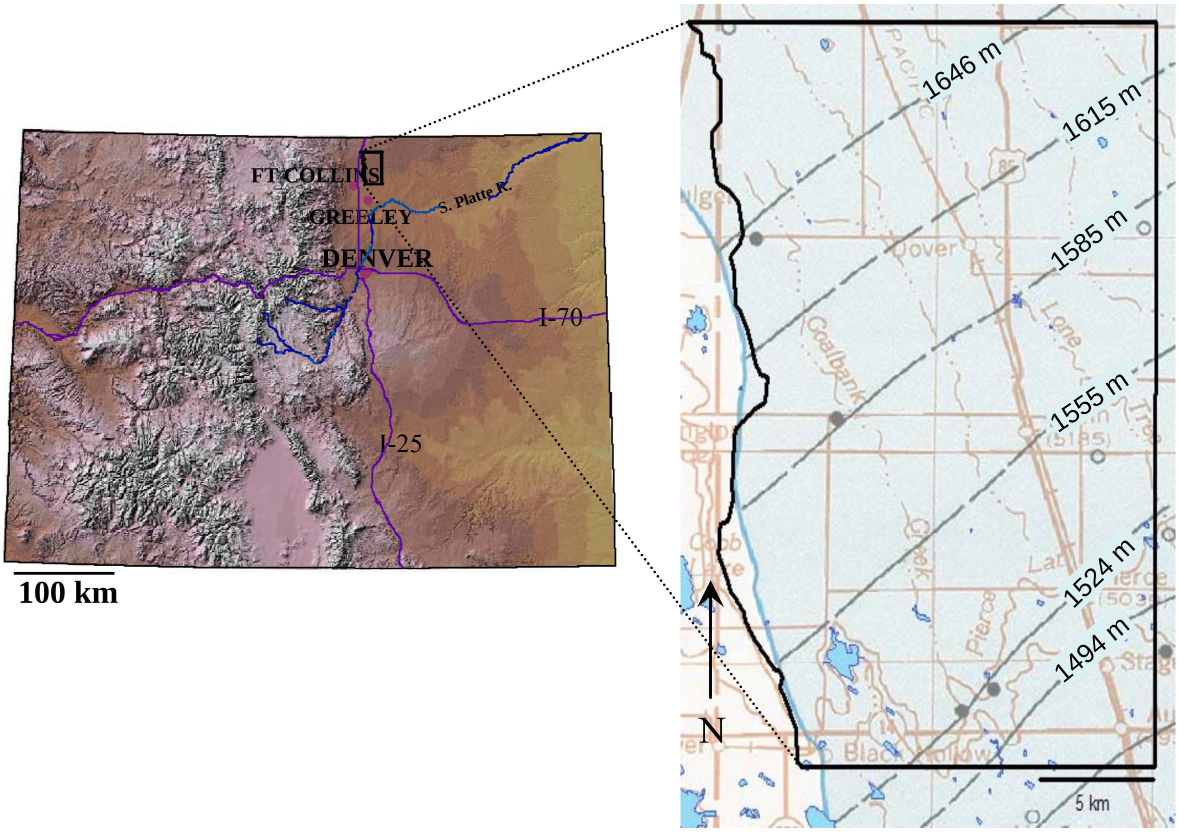

Figure 2-4. Potentiometric surface (hydraulic head) contour map of Laramie-Fox Hills aquifer (adapted from Robson and Banta, 1987).

2.3 Existing Water Level Data

To construct a detailed hydraulic head contour map of the Laramie-Fox Hills aquifer, hydraulic head information from well construction reports from the Colorado Division of Water Resources (Office of the State Engineer) online database were compiled (see *http://www.dwr.state.co.us/WellPermitSearch/default.aspx*). Information for wells drilled from 1990 to 2010 and with screen intervals less than or equal to 18.3 meters (60 feet) were included. This screen interval cutoff value was determined based on the fact that shorter screen intervals better reflect a hydraulic head value for a point within the vertical column. Given formation thicknesses on the order of tens to hundreds of feet, screens with larger intervals would indicate average values of hydraulic head across formations and may not reflect head values within one particular unit. In fact, some wells with screen intervals less than 18.3 meters may still cross geologic units defined in this study. The resulting water level dataset adequately covers the large domain of the study area. Table III-1 in Appendix III shows all well data used including permit number, UTM coordinates, recorded aquifer name, date well constructed, well depth, screen depth, screen interval, and depth to static water level.

Because land surface elevation data were not included in most well construction reports, topography was imported from the U.S. Geological Survey Seamless (2010) online tool and is accurate to 1/3 arc-second, or 1 meter in vertical elevation. To solve for water table elevation, depth to static water was subtracted from imported elevation data. Because of the resolution limitation in imported topographic data, the calculated water level elevation is an average over a 10 meter x 10 meter area. Given a large dataset, the resulting detailed water level elevation map is a more reasonable approximation for calculating hydraulic gradients and groundwater flow direction than the larger scale compilation of Robson and Banta (1987) shown in Figure 2-4.

Groundwater levels from 1990-2010 well data were contoured to provide an overall depiction of the current groundwater levels in the study area. The contour map developed shows hydraulic head for wells that are listed as screened in the “Laramie-Fox Hills Aquifer” (Fig. 2-5). These data are a subset of data for wells contained in “All Aquifers” of the study area. A contour map for wells listed as screened in “All Aquifers” can be found in Appendix IV.

The interpolation scheme used in contouring was the Inverse-Distance-Weighted method (where Power=2, Number of points=8, Cell size=50) in ArcView version 9.3.

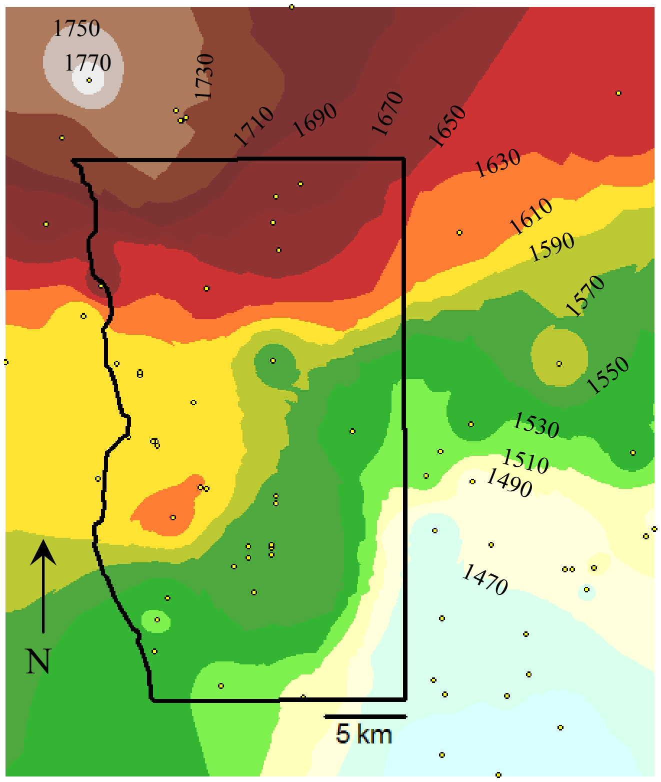

Figure 2-5. Water level contour map of data from the Colorado Division of Water Resources, Office of the Colorado State Engineer data from 1990 to 2010, in meters above sea level. Contour interval is 20 meters. Map includes well locations (yellow dots) for wells with screens in the "Laramie-Fox Hills Aquifer."

The Lower Laramie and Upper Fox Hills Formations are considered one aquifer because contacts between them are inconsistent on a regional scale. It is therefore difficult to confidently determine the depth at which one formation begins and the other ends (Robson and Banta, 1987). Within the study area, a coal layer distinguishes the boundary between the two (Fig. 1-4) (Spencer, 1986). Although the two formations may not be significantly hydraulically connected in the vertical direction due to intervening low permeability mudstones, the composite water level contour map (Fig. 2-5) of the aquifer as a whole shows groundwater trending to the south and slightly east. A similar trend is noticed in topography, where surface elevation decreases to the south and slightly east (Fig. 1-2). This suggests the groundwater configuration is largely topography-controlled, a common relationship set forth originally by Tòth (1963).

Because the Pierre Shale is likely to act as an impermeable lower boundary to the Laramie-Fox Hills aquifer, its easterly dip may be a reason for a bedrock-controlled groundwater table in the southern area of the study domain, where the thickness of the aquifer decreases to less than 90 meters. Because aquifer thickness is comparatively small in the southern area, it may allow the low-permeability Pierre Shale to become a larger controlling factor on groundwater flow direction which may become parallel to the bedrock surface. It is likely that topography most greatly influences flow in all areas of the model domain, and the dip of the Pierre Shale to the east additionally influences groundwater flow direction in the southern area.

Deviations from the general flow pattern exist and may result from either the separation of sandstone layers by shales or spatial variation of hydraulic conductivity. If the hydraulic gradient of a given area is high, denoted by closely spaced contour lines, it may indicate that hydraulic conductivity is relatively low. Conversely, if the hydraulic gradient is low, denoted by widely spaced contour lines, it may indicate relatively high hydraulic conductivity of the rock unit for the given area. Widely spaced contour lines are observed where the Fox Hills Formation outcrops on the western boundary, suggesting the Fox Hills Formation may exhibit higher hydraulic conductivity than the greater Laramie-Fox Hills aquifer. While the water level contour map in Figure 2-5 displays areas of high and low hydraulic head gradients, the hydraulic head mainly decreases to the southeast boundary of the study area. Discussion on the differences between the Laramie and Fox Hills Formations in terms of hydraulic conductivity are discussed further in Chapter 3.

Aside from the general groundwater trend to the southeast, Figure 2-5 also exhibits areas where the expected water levels are anomalous, showing unexpectedly high and low water levels. A well in the center-left shows a relatively high level because it is a shallow well in a topographically high area. Because water levels largely mimic topography (Tòth, 1963), and because of the shallow well screen interval, the water level anomaly is more likely to be a result of its location at high elevation rather than to be a representation of the deeper groundwater system. In contrast, there is a well showing a relatively low water level on the center-right. This well is screened in the Fox Hills Formation. The low and high head disparities are likely an artifact of wells screened at different depths in the Fox Hills and Laramie Formations, which may indicate the influence of confining layers between the two formations. Layers of shale or mudstone must have extremely low-permeability and must lie between the formations in order to maintain the observed hydraulic head difference between the Laramie and Fox Hills Formations.

CHAPTER 3:
HYDRAULIC CONDUCTIVITY OF MAJOR SEDIMENTARY FORMATIONS

Hydraulic conductivity distributions are expected to be heterogeneous and anisotropic due to mustone, shale, and sandstone layers throughout the regional Laramie-Fox Hills aquifer. This chapter discusses the measurement of hydraulic conductivity in the Lower Laramie Formation and the Upper Fox Hills Formation. A presentation of literature values for major formations is also included.

To measure hydraulic conductivity of rock units, aquifer tests, such as slug tests and pumping tests, can be performed. Slug tests yield hydraulic conductivity values representative of the formation in the immediate vicinity of the well. Aquifer pumping tests yield average hydraulic conductivity values of large rock volumes, tens to even hundreds of meters around the pumping well, depending on the scale of the test. Slug tests were conducted in the Lower Laramie Formation and results were analyzed to determine hydraulic conductivity as well as storativity of the rock. The Fox Hills Formation and Pierre Shale were not examined using slug tests due to prohibitive depth to water and/or lack of appropriately characterized wells. In almost all well construction reports for wells in the study area lithology was inadequately reported or a water pump was in use, rendering the wells inappropriate for slug tests.

3.1 Slug Tests

3.1.1 Background

Slug tests are one of the most commonly employed field techniques to measure hydraulic conductivity. The technique is widely used because it is cost-effective, simple, relatively quick, no water needs to be taken out or put into the test well, and the analysis is relatively straightforward (Butler, 1998). The main limitation of a slug test is that it reflects the hydraulic conductivity only in the immediate vicinity of the well screen.

This study employed a "slug"—a sand-filled PVC pipe that is closed on both ends—of 0.0508 m x 1.524 m (2 in x 5 ft) that was quickly inserted into a well to raise the water level. The slug served to add a known volume to the well without the addition of water (Fig. 3-1). The rate at which the water level recovered to its original state was measured at known intervals using a pressure transducer.

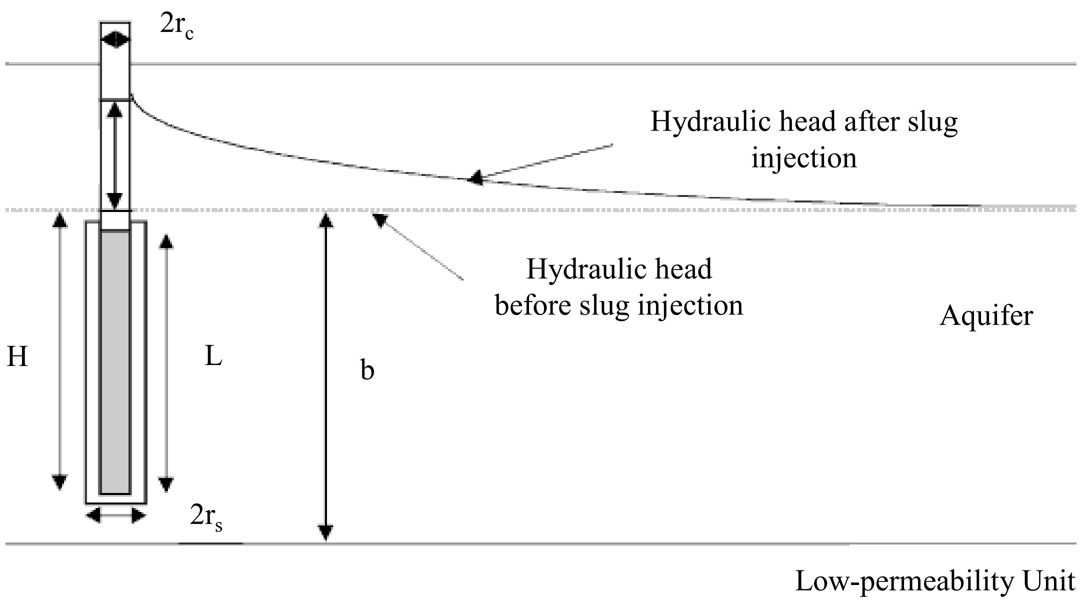

Figure 3-1. Well configuration of slug test in an unconfined aquifer showing change in hydraulic head from initial hydraulic head (H_0) after slug injection (modified from HydoSOLVE, Inc., 1996). L is length of well screen, r_w is radius of well screen, r_c is radius of the well casing, and b is the aquifer thickness.

Water level recovery is a function of the transmissivity of the aquifer, or the rate at which water is transmitted through the thickness of the aquifer. Transmissivity is dependant on properties of the water, rock, and rock unit thickness. It is mathematically defined later in this chapter. Figure 3-2 includes a picture of the slug, one of the wells tested in this study, and a pressure transducer. The pressure transducer is lowered into the well at a depth that will accommodate subsequent slug insertion. The slug is lowered into the water very quickly to achieve an "instantaneous" increase in water level.

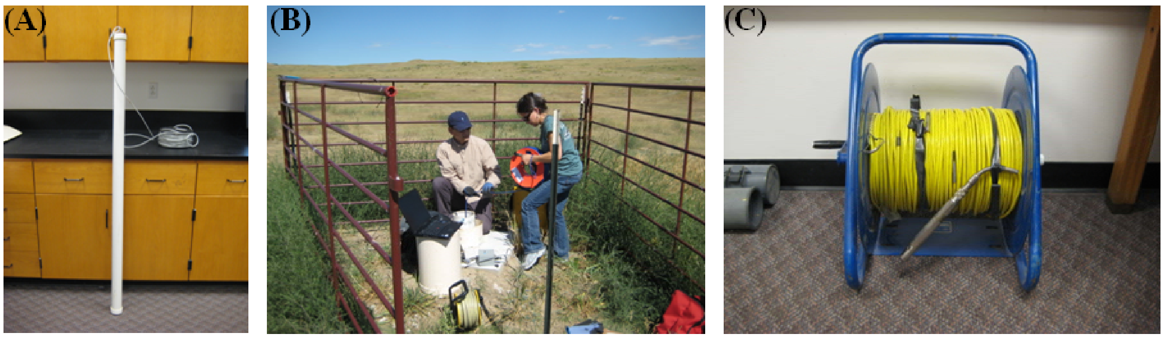

Figure 3-2. A five-foot slug with a steel cable attached (A). In-Wook Yeo and the author at well IN08-33 MO3 for Test-1 before slug insertion (B), and a pressure transducer (C).

There are several methods for analyzing the water level recovery data for different aquifer types. This study utilized the Cooper-Bredehoft-Papadopolus and Hvorslev methods for confined aquifers. The Cooper-Bredehoft-Papadopulos method works by matching normalized water level data, defined by the observed water level over the initial water level, (H/H_0), to a series of aquifer type reference curves to determine aquifer transmissivity. The method to determine hydraulic conductivity from transmissivity is discussed later in this chapter. Normalized water level data are plotted against time, and the reference curve is plotted as H/H_o versus Tt/r_c^2. This is shown in the plot below where T is transmissivity (m^2/s), r_c is the radius of the well casing (m), and t is time (s).

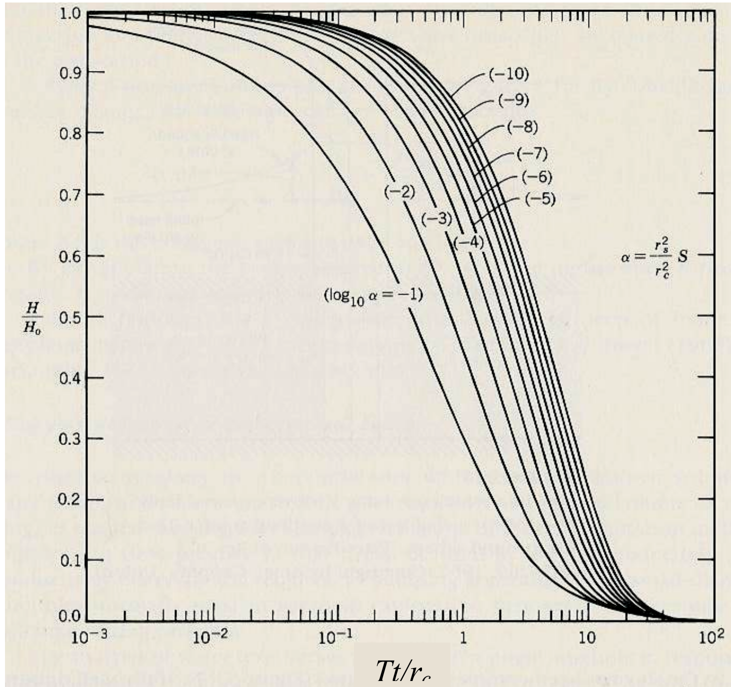

Figure 3-3. Reference type curves for slug test analysis using the Cooper-Bredehoft-Papadopolus method. (Papadopolus and others, 1973).

The measured H/H_0 data curve of water level versus time was plotted on a semilogarithmic scale and overlain to best match one of the reference curves in Figure 3-3. The point at which the x-axis value of the type curve plot was equal to 1.0 was used to find a corresponding time along the curvature of the field data curve (Fig. 3-4). This point was named t_1 and was used in the equation to solve for transmissivity,

$$T = \frac{1.0 r_c^{\,2}}{t_1} \tag{3.1}$$

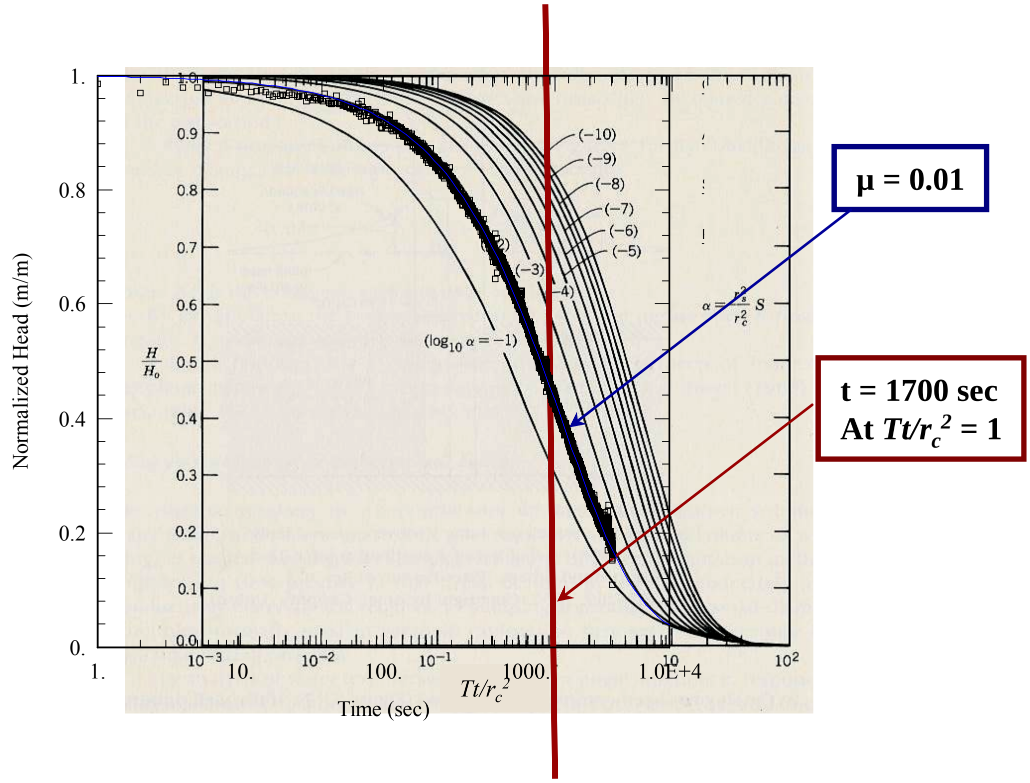

Figure 3-4. Curve matching data to reference type curves using the Cooper-Bredehoft-Papadopolus method.

From there, the hydraulic conductivity can be calculated using the equation,

$$T = Kb \tag{3.2}$$

where K is hydraulic conductivity (m/s), and b is the thickness (m) of the aquifer. The thickness of the aquifer can be determined by lithologic logs or driller's logs from well construction reports.

Storativity is an aquifer property that indicates rock matrix compressibility. It can also be estimated from the slug test using the following equation:

$$S = \left(r_c^2 \mu\right) / r_s^2 \tag{3.3}$$

Where S is storativity, r_c is the radius of the well casing (m), μ is a dimensionless value corresponding to the type curve, and r_s is the radius of the screen casing. The μ value is determined from the curve match to a reference curve as shown in Figure 3-4.

The Hvorslev method (Hvorslev, 1951) for slug test analysis was also used in this study. The ratios of water level during the test to the original water level (H/H_0) versus time are plotted on a semilogarithmic scale. From this plot, a value for t_{37} is found and the following equation is used to compute hydraulic conductivity:

$$K = \frac{r_c^{\,2} \ln(L_e / R)}{2L_e t_{37}} \tag{3.4}$$

where R is the radius of the wells screen (m), L_e is the length of the well screen (m), and t_{37} is the time (s) it takes for water level to fall to 37% of the initial water level at the start of the test. The advantage to using the Hvorslev method is calculating hydraulic conductivity in the absence of information on aquifer thickness.

Once water levels were mostly recovered, a bail test was conducted by quickly removing the slug and thereby instantaneously decreasing the water level. Water level recovery data were collected and the same analysis described above was applied to the bail test. The bail test should yield a similar hydraulic conductivity for the rock unit as the slug test, and it supplies a second set of data for the test well.

3.1.2 Analysis

Analyses for confined aquifer conditions were conducted for the slug and bail tests performed in the low sandstones of the Laramie Formation. The two slug tests and the two bail tests were performed in Powertech wells in the northern section of the study domain (Fig. 1-2). The data were recorded by an electronic pressure transducer (Fig. 3-2) and data logger. A geophysical log of the Test-1 well was completed by Powertech and subsequently posted on the Division of Reclamation Mining and Safety website.

Geophysical well logs provide primary data regarding lithologic layering in the area. An interpretation of the gamma, spontaneous potential, and resistivity logs with depth provided information on thickness and depth for sandstone, shale, and coal layers. Gamma radiation is emitted primarily by thorium, potassium, and uranium. Increased deflections in the gamma log may be caused by clays which contain high amounts of potassium, or a deposit of uranium or thorium. Coal layers reflect extremely low gamma radiation in the well log. Spontaneous potential is a measurement of electrochemical potential caused by the diffusion of dissolved ions in groundwater in the borehole. It may identify permeable units (i.e. sandstones) by increased deflections, but these data must be used in conjunction with resistivity and other geologic parameters to ensure proper lithologic interpretation. Resistivity is a general property of the rock material and is relatively low for shale units compared to sandstones. While there are significant complexities involved with understanding well log data (Ellis and Singer, 2007), these fundamental concepts were used to interpret sandstone depth and thickness for the Test-1 well, as well as other wells in the area discussed in Chapter 5.

Test-1 was conducted on August 20, 2010 at well IN-08-33 MO3. The well is located in Section 33, T 10N, R 67W and is 0.1524 meters (6 inches) in diameter. The thickness of the sandstone was estimated at 7.9 meters (26 feet) (Fig. 3-5). Total well depth is approximately 81 meters (266 feet) and the screened interval is between 72 meters and 81 meters (236 feet to 266 feet) in depth (Colorado Division of Water Resources, 2010). Depth to water was recoded at approximately 52 meters (107.3 feet).

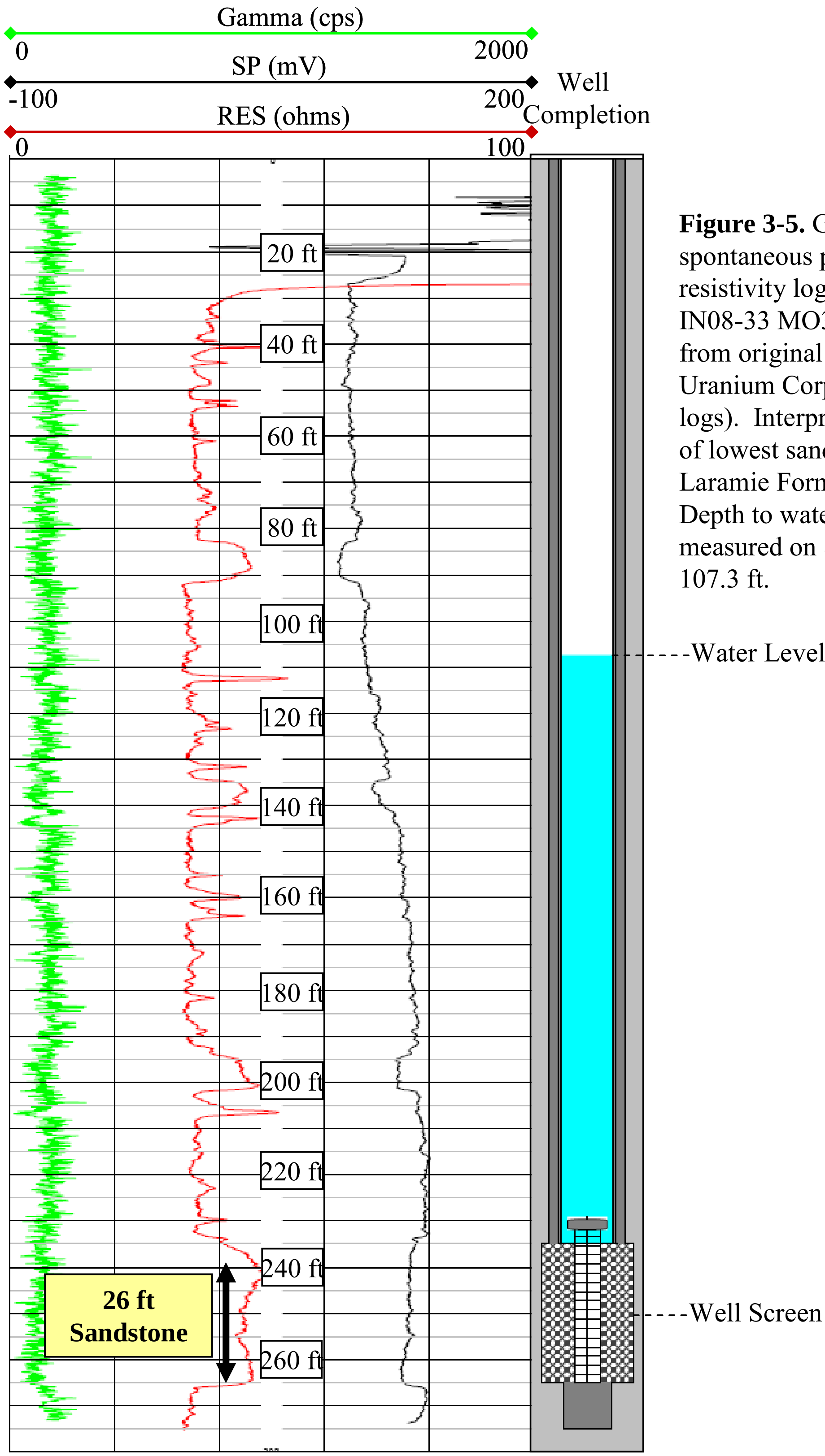

Figure 3-5. Gamma, spontaneous potential, and resistivity logs for well IN08-33 MO3 (modified from original Powertech Uranium Corporation well logs). Interpreted thickness of lowest sandstone in the Laramie Formation is 26 ft. Depth to water was measured on 8/20/2010 at 107.3 ft.

Test-2 was conducted on September 24, 2010 at well IS-010. The well is 0.01016 meters (4 inches) in diameter and is located in Section 15, T 9N, R 67W (Fig. 1-2). Total well depth is approximately 71.3 meters (234 feet) and the screened interval is between 36.6 meters and 42.7 meters (120 feet to 140 feet) (Colorado Division of Water Resources, 2010). The thickness of the sandstone was assumed to be the same as the thickness of the screen interval: 6.1 meters (20 feet). Plots of water level recovery over time for all tests are shown in Figure 3-6 through Figure 3-11. Figure 3-6 exhibits a peak (a) and trough (b) immediately after initial addition or removal of the slug in excess of the actual change in volume. This is due to the sensitivity of transducer measurements, which can be temporarily thrown off by water turbulence in the well.

(A)

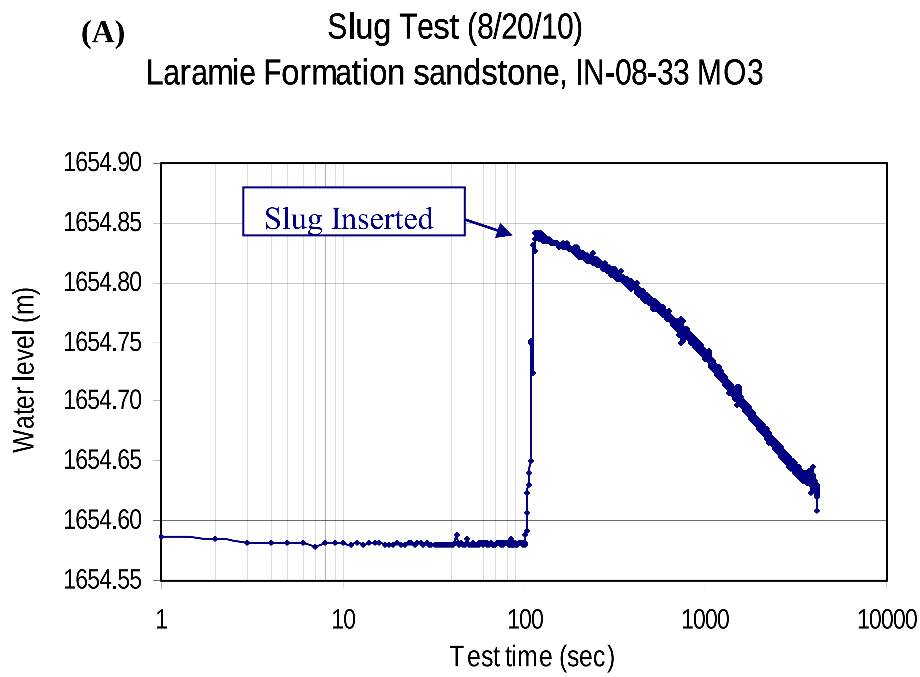

(B)

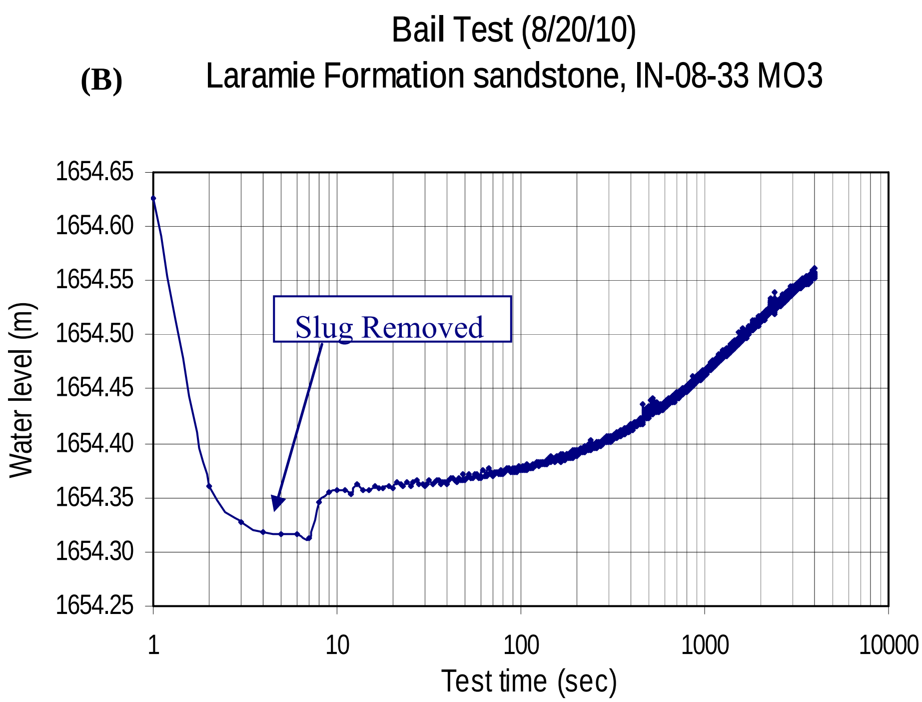

Figure 3-6. Slug and bail tests from well IN-08-33-MO3 showing decrease in water level after the addition of the slug (A) and increase after slug removal (B).

(A)

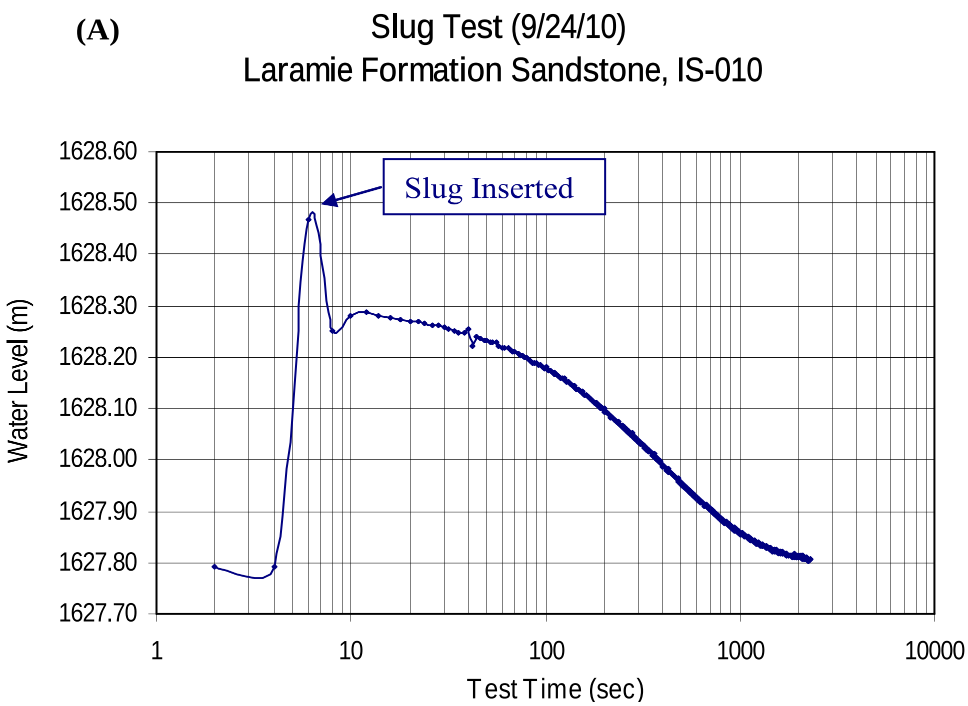

(B)

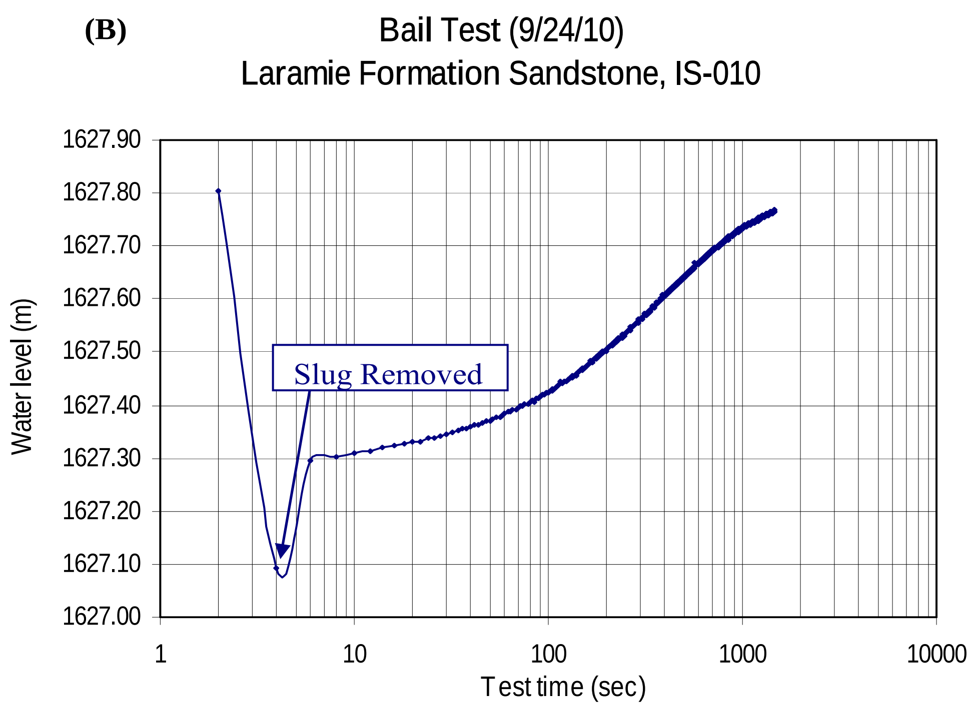

Figure 3-7. Slug and bail test from well IS-010 showing decreasing in water level after the addition of the slug (A) and increasing after slug removal (B).

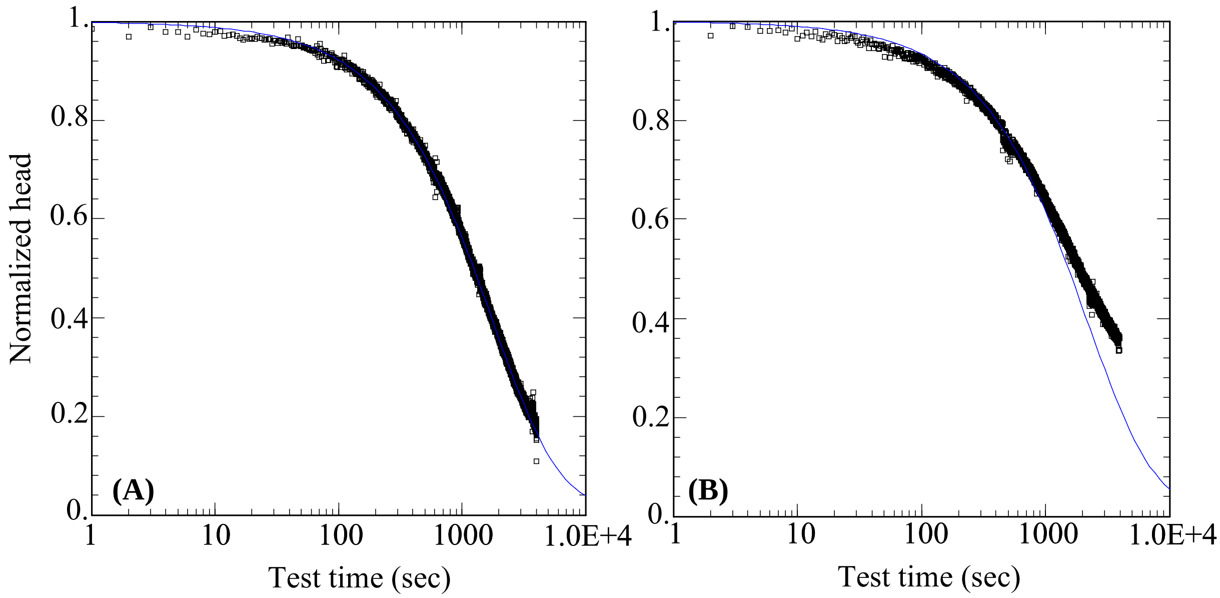

Figure 3-8. Semilogarithmic graph of normalized data for well IN-08-33-MO3 showing slug test conducted on well penetrating the lowest sandstone of the Laramie Formation on August 20, 2010. Curve matching (blue line) using Cooper-Bredehoft-Papadopolus method for confined aquifers yielded a hydraulic conductivity of 9.2×10^{-7} m/s and storativity of 0.001 (A). Result of the bail test conducted directly following the slug test. Curve matching yielded hydraulic conductivity of 7.5×10^{-7} m/s and storativity of 0.001 (B).

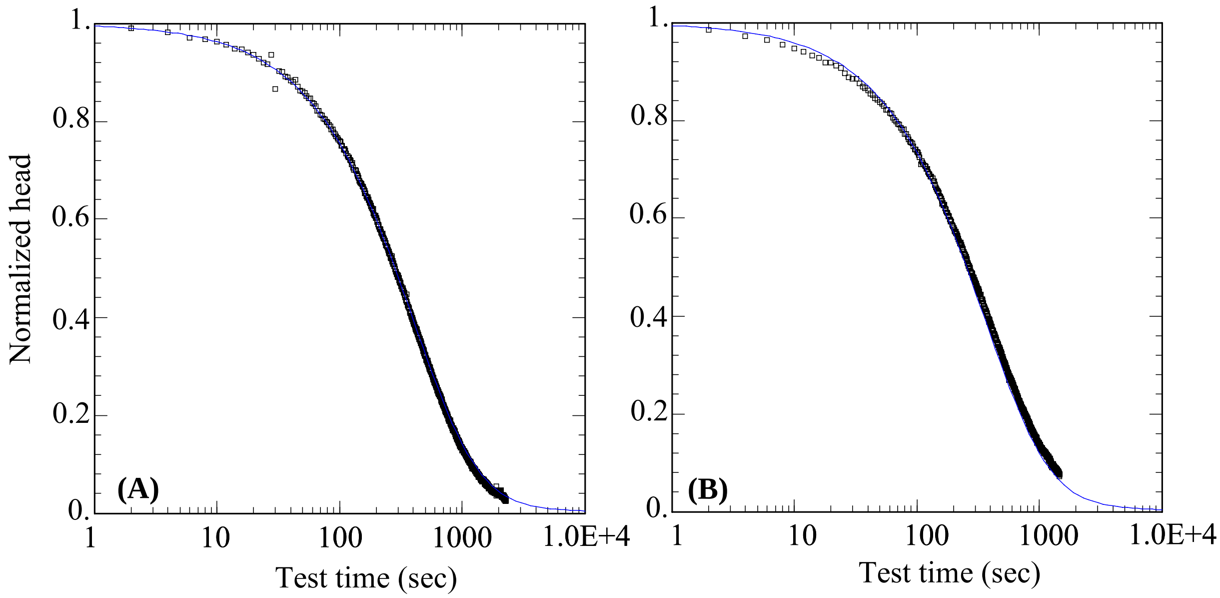

Figure 3-9. Semilogarithmic graph of well IS-010 showing slug test conducted on well IS-010 penetrating a sandstone of the Laramie Formation on September 24, 2010. Curve matching (blue line) using Cooper-Bredehoft-Papadopolus method for confined aquifers yielded a hydraulic conductivity of 1.8×10^{-6} m/s and storativity of 0.0001 (A). Result of the bail test conducted directly following the slug test. Curve matching yielded hydraulic conductivity of 2.0×10^{-6} m/s and storativity of 0.0001 (B).

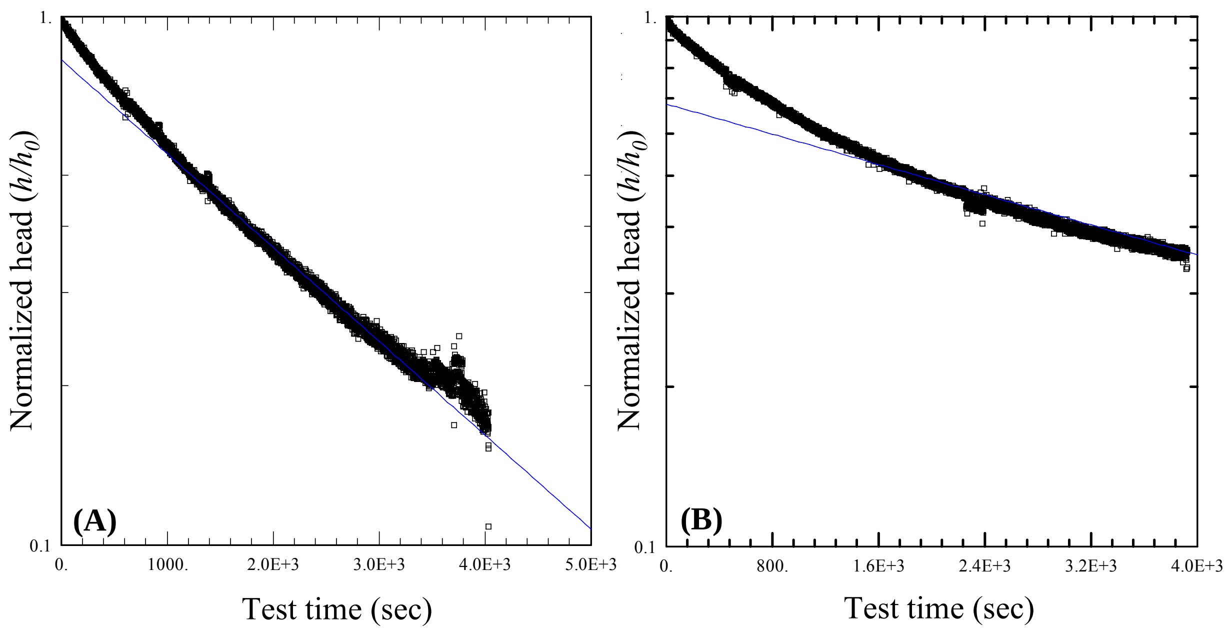

Figure 3-10. Semilogarithmic graph of normalized data for slug test conducted on well IN08-33 MO3. Straight line matching using Hvorslev method for confined aquifers yielded hydraulic conductivity of 8.0×10^{-7} m/s (A). The bail test yielded a hydraulic conductivity of 3.2×10^{-7} m/s (B).

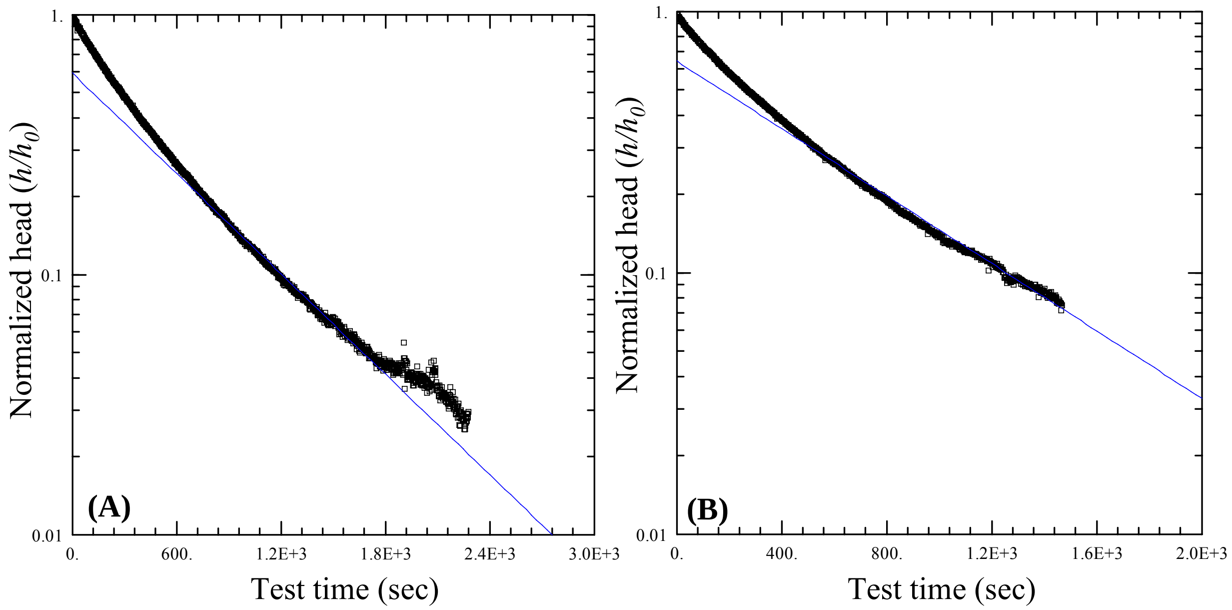

Figure 3-11. Semilogarithmic graph of normalized data for slug test conducted on well IS-010. Straight line matching using Hvorslev method for confined aquifers yielded hydraulic conductivity of 1.2 x 10^{-6} m/s (A). The bail test yielded a hydraulic conductivity of 1.2 x 10^{-6} m/s (B).

3.1.3 Results

Hydraulic conductivity of the Lower Laramie Formation sandstones was found to be between 3.2 x 10^{-7} m/s and 9.2 x 10^{-7} m/s from Test-1 and between 1.2 x 10^{-6} m/s and 2.0 x 10^{-6} m/s from Test-2 using both the Cooper-Bredehoft-Papdopolus and Hvorslev methods for confined aquifers. Analyses were conducted using AQTESOLV (HydoSOLVE, Inc., 1996), a computer program designed for perform curve-matching and calculation described in Section 3.1. Slug Test-1 yielded a storativity of 0.001 and slug Test-2 yielded 0.0001. Robson and Banta (1995) estimated the storativity of the Laramie-Fox Hills aquifer to be 0.0001. These results compare well to the characteristically low storativity of confined aquifers, typically 0.005 or less (Fetter, 2001). Because the wells are screened in sandstone units, these values likely represent high hydraulic conductivity of sandstone layers of the formation, given that most of the Laramie is comprised of low hydraulic conductivity shale. On the other hand, these localized slug and bail test results for hydraulic conductivity may be lower than values of a larger scale.

Little is known about the hydraulic conductivity of intervening shales within the formations and reference values from literature are employed in the absence of data. One study by Barkmann (2004) searched for reported values for vertical hydraulic conductivity of shales in Denver Basin aquifers. Values ranged widely between 1 x 10^{-13} m/s and 1 x 10^{-5} m/s.

Results for hydraulic conductivity from slug and bail tests are summarized in Table 3-1 along with literature values for other formations in the study area. Results from an aquifer pumping test discussed in the next section are also shown. Storativity is not shown in the summary table because it is not a parameter used in the steady state flow modeling of this study.

Formation	Rock type (Braddock and Cole, 1978)	Hydraulic Conductivity (m/s)	Source
Quaternary Alluvium	Gravel, alluvium	5.4×10^{-4} to 3.1×10^{-3}	Topper and others (2003), assumed value from Cache La Poudre Alluvial aquifer
White River (Tertiary)	Conglomerate	1.1×10^{-3} to 7.4×10^{-3}	Topper and others (2003), assumed value from Lone Tree Creek Alluvial aquifer
Ogallala (Tertiary)	Alluvium	1.1×10^{-3} to 7.4×10^{-3}	Topper and others (2003), assumed value from Lone Tree Creek Alluvial aquifer
Laramie (Cretaceous)	Inter-fingering sandstone, shale, coal	3.2×10^{-7} to 9.2×10^{-7} 1.2×10^{-6} to 2.0×10^{-6} 9.5×10^{-7} to 2.4×10^{-6}	Slug and Bail Test-1 conducted on 8/20/2010 Slug and Bail Test-2 conducted on 9/24/2010 Sherman and others (1978)
Fox Hills (Cretaceous)	Sandstone, shale	7.2×10^{-6}	Powertech (2009), multi-well aquifer pumping test conducted in 2008
Laramie-Fox Hills Aquifer	Inter-fingering sandstone, shale, mudstone, coal	1.8×10^{-7} to 2.5×10^{-5} 9.5×10^{-7} to 2.4×10^{-6}	Robson (1983) Sherman and others (1978)
Pierre (Cretaceous)	Shale, sandstone	1.0×10^{-9} to 1.0×10^{-5}	Freeze and Cherry (1979)

Table 3-1. Geologic description and hydraulic conductivity of formations in the study area.

3.2 Aquifer Pumping Test

An aquifer pumping test can be conducted to derive hydraulic parameters of an aquifer, such as hydraulic conductivity and storativity. It entails pumping at one well and recording water level change in surrounding wells. Using a constant pumping rate, a cone of depression (area of lowered head around the pumping well) is induced. The water level response from neighboring observation wells are often analyzed by various graphical methods. Most commonly used are the Thies method and the Cooper-Jacob straight-line method discussed in this section.

The Theis equation for transient flow conditions in a confined aquifer is as follows:

$$T = \frac{Q}{4\pi(h_0 - h)} W(u) \tag{3.5}$$

Where T is transmissivity (m^2/d), Q is the pumping rate (m^3/d), h_0 is initial hydraulic head, h hydraulic head at a specified time, and $W(u)$ is a dimensionless well function used in curve matching to a reference type curve. Similar to the curve matching in Section 3.1, drawdown data versus time is plotted and matched to a type curve (see Fetter, 2001). Analysis with the Theis solution requires adequate water level records in early stages of the pumping test.

The Cooper-Jacob straight-line method involves plotting water level drawdown versus distance of the observation wells and computing transmissivity and storativity:

$$T = \frac{2.3Q}{2\pi(h_0 - h)} \tag{3.6}$$

$$S = \frac{2.25Tt}{r_0^{\ 2}} \tag{3.7}$$

Where S is aquifer storativity (dimensionless), t is the time since pumping began (s), and r_0 is the distance at which the straight line intercepts the zero-drawdown axis (m). Hydraulic conductivity is found by using the calculated transmissivity in Equation 3.2.

Hydraulic conductivity of the A_2 Sandstone in the Upper Fox Hills Formation was investigated by Powertech in 2008 by conducting a multi-well aquifer pumping test (Powertech, 2009). The test was conducted within the northern proposed mine site in Section 33, T 10N, R 67W (cross-hatch in Fig. 1-2). Hydraulic conductivity was calculated to be 7.2×10^{-6} m/s (Table 3-1) and storativity was found to be 4.18×10^{-5} (Powertech, 2009). Another aquifer test by Powertech has been approved by the Environmental Protection Agency and may occur in 2011.

CHAPTER 4:
REGIONAL GROUNDWATER MODELING

Computer modeling of groundwater flow systems using geological information can help support a conceptual understanding of the dynamics of groundwater flow in the study area. This study used Visual MODFLOW (Schlumberger Water Services, 2009) to model groundwater flow in the Laramie-Fox Hills aquifer. MODFLOW (McDonald and Harbaugh, 1988) is a finite difference program for simulating three-dimensional, saturated groundwater flow. It can handle heterogeneous and anisotropic conditions and can incorporate evapotranspiration, recharge, pumping, and other hydrologic features. At the heart of groundwater flux determination is Darcy's Law, derived by Henry Darcy in 1856 (Freeze and Cherry, 1979):

$$q = -K\frac{\partial h}{\partial l} \tag{4.1}$$

where q is specific discharge (m/s), K is hydraulic conductivity (m/s), h is hydraulic head (m), and l is length (m). Darcy's Law (Equation 4.1) describes one-dimensional flow through a homogeneous material. It can be expanded to three dimensions for heterogeneous and anisotropic conditions. A mass balance principle requires that the difference in fluid mass flowing into and out of a given volume must be equal to the change in mass of fluid within the volume. Combining Darcy's law and the mass balance equation, with additional consideration for sources and sinks of groundwater, the equation governing hydraulic head distribution can be derived as below (Frezee and Cherry, 1979):

$$\frac{\partial}{\partial x}\left(K_{xx}\frac{\partial h}{\partial x}\right)+\frac{\partial}{\partial y}\left(K_{yy}\frac{\partial h}{\partial y}\right)+\frac{\partial}{\partial z}\left(K_{zz}\frac{\partial h}{\partial z}\right)-W = S_s\frac{\partial h}{\partial t} \tag{4.2}$$

Where K_{xx}, K_{yy}, and K_{zz}, represent hydraulic conductivity (m/s) in the x, y, and z directions respectively, h is hydraulic head (m), W is a water source or sink (1/s), S_s is specific storage (1/m) , and t is time (s) (McDonald and Harbaugh, 1988). Analytical techniques for solving the equation are complex and sometimes not feasible. Instead, numerical techniques such as finite element and finite difference methods may be used to approximate the solution. MODFLOW solves the governing equation (Equation 4.2) for hydraulic head distribution under specified boundary conditions. When using numerical modeling, a study domain is discretized into three-dimensional cells described by Δx, Δy, and Δz, where hydraulic head is solved for a central node within each cell.

This study examines steady state head conditions for a general understanding of the background groundwater flow system. Thus, the assumption that the right hand side of Equation 4.2 is equal to zero is applied because hydraulic head does not change with time:

$$\frac{\partial}{\partial x}\left(K_{xx}\frac{\partial h}{\partial x}\right)+\frac{\partial}{\partial y}\left(K_{yy}\frac{\partial h}{\partial y}\right)+\frac{\partial}{\partial z}\left(K_{zz}\frac{\partial h}{\partial z}\right)-W=0 \tag{4.3}$$

The regional groundwater model in this study encompasses an area to the northeast of Fort Collins and is bounded on the west by a generally north-south trending water divide where the formations of interest crops out at the land surface (Fig. 1-4). Boundary conditions are assigned based on head contour maps created from water level records from 1990 to 2010 (Fig. 2-4) discussed in Chapter 2, and digital topographic maps from the U.S. Geological Survey Seamless (2010) website *(http://seamless.usgs.gov)*. Hydrogeologic parameters were assigned given reported literature values as well as aquifer test data.

4.1 Model Design

The model domain (Fig. 1-2) is 33.8 kilometers from north to south and 20.5 kilometers from east to west. The model domain covers a land surface area of approximately 650 square kilometers. The thickness in the vertical direction varies from 1200 meters to 1765 meters, and the maximum thickness is 565 meters. The maximum depth of the Fox Hills Formation in the study area was used to determine the maximum depth of the model. Cell size is 100 m x 100 m x 20 m, but layer thickness is refined near the surface to accommodate large changes in topography. Topographic data were imported into MODFLOW to form the upper boundary of the model domain and cell thickness, Δz, in the uppermost layers was modified to fit topographic constraints. As a result, cells in the upper layers have smaller thicknesses compared to the layers below them. Horizontal to vertical cell dimensions maintain a ratio of 5:1. The model consists of 338 rows, 205 columns, and 58 layers.

The steady state model was developed under heterogeneous, anisotropic conditions. The aquifers were considered heterogeneous because lithologic properties change spatially. Anisotropy, where hydraulic conductivity is greater in the lateral directions as compared to the vertical direction, was likely because of sub-horizontal layering of low-permeability mudstones and shales. Generalized stratigraphy includes, in ascending order, the Upper Pierre Shale, the Fox Hills Sandstone, and the Laramie Formation (Fig. 1-3). These tilted formations generally strike north-south within the study domain and are unconformably overlain by flat lying Tertiary and Quaternary deposits (Fig. 1-4) discussed in Chapter 1. These younger deposits were simulated in the model by surficial layers between 10 meters and 50 meters thick. The three-dimensional rendering of this information is shown in Figure 4-1.

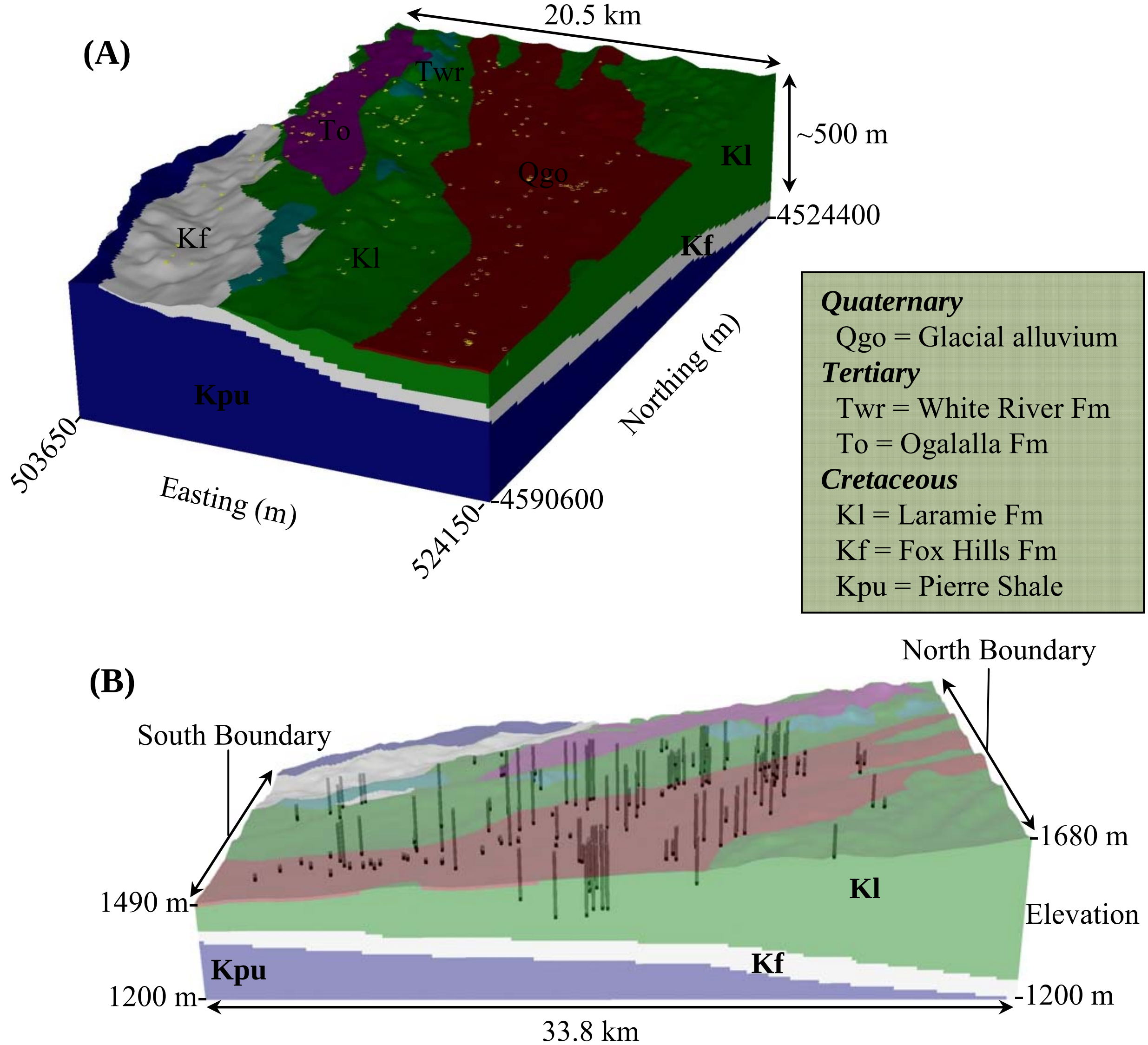

Figure 4-1. Three-dimensional model geometry and hydrostratigraphy based on geologic mapping (Green, 1992) and isopach and structural contour maps (Robson and Banta, 1987). Well locations are shown as dots (A). Three-dimensional view looking west is shown in semi-transparency to display observation wells mostly in the Laramie and Fox Hills Formations. Well casing is shown in gray and the point of calibration at the center of the well screen is in black (B). Vertical exaggeration is 15x.

Groundwater flow into the model comes from two sources: areal recharge and flow across the north constant head boundary. Recharge is a specified flux boundary condition applied to the uppermost layer. Because it is a steady state model, the volumetric flow entering from the north boundary combined with groundwater entering from recharge will be equal to the volume of groundwater exiting the south boundary of the model plus volume lost to evapotranspiration. Recharge, constant head boundaries, and other hydrologic parameters used in modeling are discussed below.

4.2 Recharge and Evapotranspiration

Recharge to groundwater is low in the study area, between 5 mm and 15 mm per year. This is a result of low precipitation as well as evaporation and plant transpiration (evapotranspiration) from non-irrigated or natural grasslands (Arnold, 2010). A range for recharge values is estimated by Arnold (2010) using the chloride mass-balance method in which soil profiles of chloride concentration are used to estimate water flux from the land surface to the groundwater table. In non-irrigated areas, chloride originates from wet and dry deposition. Chloride accumulates at the extinction depth, the depth limit below which there is no groundwater lost to evapotranspiration. Chloride concentration is related to recharge rate according to the equation of Allison and others (1994):

$$q_w = (C_p P)/C_s \tag{4.4}$$

Where q_w is the recharge rate (mm/yr), C_p is the effective chloride concentration in precipitation (mg/L), P is the precipitation rate (mm/yr), and C_s is the average chloride concentration in soil water below the depth of effective evapotranspiration (mg/L). Using this relationship, Arnold (2010) quantified recharge rates for the Lost Creek designated groundwater basin in Weld, Adams and Arapahoe Counties in Colorado. This current study assumes a similar value for recharge rate given the proximity of the Lost Creek drainage basin to the study domain. The study area lies approximately 40 kilometers to the northwest of the Lost Creek groundwater basin. A recharge rate of 10 mm/yr is used in the model, based on the median value of the range given by Arnold (2010) for natural or non-irrigated grasslands. This value implicitly accounts for evapotranspiration in Equation 4.4 used to calculate recharge. Therefore evapotranspiration is set to zero in the model.

4.3 Hydrologic Boundaries

Hydrogeologic boundaries used in regional groundwater modeling include constant head boundaries (where hydraulic head does not change with time) and no-flow boundaries. Constant heads with a linear gradient from west to east were assigned to the north and south boundaries of the model domain (Fig. 4-2). The constant head boundaries set forth are the factors that most greatly affect calculated hydraulic head in the simulation. Large surface water bodies are assumed to be constant heads as well. For example, the Black Hollow Reservoir in the southern area of the study domain is filled with water year-round. This study assumes the water level (hydraulic head) in the reservoir is fixed at the adjacent surface elevation. Hydraulic heads at the northern and southern boundaries were approximately assigned according to the steady state groundwater level data (Fig. 2-4). The model set up showing boundary conditions and bodies of water are shown in Figure 4-2. Small seasonal streams and irrigation ditches in the study area were not simulated.

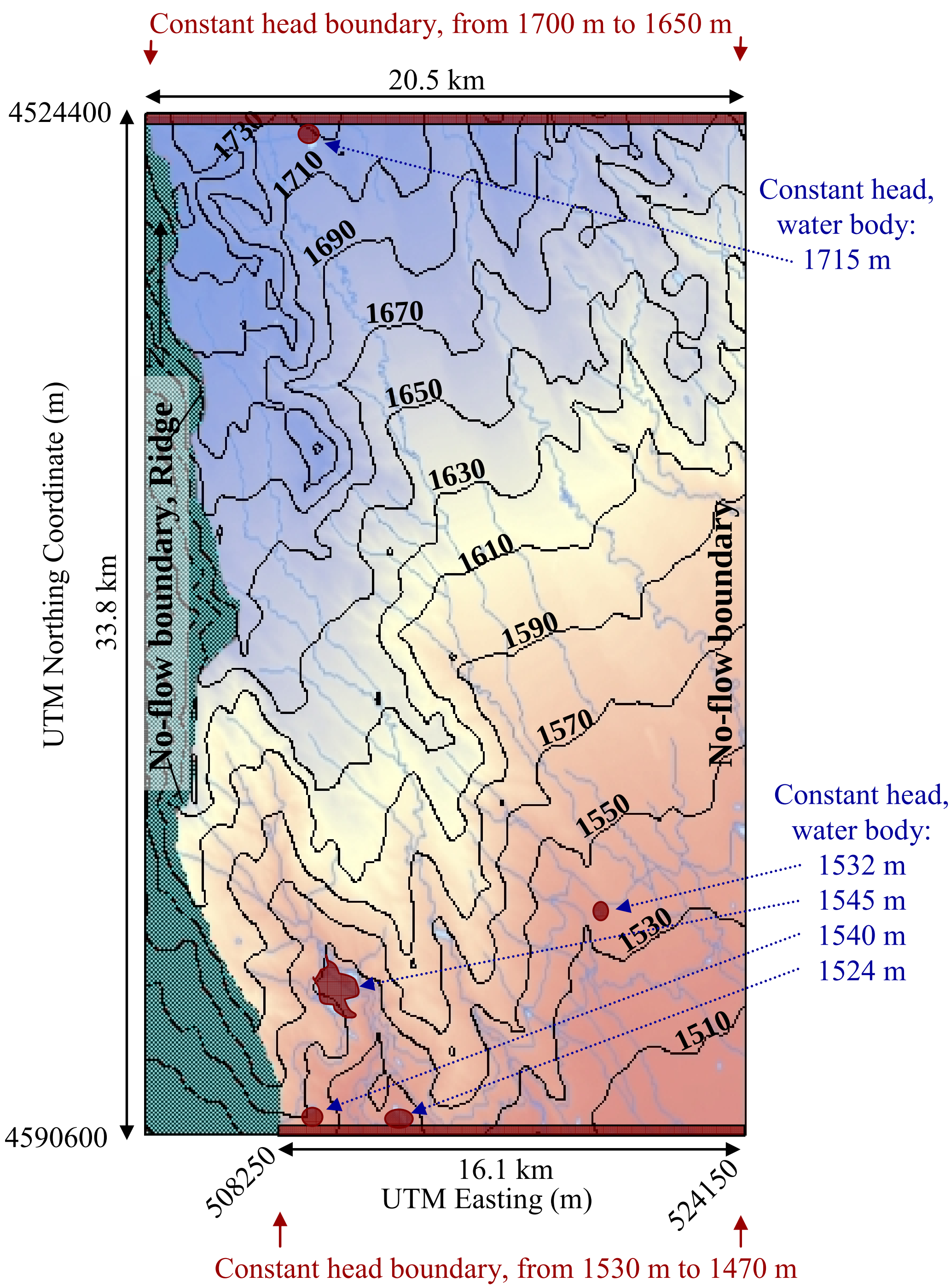

Figure 4-2. Boundary conditions for MODFLOW model. Shaded relief and contour map of topography, in meters, is shown decreasing in elevation to the southeast. Green shaded area represents the inactive zone which lies outside the model domain. North American Datum 1983 coordinate system is shown.

A no-flow boundary was assigned to the west boundary to represent a topographic divide. The low ridge defines a natural drainage divide which extends vertically downward from the ridge. It corresponds to the natural condition that groundwater along this ridge flows to the south or east. This assumption coincides with groundwater trends shown in previous contour maps (Fig. 2-4 and 2-5). The depth of the groundwater table varies between 3 meters and 9 meters below the surface.

At the east boundary, there is no obvious natural surface water divide reasonably close to the mining zone (area of interest). A north to south no-flow boundary is assigned at a far enough distance from the proposed mining zone, so that the boundary condition does not impact the hydraulic head in the area of interest.

4.4 Hydraulic Conductivity

Field data were used to constrain hydraulic conductivity values employed for modeling. Usage of values within one order of magnitude of the field data (Table 3-1) were necessary for optimal calibration. Modeling within such a range for hydraulic conductivity is not uncommon practice. Horizontal conductivity values were initially assigned using the highest conductivity values from the slug, bail, and multi-well aquifer pumping tests.

Conductivity values used in the model are listed in Table 4-1 below. Anisotropic conditions were assigned, where horizontal conductivity, $K_{x,y}$, was three times greater than vertical conductivity, K_z, so $K_{x,y}$:K_z is equal to 3:1. Other common relationships between $K_{x,y}$ and K_z were possible. Ratios of 10:1 and 5:1 for $K_{x,y}$:K_z were explored but did not achieve comparable model calibration; correlation to observed data was 47% or less in those cases.

Pierre Shale		Fox Hills Fm		Laramie Fm	
$K_{x,y}$ (m/s)	K_z (m/s)	$K_{x,y}$ (m/s)	K_z (m/s)	$K_{x,y}$ (m/s)	K_z (m/s)
1.0×10^{-8}	3.3×10^{-9}	2.0×10^{-5}	6.7×10^{-6}	1.7×10^{-5}	5.7×10^{-6}

Tertiary and Quaternary Deposits (isotropic) (m/s)		
White River	Ogallala	Quaternary Deposits
4.0×10^{-4}	7.3×10^{-3}	3.1×10^{-3}

Table 4-1. The hydraulic conductivities for each geologic formation used in modeling.

4.5 Model Results

Model results are measured against observed water levels from the Colorado Division of Water Resources (Office of the State Engineer) online database. The comparison between calculated hydraulic heads (water levels) and observed water levels is a measure of the degree of model calibration. Calibration to existing well data is essential to understanding model results at a fundamental level. The models presented in this study are non-unique in their solutions because adjustments to boundary conditions or different model set ups may lead to similar calibration seen in this study. Model calibration to existing water level data will be discussed in this section.

Modeled hydraulic heads are shown in plan view as well as in north-south and east-west cross section in Figure 4-3. Groundwater flow is depicted with arrows showing flow direction through the Laramie and Fox Hills Formations. Arrow magnitude depicts the relative magnitude of velocity of groundwater. The highest flow velocity calculated in the model is 1.3×10^{-5} m/s.

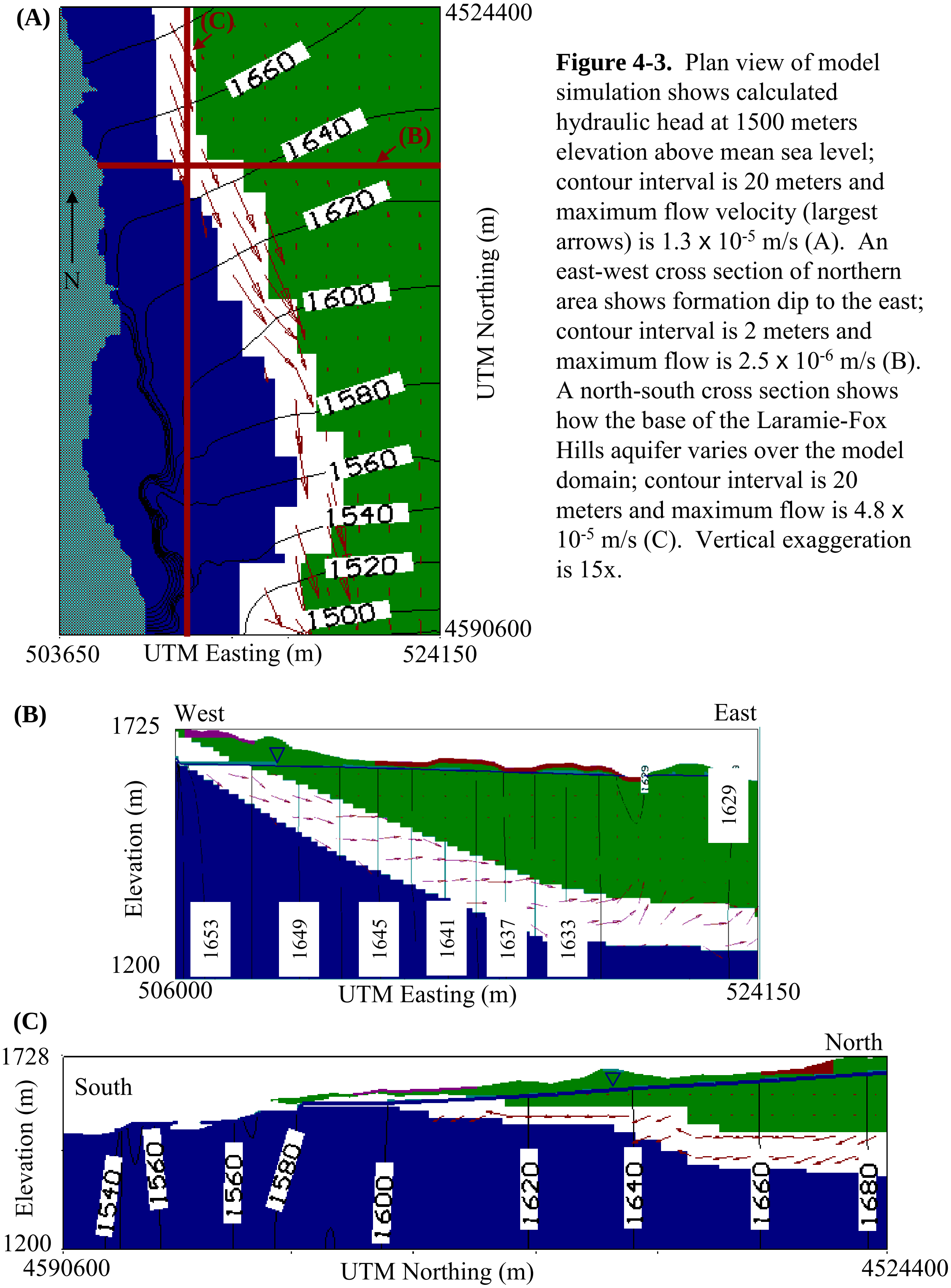

Figure 4-3. Plan view of model simulation shows calculated hydraulic head at 1500 meters elevation above mean sea level; contour interval is 20 meters and maximum flow velocity (largest arrows) is 1.3×10^{-5} m/s (A). An east-west cross section of northern area shows formation dip to the east; contour interval is 2 meters and maximum flow is 2.5×10^{-6} m/s (B). A north-south cross section shows how the base of the Laramie-Fox Hills aquifer varies over the model domain; contour interval is 20 meters and maximum flow is 4.8×10^{-5} m/s (C). Vertical exaggeration is 15x.

Observed hydraulic head contours discussed in Chapter 2 (Fig. 2-5) are compared to the model output in Figure 4-4. The model output plot represents head contours at an elevation of 1500 meters. The southeast-trending general flow pattern is consistent between the two plots, although the model does not appear to account for local anomalies seen in the composite water level map of the Laramie-Fox Hills aquifer (Fig. 2-5). Model results show the influence of the low hydraulic conductivity of the Pierre Shale in the southwest corner, where contour lines are closely spaced and water level (hydraulic head) decreases with the dip of the formation.

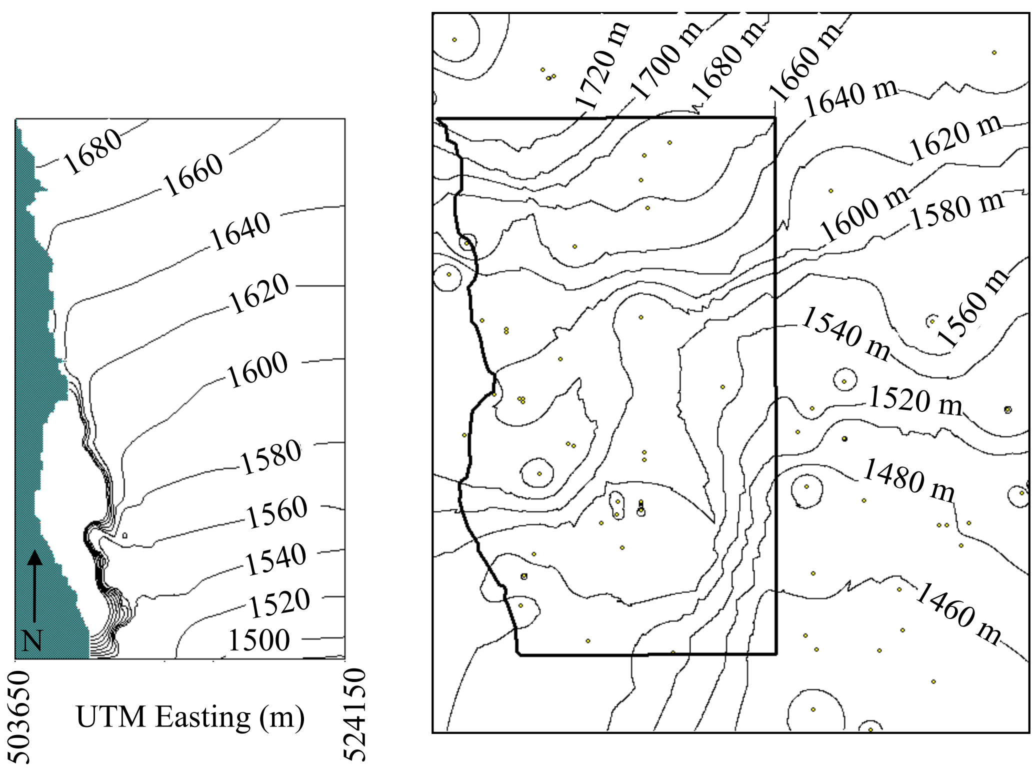

Figure 4-4. Comparison of modeled hydraulic head at 1500-meter elevation (left) with the Colorado Division of Water Resources well data for the Laramie-Fox Hills Aquifer (right), as seen in Figure 2-5.

The composite water level map of the Laramie-Fox Hills aquifer (Fig. 2-5) is an average over the vertical domain of the aquifer, thereby representing average hydraulic head spanning both the Laramie and Fox Hills Formations. When viewing various layers in the model, specified by real-world elevations, hydraulic head contours may appear to be somewhat mismatched from the Laramie-Fox Hills aquifer map due to changes in hydraulic head through the vertical column. Figure 4-4 shows overprediction of the model results approximately between 0 meters and 20 meters, although other model layers may compare differently. Given this, additional means of representing model calibration are discussed below.

Model residual (R_i) is the difference between calculated model results (X_{cal}) and observed water levels (X_{cal}), defined as

$$R_i = X_{cal} - X_{cal} \tag{4.4}$$

The residual mean ($\overline{R}$) is a measure of the average residuals for all data points used in calibration:

$$\overline{R} = \frac{1}{n}\sum_{i=1}^{N} R_i \tag{4.5}$$

Once residual mean is calculated, the root mean squared error value (RMS) can be computed:

$$RMS = \sqrt{\frac{1}{n}\sum_{i=1}^{N} R_i^{\,2}} \tag{4.6}$$

The normalized root mean squared value (Equation 4.7) is a measure of degree of fit of the calculated data to the observed data that accounts for the range of data values used. Because this study incorporates a large number of calibration points and a large range of water levels, it is important to statistically describe the degree to which the model predicts water level. The normalized root mean squared value is expressed as a percentage, and is ideally 10% or less

(Delaney, P.G. and Loveys, J., 2000). The best degree of fit achieved for the model was 14.8%.

$$NormalizedRMS = \frac{RMS}{(X_{obs})_{\max} - (X_{obs})_{\min}} \tag{4.7}$$

The relationship between calculated model results and observed water levels can also be described by a correlation coefficient ranging between -1.0 (negative correlation) and 1.0 (positive correlation). A correlation coefficient of zero means the data sets are unrelated. The model achieved a correlation coefficient of 0.86, suggesting the water levels predicted by the model are fairly well related to observed water levels.

Figure 4-5 shows a plot of calculated versus observed hydraulic head values. The region bound by the upper and lower blue dashed lines contains the region where 95% of the plotted points are *expected* to occur given water level data variability. Model results for Equations 4.4 to 4.7 are also shown. Most calculated values fall within a 40 meter range of the observed values. The confidence interval, denoted by red lines in the Figure 4-5, is calculated for each observed value and indicates the model range that would be acceptable for that data point. It is determined by adding (or subtracting) the upper and lower limit of the residual mean (Equation 4.6) from the observed value. The range falls above and below the observed value to the standard deviation of observed values.

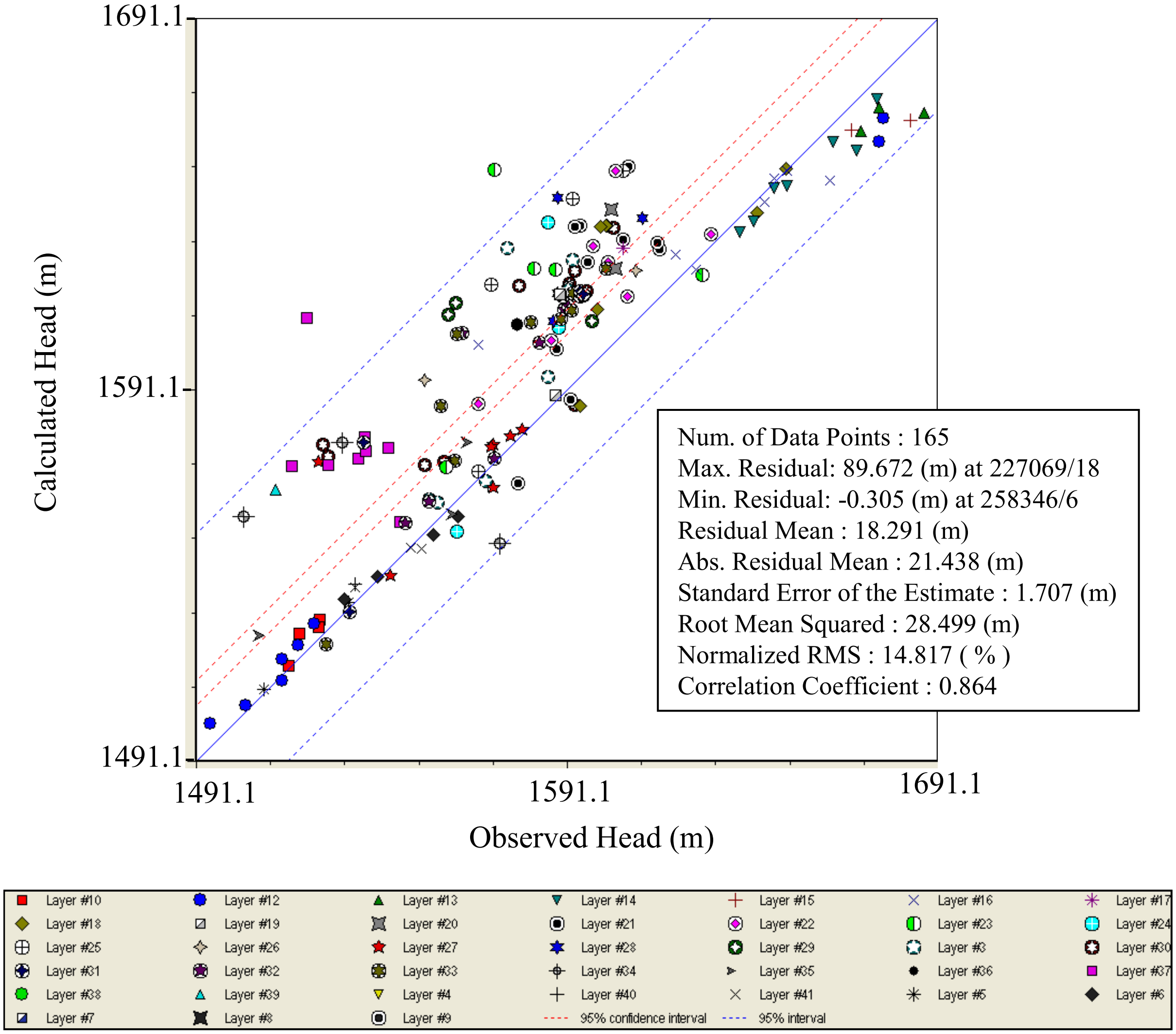

Figure 4-5. Modeled calculated head versus observed head. Dotted blue lines denote the boundary within which 95% of the points are expected to occur. The red lines denotes the confidence interval.

General overprediction of the model may be due to increased pumping in the area over the time span of water level records (20 years). Because observed values represent water levels measured any time between 1990 and 2010, observed heads today may be lower than predicted by the model if pumping in the aquifer was higher than aquifer recharge.

Water levels for wells in Nunn, Colorado and the Powertech proposed mining zone were overpredicted by the model. The water level data recorded for wells in Nunn may have been lower than actual aquifer conditions due to pumping from neighboring wells at the time of construction and water level measurement. This may have contributed to an overprediction of hydraulic head for these wells. Wells in the Powertech proposed mining zone may have lower hydraulic head than was calculated because they are screened in specific sandstones known for low-hydraulic head in the Fox Hills Formation. This is further discussed in Chapter 5 where details of the hydrogeologic structure of the Fox Hills Formation are presented.

Figure 4-6 shows hydraulic head residuals, or model head minus observed head, on the x-axis and the frequency at which the residuals occur on the y-axis. The model appears to slightly overpredict the hydraulic heads with a mean residual of 4.6 meters. Generally, residuals are expected to follow a normal distribution. Fifty-one out of 204 data points fall between zero and 6 meters of residual. This indicates that residuals are more tightly distributed about a residual of zero than would be predicted assuming a typical normal distribution of data.

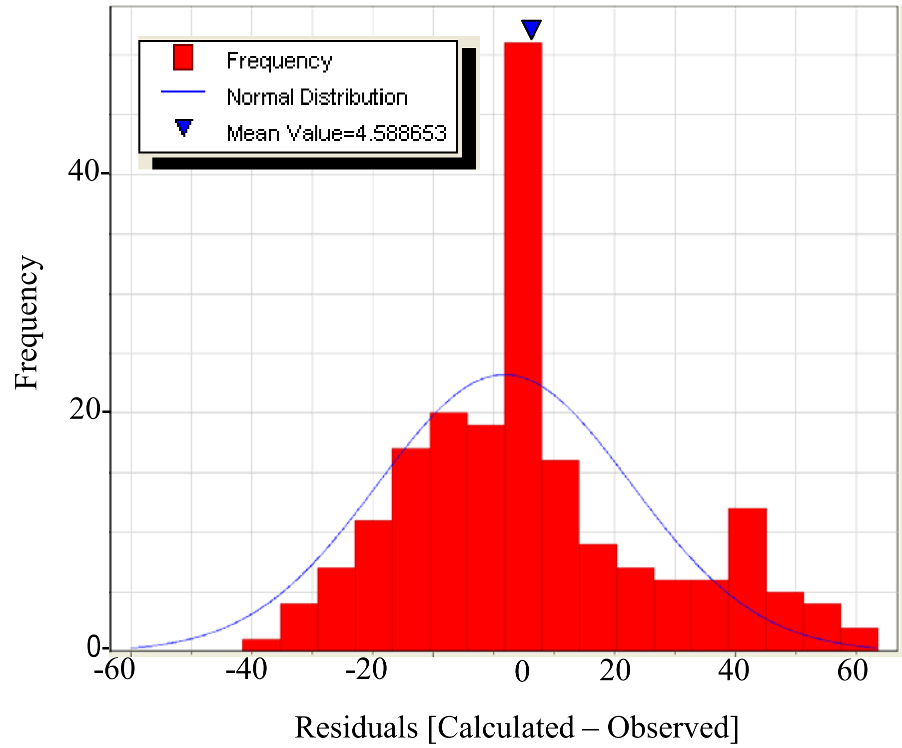

Figure 4-6. Model calibration residual histogram showing a spike between zero and 6 meters of residual (calculated minus observed head). The blue line denotes a normal distribution curve.

The resulting mass balance of the model (Fig. 4-7) consists of inflow into and outflow leaving the groundwater system. In this model, groundwater flow input includes aquifer recharge, flow entering through the north constant head boundary, and flow entering from constant head water bodies at the land surface. Output of flow is through the southern constant head boundary.

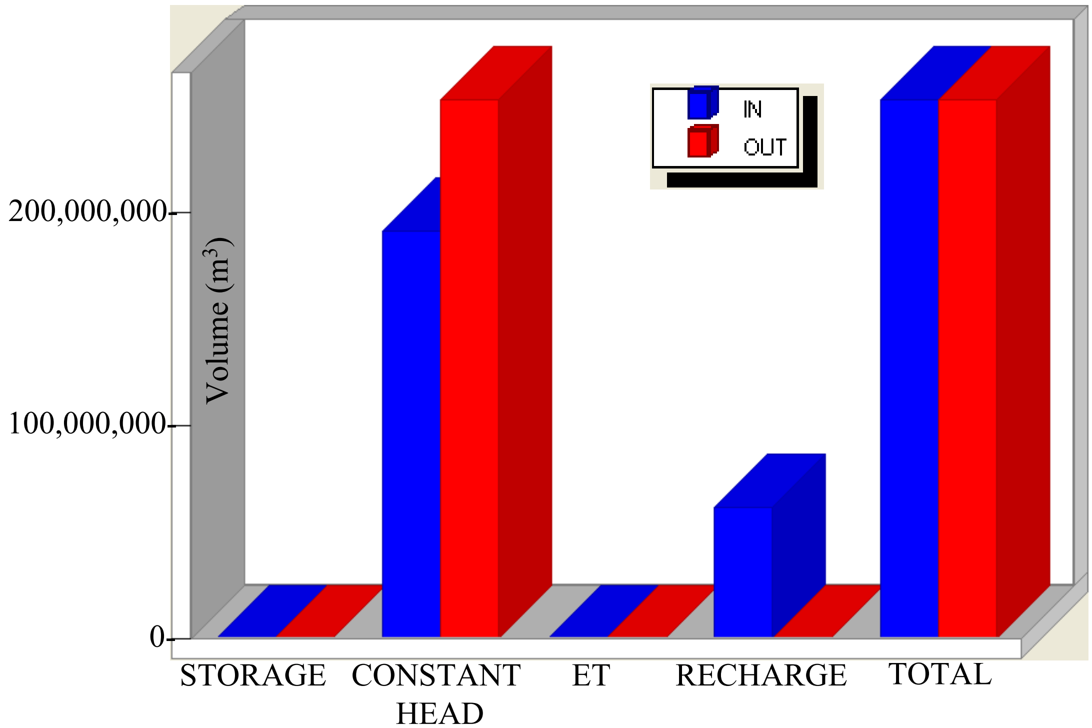

Figure 4-7. Mass balance bar chart of model output. Boundary conditions (constant heads at the north and south boundaries) account for the majority of volumetric flow through the Laramie-Fox Hills aquifer. Evapotranspiration (ET) is incorporated in the recharge value which accounts for roughly one quarter of the model volumetric input. Storage is not a parameter used in steady state calculations.

Hydraulic head values decreased to the south and east. Approximate hydraulic head gradients from this calibrated model showed a north-south gradient of 0.005, and an east-west gradient of 0.0037. These gradients represent the average lateral change in hydraulic head of the Laramie-Fox Hills aquifer. Lithologies affect groundwater flow velocity and can be related to the hydraulic head gradient within sedimentary units. In units of low hydraulic conductivity, such as a shale, the hydraulic head gradient is expected to be higher than that of more permeable sandstones. Because the Laramie Formation includes more shale units than the Fox Hills Formation (Chapter 2.1), higher gradients are expected within the Laramie Formation. The composite hydraulic head gradients represented in the model may be the average of high gradients in the Laramie Formation and low gradients in the Fox Hills Formation.

4.6 Sensitivity analysis

Once constant head boundaries were assigned, the most important adjustments affecting model results were in selecting hydraulic conductivity values within the constraints of field and literature values. Deviations from the calculated slug test hydraulic conductivity for the tested formation are expected in natural systems. For hydraulic conductivity within a formation, model calibration required using hydraulic conductivities that were within one order of magnitude of reported values (3-1). When upscaling local field test data, hydraulic conductivity increases are expected.

During iterations of model calculations, $K_{x,y}$ and K_z values were adjusted to reach optimal calibration (Table 4-1). Hydraulic conductivity anisotropy of 5:1 and 10:1 were examined, but did not calibrate with observed data as well as 3:1 anisotropy. This may represent the connection of sandstone units at the regional scale of the system modeled in this chapter.

Model simulations under variable evapotranspiration rates showed little to no change in hydraulic head results for the Fox Hills Formation. Similarly, model results were not affected by fluctuating recharge within the 5-15 mm/yr range. Given the estimated low recharge rates for the region, it is likely that recharge would have a minor role in groundwater flow of the study area.

The model forced groundwater flow to the south and somewhat east. Groundwater flow in the east direction within the sandstone was seen as a result of the hydraulic head gradients assigned in the east-west orientation at both north and south constant head boundaries (Fig. 4-

2). A small component of flow travels east and then is forced south along the eastern no-flow boundary. Therefore calculated hydraulic head along this boundary is a product of numerical modeling rather than the natural system. Wells within 2 kilometers of the east boundary were excluded from use in model calibration.

4.6.1 Alternative Model Design

One of the uncertainties in model input is the assignment of boundary conditions. The north boundary in the model was constant through the vertical column, regardless of geologic formation. An alternative model was created to examine model sensitivity to the north boundary condition. It included lower constant head values in the Fox Hills Formation along the north boundary. The south constant head boundary remained the same as in the original model where constant head values were invariable through the vertical column. The value for constant head assignments in the Fox Hills Formation at the north boundary were calculated based on a gradient of 0.004 from the south constant head boundary, less than the average gradient found in the original model (0.005). A decrease in hydraulic head gradient represented higher hydraulic conductivity in the Fox Hills Formation given greater sandstone composition compared to the Laramie Formation. Similarly, an east-west gradient of 0.001 was assigned because it was less than the original model average (0.0037). North constant head boundary assignment along the dip of the Fox Hills Formation begins at 1665 meters in the west and ends with 1631.2 meters in the east. The area with this constant head assignment extends the thickness of the Fox Hills Formation (Fig. 4-8).

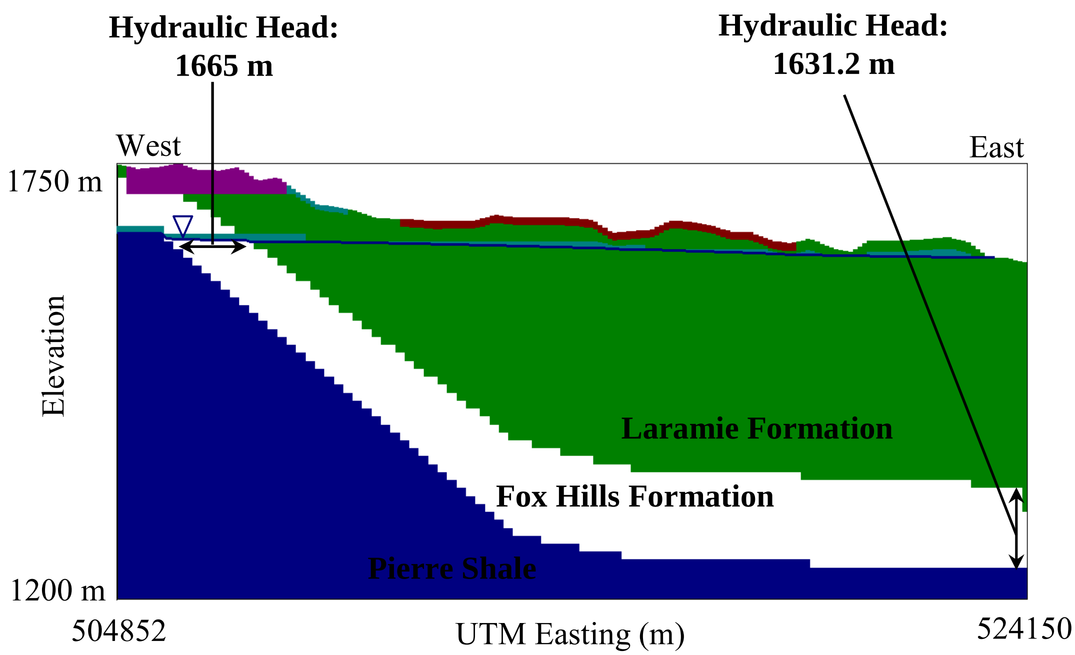

Figure 4-8. North constant head boundary assignment of the Fox Hills Formation with an east-west gradient of 0.001. Hydraulic head decreases linearly toward the east boundary. Vertical exaggeration is 15x.

4.6.2 Alternative Model Results

Hydraulic head results are shown in plan view as well as in north-south and east-west cross section in Figure 4-9. Groundwater flow is depicted with arrows showing flow direction through the Laramie and Fox Hills Formations. Arrow magnitude depicts the relative magnitude of velocity of groundwater. The highest flow velocity calculated is 1.1 x 10^{-4} m/s. One east-west cross section (Fig. 4-9b) illustrates the decrease in dip of the Pierre Shale in the northern portion of the model domain, where flow on the east side is affected by the no-flow boundary. Because upward flow at the east boundary is an artifact of numerical modeling, observation wells within 2 kilometers of the east boundary were not included in calibration. Similarly, observation wells within 4 kilometers of the north boundary were not included in model calibration because of the forced north-bound flow (Fig. 4-9c) due to model boundary assignments.

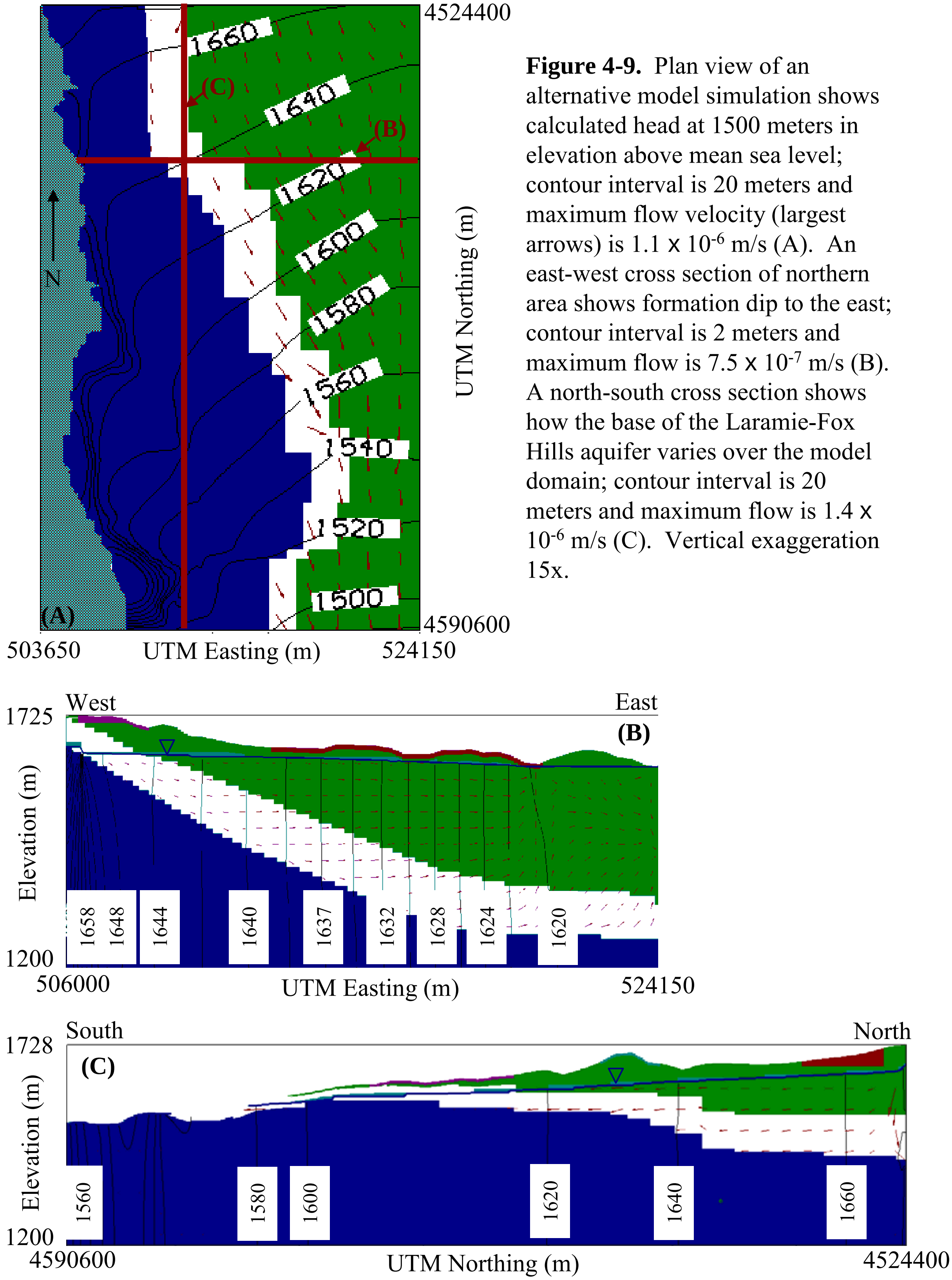

Figure 4-9. Plan view of an alternative model simulation shows calculated head at 1500 meters in elevation above mean sea level; contour interval is 20 meters and maximum flow velocity (largest arrows) is 1.1×10^{-6} m/s (A). An east-west cross section of northern area shows formation dip to the east; contour interval is 2 meters and maximum flow is 7.5×10^{-7} m/s (B). A north-south cross section shows how the base of the Laramie-Fox Hills aquifer varies over the model domain; contour interval is 20 meters and maximum flow is 1.4×10^{-6} m/s (C). Vertical exaggeration 15x.

Observed hydraulic head contours discussed earlier in this study (Fig. 2-5) are compared to the model output in Figure 4-10. The model results are plotted against available groundwater level data.

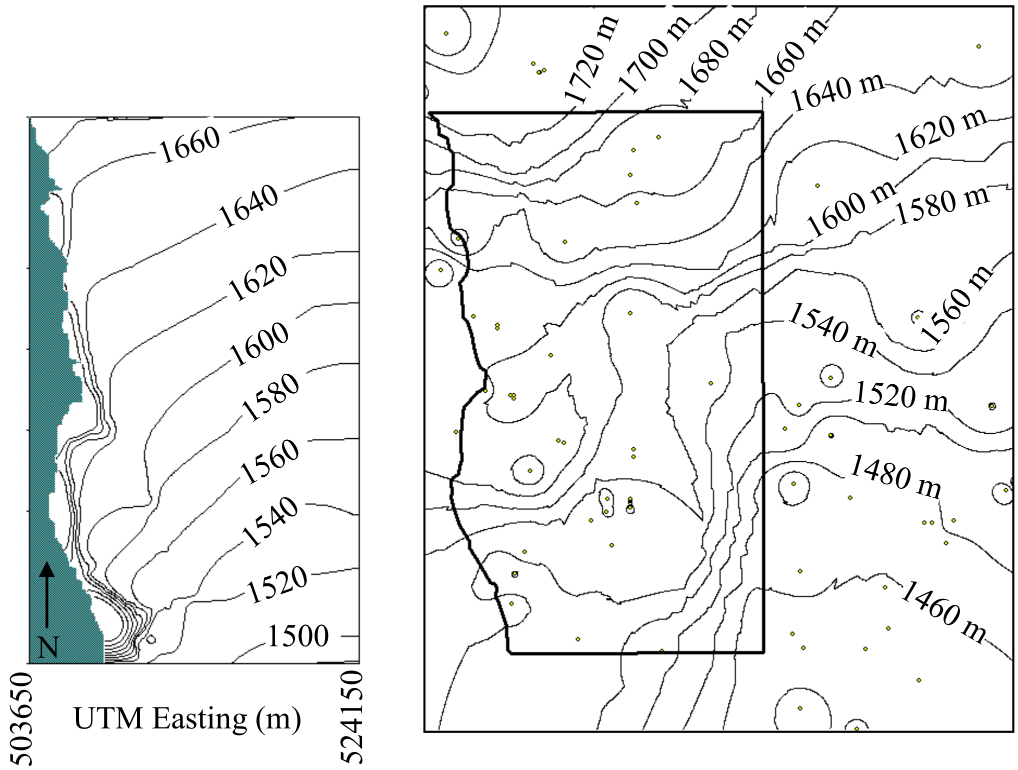

Figure 4-10. Comparison of an alternative model hydraulic head distribution (left) with Colorado Division of Water Resources well data for the Laramie-Fox Hills aquifer (right), as seen in Figure 2-5.

Similar to Chapter 4.5, model calibration results are discussed below. Figure 4-11 shows a plot of calculated versus observed head values compared to the 1:1 agreement reference line. The region bound by the upper and lower blue lines contains the area in which 95% of the plotted points are *expected* to occur given the statistical variability in water level data. The normalized root-mean-squared is 15.7% and the correlation coefficient is 0.87.

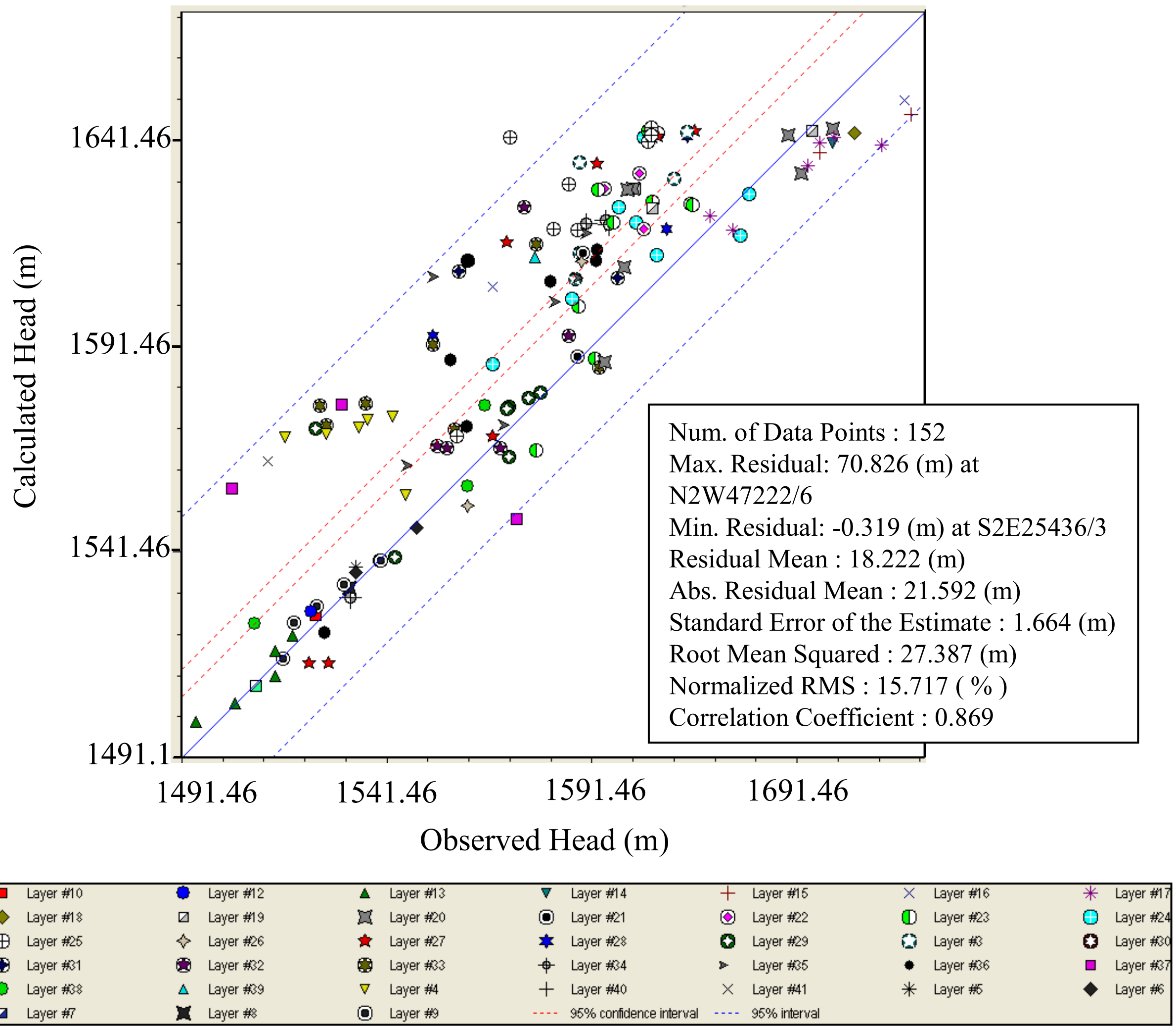

Figure 4-11. Alternative model plot of calculated versus observed head. Dotted blue lines denote the boundary within which 95% of the points are expected to occur. The red line denotes the confidence interval for the given dataset.

The results shown in Figures 4-12 and 4-13 show that boundary condition adjustments accounting for relatively low hydraulic head in the Fox Hills Formation compared to the Laramie Formation can have a significant impact on model calibration. Residuals were computed as the difference between the observed head and calculated head. The residual mean is 18.22 meters, signifying a significant overprediction of hydraulic head by the alternative model compared to the original model. Figure 4-12 shows more than 25% of the values fall within 6 meters of the observed value, but many calculated heads overpredict by 30 meters. Figure 4-13 shows a volumetric mass balance of flow similar to the original model where constant head and recharge are primary influxes of flow. However, recharge has less of an influence on the system in the alternative model. While the original model shows better calibration to observed water level data, the alternative model may be a more reasonable representation of the observed low hydraulic head values in the Fox Hills Formation specifically. Therefore it is important for future modeling to account for differences in hydraulic head between the Laramie Formation and the Fox Hills Formation.

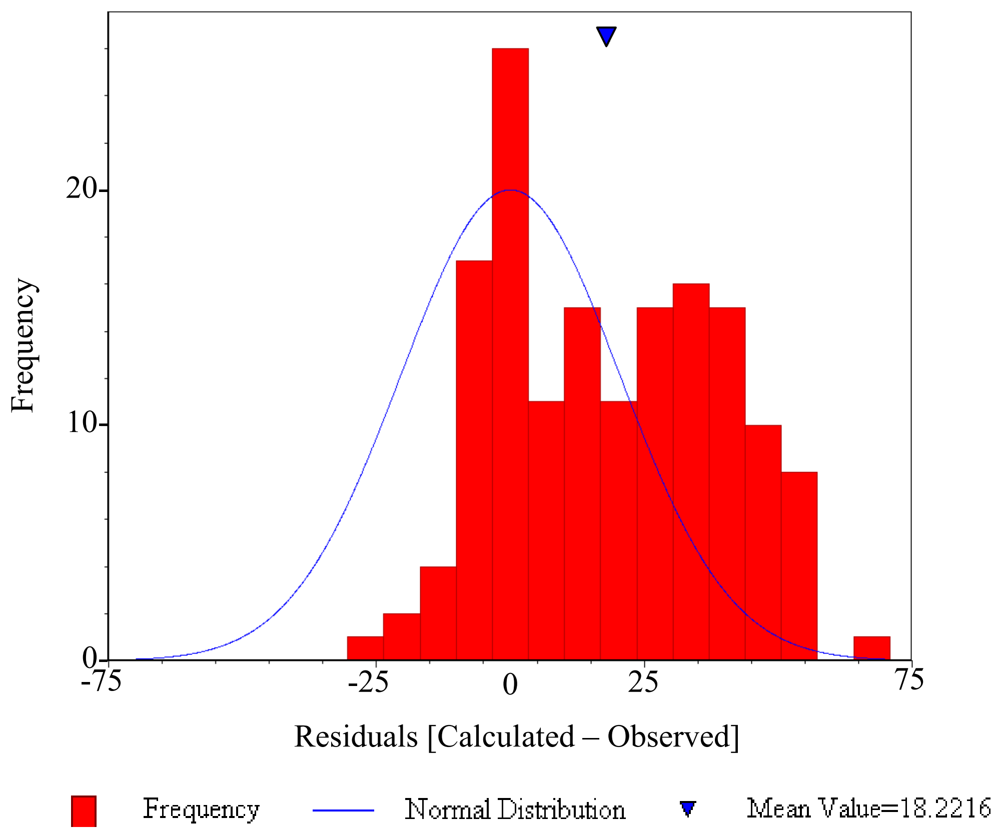

Figure 4-12. Alternative model calibration residual histogram showing a spike between zero and 5 meters of residual (calculated minus observed head).

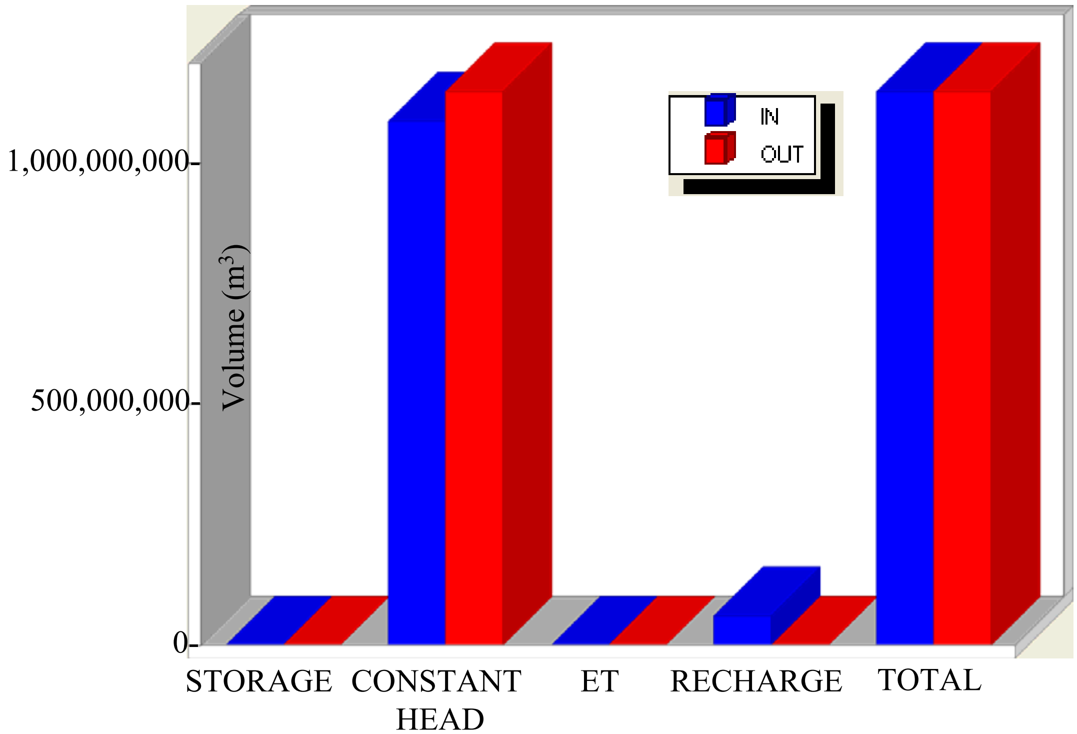

Figure 4-13. Mass balance bar chart of alternative model output. Boundary conditions (constant head at the north and south boundaries) account for the majority of volumetric flow through the Laramie-Fox Hills aquifer. Evapotranspiration (ET) is incorporated into the recharge value, which is minimal according to the model volumetric input. Storage is not used in steady state calculations.

4.7 Limitations

It should be noted that there are local variations in flow direction given strata orientation and variability between rock units of disparate hydraulic conductivity. The model does not account for the interfingering of shale, mudstone, coal, and sandstone within the larger formations other than through anisotropy in bulk hydraulic conductivity. Intermittent surface streams in the study area are not included in the model due to their seasonality and low flow. They are assumed to have a low impact on the deeper groundwater system.

Reported water levels in some wells may not accurately represent natural or background conditions. For example, the water level recorded by drillers may have been influenced if measurement immediately followed drilling of the well. In addition, nearby pumping from wells may lead to drawdown in the measured well causing an underestimation of natural water levels. This scenario is likely in areas of Nunn, Colorado (Fig. 1-2), where wells are densely clustered and water level measurements may not represent regional conditions. Therefore, model calibration based on these wells may not be reliable at local scales.

Because the majority of wells in the region are screened in the Fox Hills and Laramie Formations, the model results were biased to these zones. Therefore the true influence of the Pierre Shale on groundwater flow may not be fully captured in model results. While there are inherent limitations to the regional model presented in this chapter, general flow patterns were confirmed and dynamics between the Laramie and Fox Hills Formation were more fully understood. Given the lithologic composition of the Laramie Formation and observed water level data, hydraulic heads and hydraulic gradients within the formation are both higher than those of the Fox Hills Formation. Thus, in addition to general south-bound flow within the model, there is a small component of groundwater which flows vertically from the Laramie Formation downward into the Fox Hills Formation.

CHAPTER 5:
LOCAL SCALE MODEL OF IN-SITU RECOVERY

While regional groundwater flow modeling discussed in Chapter 4 lends an understanding of steady state regional groundwater flow, a smaller scale model is needed to simulate and predict groundwater flow around the mining zone. Visual MODFLOW (described in Chapter 4) was used along with MT3D (Zheng, 1990) to simulate generalized mining processes. MODFLOW was used to approximate drawdown during mining. MT3D was used to simulate a solute concentration distributions during in-situ recovery pumping conditions. When used together, a depiction of mining fluid transport during mining was produced for specific pumping and injection rates in generalized hydrogeologic conditions.

MT3D is a modular three-dimensional transport model used in this study for simulating advection and dispersion of a tracer with an assumed solute concentration. MT3D has the capability to also incorporate chemical reactions¸ but they were excluded from this study along with sorption reactions that may take place. The program solves for transient concentration of the simulated tracer injection fluid. The governing equation for contaminant transport is as follows:

$$\frac{\partial(\theta C^k)}{\partial t} = \frac{\partial}{\partial x_i}\left(\theta D_{ij}\frac{\partial C^k}{\partial x_j}\right) - \frac{\partial}{\partial x_i}\left(\theta v_i C^k\right) + q_s C_s^{\ k} + \sum R_n \qquad (5.1)$$

Where θ is porosity of the rock (dimensionless), C^k is the dissolved concentration of species k (mg/L^3), t is time (s), $x_{i,j}$ is distance (m), D_{ij} is the hydrodynamic dispersion coefficient tensor (m^2/s), v_i is the linear pore water velocity (m/s), q_s is the volumetric flow rate per unit volume of aquifer representing fluid sources (1/s), $C_s^{\,k}$ is the concentration of the source or sink flux for species k (mg/L^3), and ΣR_n is the chemical reaction term (mg/L^3·s). Porosity is the ratio of pore space to total volume, and effective porosity is the ratio of connected pore spaces to the total volume. An effective porosity of 0.15 was used in the model to calculate the area that is able to transmit a contaminant or tracer. Species *k* is the tracer species added at injection wells to simulate mining fluid injection.

The linkage between MT3D and MODFLOW is through groundwater average linear velocity which is used to calculate the advective part of the concentration term in Equation 5.1. The average linear velocity is defined as:

$$v_{i_i} = \frac{q_i}{\theta} \tag{5.2}$$

Where v_i is the average linear velocity (m/s), q_i is specific discharge (m/s), and θ is rock porosity (dimensionless). See Chapter 4 for the hydraulic head solution of the steady state, three-dimensional groundwater flow equation. The advection term, $\partial(\theta v_i C)/\partial x$, of the transport equation describes the transfer of contaminants at the same velocity as groundwater. Dispersion, D_{ij}, is the sum of mechanical dispersion and molecular diffusion. The spreading of contaminants by mechanical processes at a microscale and accounts for velocity deviations from average groundwater flow. Molecular diffusion is driven by concentration gradients. At the field scale, molecular diffusion is negligible compared to mechanical dispersion unless flow velocity is extremely low.

This study does not model aqueous geochemistry of in-situ recovery processes. This chapter focuses on groundwater dynamics in the Laramie Formation and the underlying Fox Hills Formation under generic mining conditions using tracer concentrations to infer the non-reactive transport of mining fluids. A local model of this area may provide insight to the impact of in-situ recovery on local groundwater in the northern area of the project site.

This chapter examines a local scale flow model of an area within the proposed mining zone (Fig. 5-1) during the in-situ recovery process. First, the model simulates natural conditions of one square mile of land in the northern project area. Pre-mining hydrogeologic conditions are based on information from regional flow modeling results as well as 11 wells in the area. Two 7-spot well configurations of pumping and injection wells (Fig. 5-1) are used to simulate in-situ recovery in the ore-bearing A_2 sandstone of the Upper Fox Hills Formation (proposed mining zone). Tracer addition at injection wells simulates mining fluid injection, and pumping at central extraction wells creates cones of depression needed to contain fluids in the mining zone. Ideally fluids are contained because groundwater flows from relatively high pressure zones at the injection wells to relatively low pressure zones at the pumping wells. Tracer (solute) transport is based on advection and dispersive processes in groundwater. Once steady state pumping conditions are reached the distribution of solute concentrations can be viewed to postulate a final distribution of mining fluids under circumstances where no geochemical processes are taking place. In this way a conservative approximation of mining fluid transport during in-situ recovery is simulated. The total pumping rate typically exceeds the total injection rate by 1-3% during in-situ recovery.

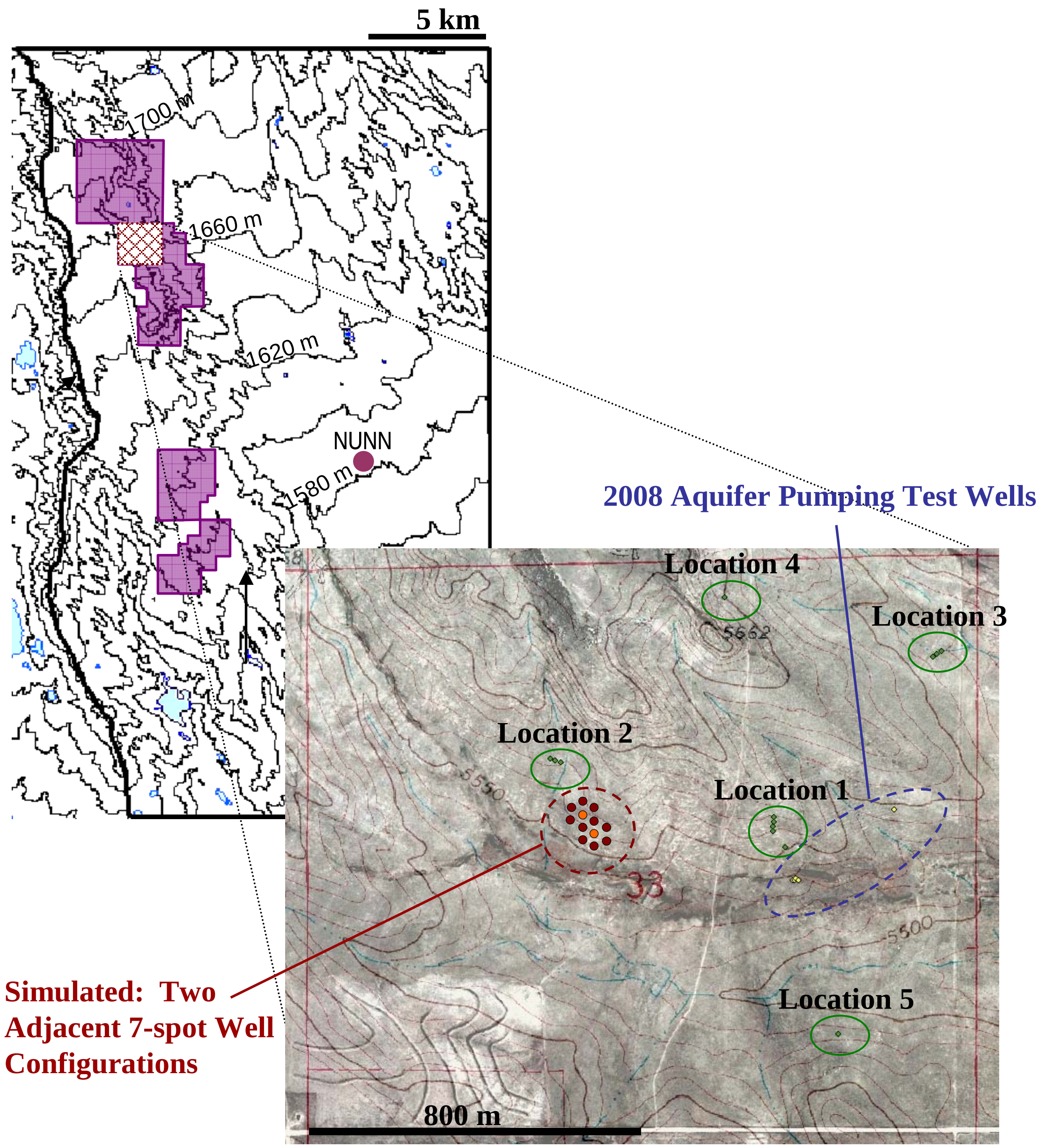

Figure 5-1. Local model domain within the regional study domain showing locations of Powertech wells. Proposed northern area of the Centennial Project is outlined in purple (Powertech, 2009) and local model extent shown in cross-hatch. Inset shows Section 33, Township 10N, Range 67W with topography and seasonal water features (U.S. Geological Survey, 1972). Well locations of a 2008 aquifer pumping test in the Fox Hills Formation are circled (yellow dashed line), and wells in Locations 1 through 5 are used to model local groundwater flow. Model location of central pumping wells (orange) and surrounding injection wells (red) are shown by two adjacent 7-spot well configurations.

Section 33, Township 10N, Range 67W was chosen for local scale modeling because lithologic logs, detailed well characterization, and monthly water level measurements taken over five months were available. Logs of self-potential, gamma and resistivity characterize the stratigraphic layers in the proposed mining zone (uranium host sandstone) as well as overlying and underlying sandstones in the Lower Laramie and Lower Fox Hills Formations. Geologic layering in the model is based on well logs submitted by Powertech to the Colorado Division of Reclamation Mining and Safety and are available at the agency website (*http://drmsweblink.state.co.us/drmsweblink/*) in Completion Issue Item #7 Attachment.

5.1 Site Characterization

Well information from 11 wells in the model area were used to characterize the boundary conditions and conductivity structure of the hydrogeological system. Detailed assignment of lithologic layers in the Laramie and Fox Hills Formation were determined from geophysical logs, with Location 1 bearing the most wells for characterization (wells IN08-33 MO1, IN08-33 MM1, IN08-33 PW1, IN08-33 MUU1). Layers are assigned horizontally and represent the upper sandstone of the Lower Fox Hills Formation, the Upper Fox Hills Formation, and the Laramie Formation toward the surface. Lithologies interpreted from the geophysical logs include sandstone, mudstone or shale, and coal. Coal seams separating the Laramie Formation from the Upper Fox Hills Formation were used as a stratigraphic marker for lithologic characterization of the area (Fig. 5-2). In total, information from 3 wells in the lowest sandstone of the Laramie Formation, 4 wells in the A_2 sandstone of the Upper Fox Hills Formation, 1 well in the WE sandstone, and 3 wells in the B sandstone of the Lower Fox Hills Formation were used for site characterization. Characterization of stratigraphy was accomplished by well log analysis to determine lithology and thickness of sedimentary layers (Fig. 5-2). Analysis was completed using principles discussed in Chapter 3.1.2. Regional gradients found in Chapter 4 were used along with hydraulic head gradients in the north-south and east-west directions calculated between local wells to simulate pre-mining hydraulic head distribution.

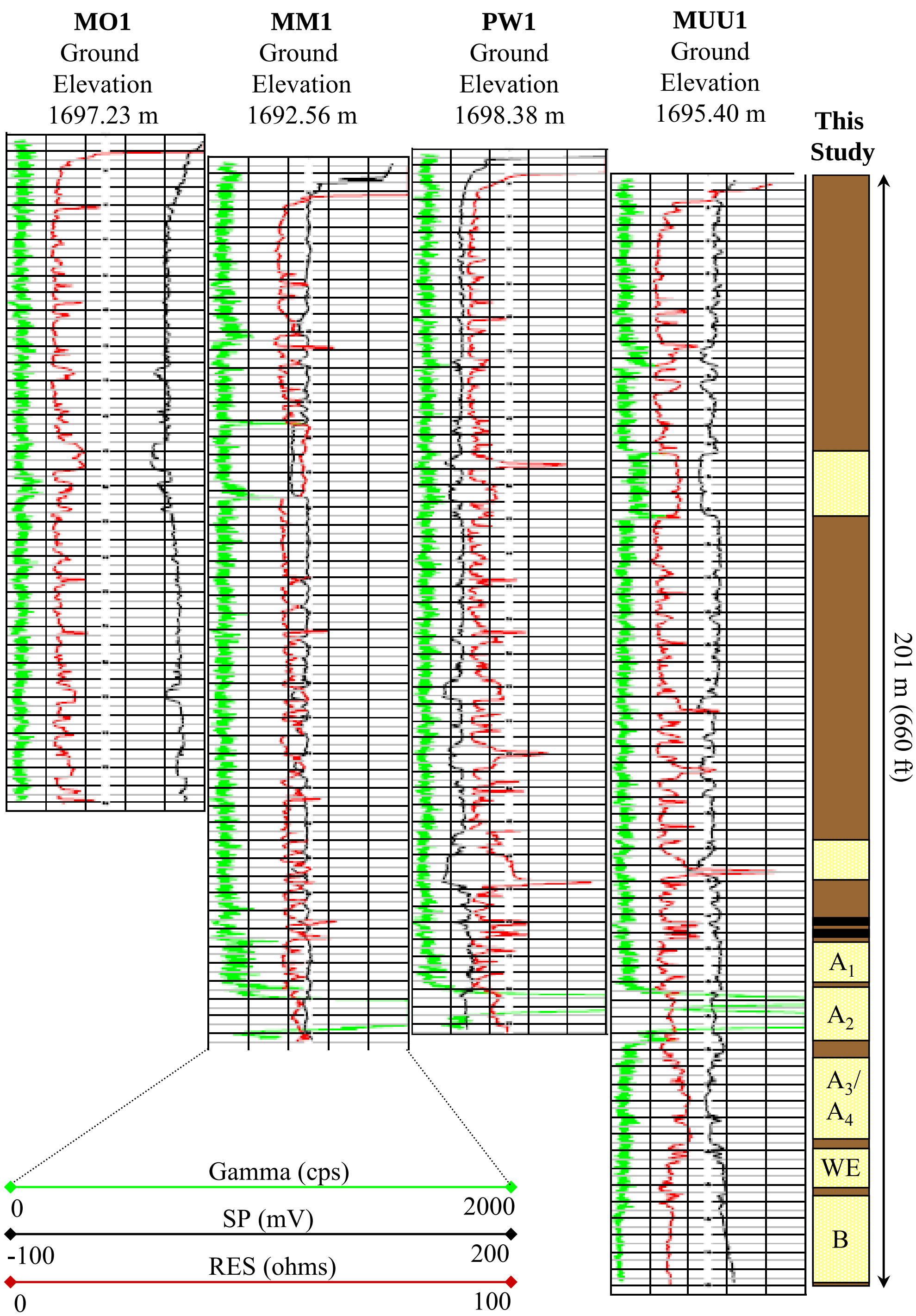

Figure 5-2. Lithologic interpretation of geophysical logs for Location 1 wells (interpretation shown on right). Coal seams above the A_1 sandstone are used as a stratigraphic marker for geophysical logs. The Upper Fox Hills Formation consists of A_1, A_2, A_3, A_4, and WE Sandstones.

Water levels (hydraulic head) were reported between August and November 2009 (Table 5-1). Location coordinate conversions to North American Datum 1983 and ground surface elevation into meters are shown in Table 5-2 along with computed mean values for water level in each well. Water levels vary minimally between measurements at each well. Variation does not exceed 1.1 meters over the 4 month period. Given tight well spacing, water level differences between wells in the same formation is small. Therefore, calculation of water level changes across the model domain in any particular sandstone is sensitive to reported water level data. While this may be the case, simulated groundwater flow trends based on this water level data agree with regional trends discussed in Chapters 2 and 4.

Well ID	**As Built Easting (NAD 27 CO, NT, ft)**	**As Built Northing (NAD 27 CO, NT, ft)**	**As Built Elevation of TOC (ft)**	**As Built Elevation of Ground Surface (ft)**	**Depth to Water Level from TOC (ft)-8/29/09**	**Depth to Water Level from TOC (ft)-9/17/09**	**Depth to Water Level from TOC (ft)-9/28/09**	**Depth to Water Level from TOC (ft)-10/22/09**	**Depth to Water Level from TOC (ft)-11/12/09**	**Depth to Bottom of Screen**	**Water Level (ft)**
IN08-33-MM1	2168510.670	531821.688	5554.86	5553.30	286.79	286.60	286.60	286.39	286.42	500.00	5268.3
IN08-33-MM2	2166640.996	532523.937	5574.40	5573.20	307.85	307.75	307.68	307.50	307.33	485.00	5266.8
IN08-33-MM3	2169754.080	533383.508	5533.90	5532.60	266.92	266.62	266.59	266.45	266.46	555.00	5267.3
IN08-33-MM4	2168026.071	533812.217	5613.96	5612.90	345.12	344.85	344.83	344.64	344.45	590.00	5269.2
IN08-33-MM5	2168932.132	530326.394	5517.14	5515.50	251.25	251.03	250.94	250.81	250.66	470.00	5266.2
IN08-33-MO1	2168417.487	532023.301	5569.97	5568.60	191.32	191.20	191.19	191.02	190.99	365.00	5378.8
IN08-33-MO2	2166679.637	532512.838	5574.36	5573.30	177.15	176.58	176.43	176.18	175.98	340.00	5397.9
IN08-33-MO3	2169716.190	533362.118	5535.89	5534.30	100.80	100.63	107.41	107.29	107.29	265.00	5431.2
IN08-33-MU1	2168415.697	531984.852	5566.11	5565.00	292.23	292.07	292.06	291.85	291.85	597.50	5274.1
IN08-33-MUU1	2168413.498	531947.023	5563.76	5562.60	267.50	266.33	266.33	266.13	266.12	635.00	5297.3
IN08-33-MUU2	2166729.117	532498.209	5573.97	5572.60	271.23	270.42	270.33	269.34	268.98	600.00	5303.9
IN08-33-MUU3	2169684.680	533337.038	5537.34	5536.00	240.25	239.53	239.44	239.19	239.20	657.50	5297.8
IN08-33-PW1	2168420.256	532060.300	5573.34	5572.40	302.84	304.55	304.55	304.42	304.43	525.00	5269.2

Table 5-1. Powertech data for water level in wells in study area over a 4 month period.

Well Name	Sandstone	Easting (NAD 83)	Northing (NAD 83)	Elevation of Ground Surface (m)	Depth to Screen Bottom (m)	Hydraulic Head (m)
IN08-33-MM1	A_2	509108.86	4515634.5	1692.56	152.39256	1605.6995
IN08-33-MM2	A_2	508540.42	4515851.7	1698.63	147.82079	1605.2356
IN08-33-MM3	A_2	509490.37	4516108.2	1686.25	169.15575	1605.3923
IN08-33-MM4	A_2	508964.62	4516241.8	1710.73	179.82322	1605.9683
IN08-33-MM5	A_2	509234.7	4515178.2	1681.04	143.24901	1605.06
IN08-33-MO1	Laramie	509080.81	4515696.1	1697.23	111.24657	1639.3862
IN08-33-MO2	Laramie	508552.17	4515848.2	1698.66	103.62694	1645.1984
IN08-33-MO3	Laramie	509478.79	4516101.8	1686.77	80.768059	1655.3508
IN08-33-MU1	WE	509080.2	4515684.4	1696.13	182.10911	1607.4666
IN08-33-MUU1	B	509079.46	4515672.8	1695.40	193.53856	1614.5315
IN08-33-MUU2	B	508567.22	4515843.7	1698.45	182.87108	1616.5529
IN08-33-MUU3	B	509469.14	4516094.2	1687.29	200.39622	1614.6961
IN08-33-PW1	A_2	509081.72	4515707.3	1698.38	160.01219	1605.9683

Table 5-2. Mean water level data including sandstone, UTM coordinate system in North American Datum 1983, and elevation in meters.

Hydraulic head gradients are computed by the change in water level over the change in lateral distance between two wells. Hydraulic head gradients in the north-south and east-west directions used in modeling are average gradients between wells hosted in their respective sandstones. Hydraulic gradients are small, between 0.001 and 0.04 as seen in the regional model. All gradients exhibit a decrease in hydraulic head either to the south or to the east, in agreement with regional flow patterns. Average gradients for each formation are shown in Table 5-3.

Sandstone	North-South Hydraulic Head Gradient	East-West Hydraulic Head Gradient
Lowest Sandstone of Laramie Formation	0.04	0.011
A_2 Sandstone of Upper Fox Hills Formation	0.001	0.001
WE Sandstone of Upper Fox Hills Formation	0.006 (assumed to be the same as B Sandstone)	0.003 (assumed to be the same as B Sandstone)
B Sandstone of Lower Fox Hills Formation	0.006	0.003

Table 5-3. Hydraulic head gradients for sandstones in (A_2) and overlying (Lowest Sandstone of Laramie Formation) and underlying (WE, B) the mining zone.

In addition to lateral flow gradients, the relationship between layers can be understood by plotting a vertical head profile of water level data of the wells. A vertical head profile shows hydraulic head data against well screen depth (Fig. 5-3). These wells are used as hydraulic head constraints in the local model. At all 5 locations, the A_2 Sandstone hydraulic heads are 10 meters to 35 meters lower than that of the overlying and underlying units. The large disparity between hydraulic heads suggests extremely limited vertical connectivity between the sandstones. Low permeability layers between these sandstones likely act as confining units. While flow may be limited, flow direction is important to characterize when considering long term flow following in-situ recovery. Flow direction is governed by the direction of decreasing hydraulic head. The A_2 sandstone exhibits relatively low hydraulic head compared to adjacent units, especially in comparison to the Laramie Formation sandstone. Therefore, the vertical direction of flow is into the A_2 sandstone from the Laramie Formation above and from the Lower Fox Hills Formation below. The natural hydrologic conditions, which are consistent at all 5 locations in the study area, help to constrain vertical flow in the ore zone from leaking into overlying and underlying units.

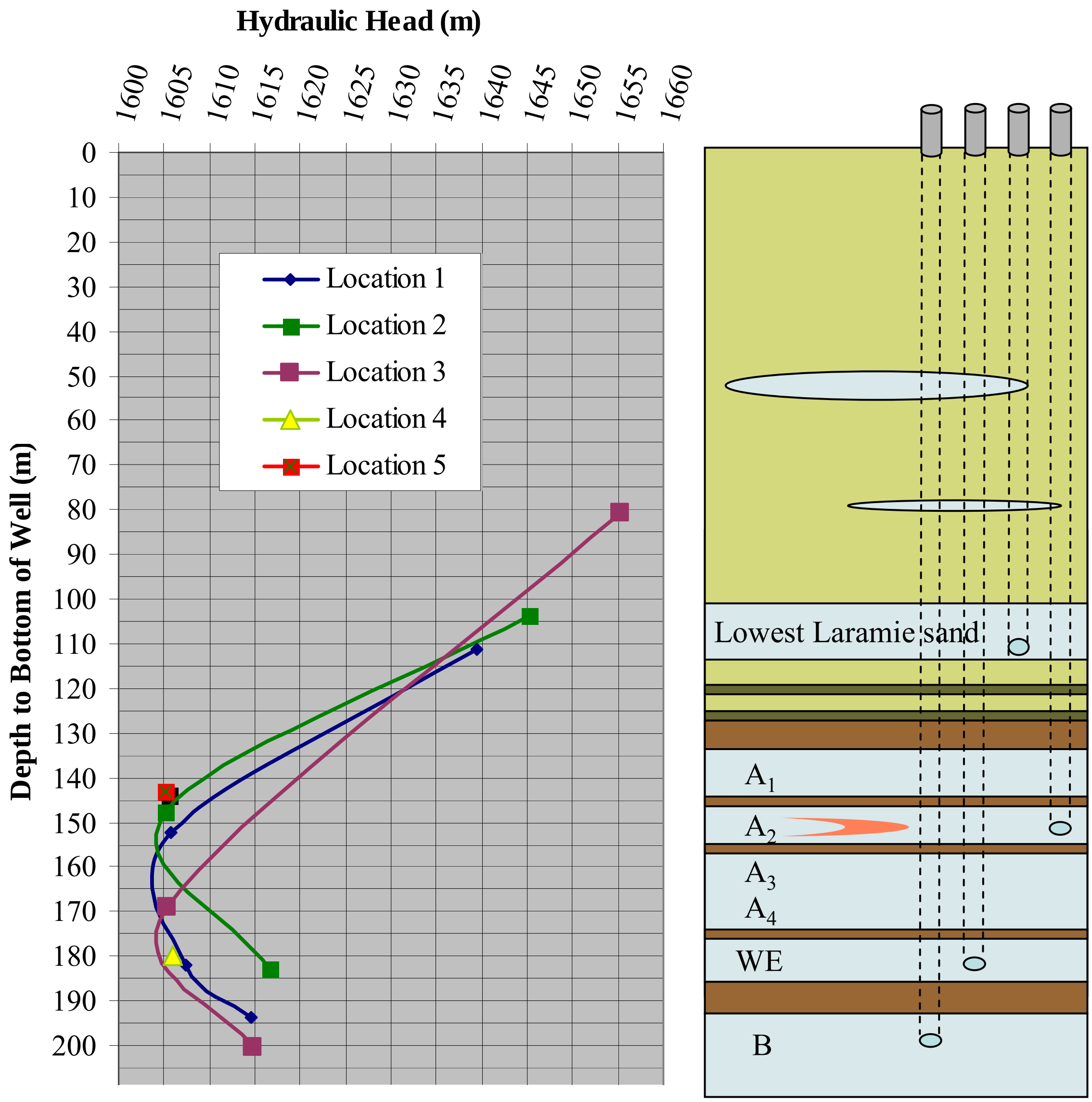

Figure 5-3. Vertical head profile of 11 wells in Section 33, T 10N, R 67W at 5 locations (Fig. 5-1). Host sandstones corresponding to Location 1 wells are shown to the right of profile.

In addition to vertical change in hydraulic head, Figure 5-3 shows relative horizontal gradients within each sandstone unit. Among the wells in the lowest sandstone of the Laramie Formation, hydraulic head ranges between 1639.38 meters and 1655.35 meters, a large range relative to the A_2 sandstone that varies between 1605.06 meters and 1605.96 meters. The B sandstone hydraulic head ranges from 1614.69 meters to 1614.53 meters. Generally, a greater difference between hydraulic heads in the same unit suggests that hydraulic conductivity is relatively low. In highly conductive units, hydraulic head gradients approach zero at local scales as groundwater levels equilibrate. Given a smaller total difference between observed water levels in the A_2 Sandstone, which hosts uranium ore (Voss and Gorski, 2007), it likely exhibits higher hydraulic conductivity than neighboring units.

5.2 Model Design

The local model is in the proposed northern project area (Fig. 5-1). It represents 1610 m x 1610 m in surface area (approximately one square mile) and is modeled to a depth of approximately 250 meters (~760 feet). The highest land surface elevation is 1730 meters, and the model extends down to an elevation 1470 meters above mean sea level. Elevation was imported from the U.S. Geological Survey Seamless website (2010). Cell size is approximately 10 m x 10 m x 5 m, but cell thickness decreases to 1 meter near the surface as MODFLOW adjusts for variable elevation. The model includes 161 rows, 161 columns, and 46 vertical layers. In addition, the model is refined in the areas directly surrounding pumping and injection wells, where cell dimensions are 5 m x 5 m x 2.5 m.

Regional hydraulic head gradients were used with local controls to simulate hydrogeologic conditions of the local model. Constant heads were assigned with linear gradients across the north, south, east and west boundaries according to observed hydraulic head gradients in each sandstone unit discussed in the last section. See Figure 5-4 for hydrogeologic structure of layers in cross section view. Hydraulic conductivity anisotropy was equal to the regional model ($K_{x,y}$:K_z is 3:1). In both models, the major component of flow is south-trending.

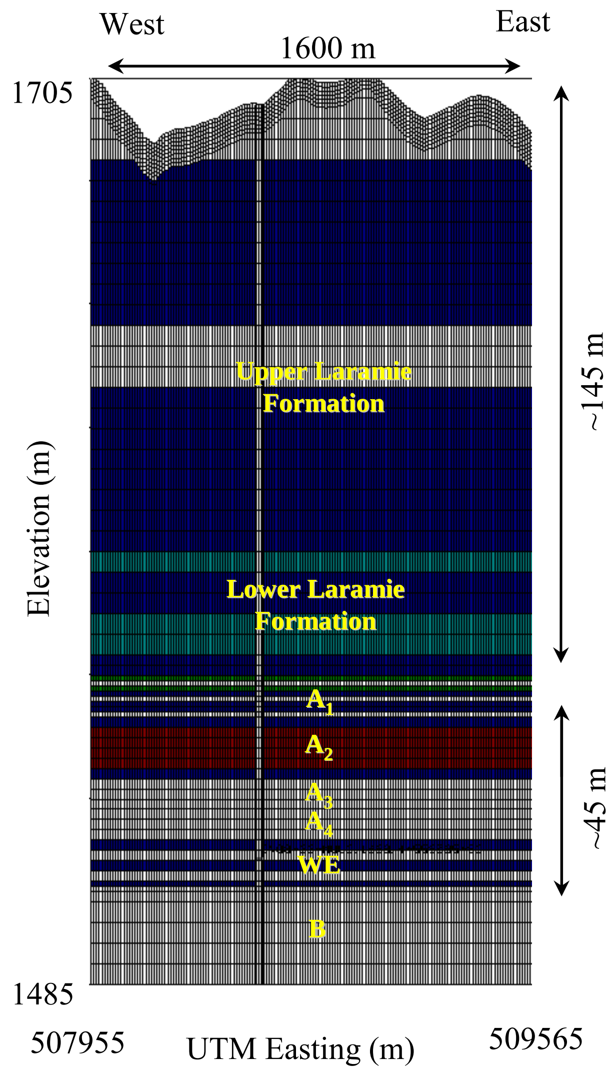

Figure 5-4. Cross section of local model showing lithological interpretation in the vertical column. Mudstones (blue), sandstones (white), coals (green), Lower Laramie Formation sandstones (teal), and the A_2 Sandstone (red) are assigned horizontally. Vertical exaggeration is 15x.

Constant head boundaries and hydraulic conductivity assignments used in modeling of each layer are shown in Figure 5-5. Boundary conditions for the Fox Hills Formation (A_1, A_2, A_3, A_4, WE, B Sandstones) and the Lower Laramie Formation were assigned based on water level data in the study area and gradients observed in regional modeling. Constant head boundaries for the Upper Laramie Formation were assigned approximately from regional modeling results (Chapter 4). The uppermost layers in the model were not assigned north and south constant head boundaries since water levels would have been below the model cell elevation. Instead, recharge (Chapter 4) of 12 mm/yr was used in the local model. This value is similar to the Arnold (2010) range of 5 mm/yr to 15 mm/yr. Recharge to the topmost layer provided an upper-boundary flux so that hydraulic head could be computed for the upper layers (in the zone where a constant head boundary was not applicable).

Values for hydraulic conductivity of various sedimentary layers were assigned based on single-well test data in the Lower Laramie Formation, the aquifer pumping test in the A_2 Sandstone (performed by Powertech), and literature values discussed in Chapter 3 used in regional modeling. Anisotropy was assumed to be the same as the regional model, where $K_{x,y}$:K_z was equal to 3:1. The hydraulic conductivity of coal layers in the Northern Great Plains vary roughly between 10^{-4} m/s and 10^{-8} m/s (Rehm, 1980). A high (conservative) value of 3.0×10^{-4} m/s for hydraulic conductivity was chosen for this study. Coal layers in the region are relatively thin (~2.5 meters to 5 meters) and are used primarily as stratigraphic markers in this study. High values used for hydraulic conductivity for these layers allowed for an increased estimate of groundwater flow, in both lateral and vertical directions, through the layers. Regardless of hydraulic conductivity for the coal layers, groundwater flow is likely to be most influenced by low-permeability shales that bound conductive coal seams.

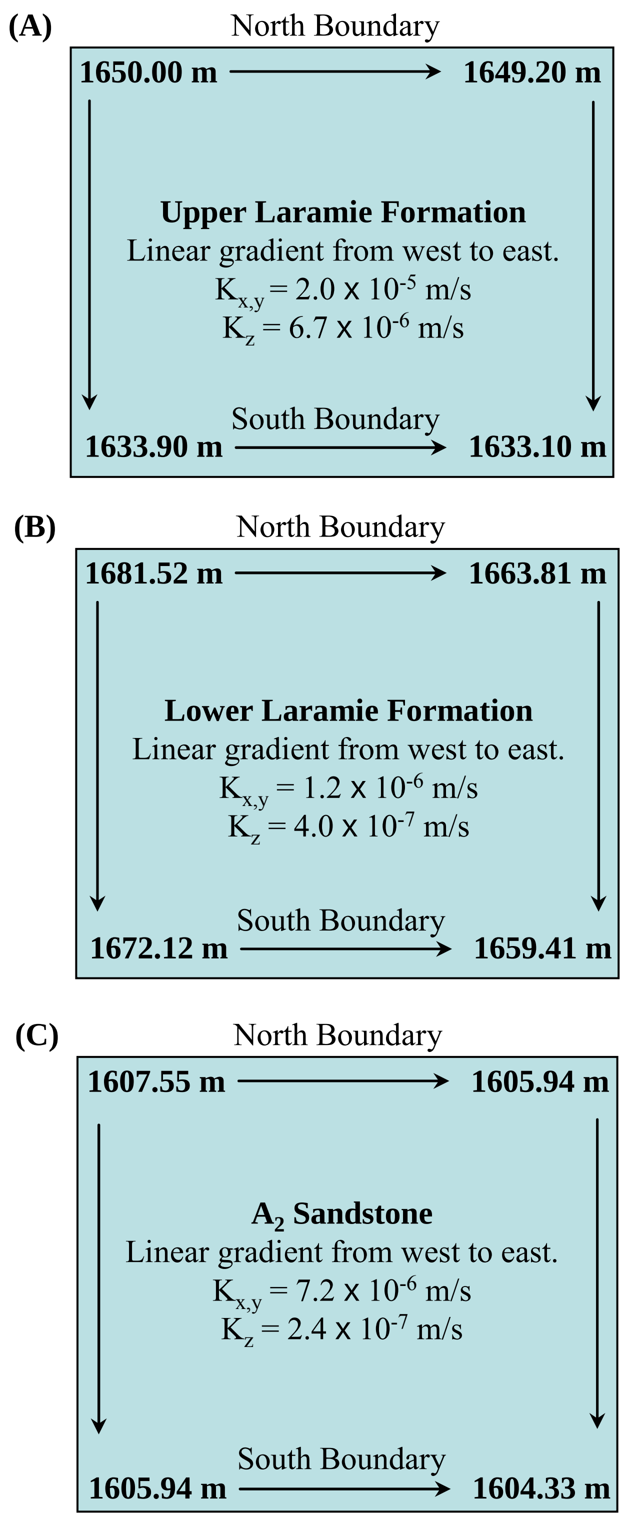

(Continued next page)

(D)

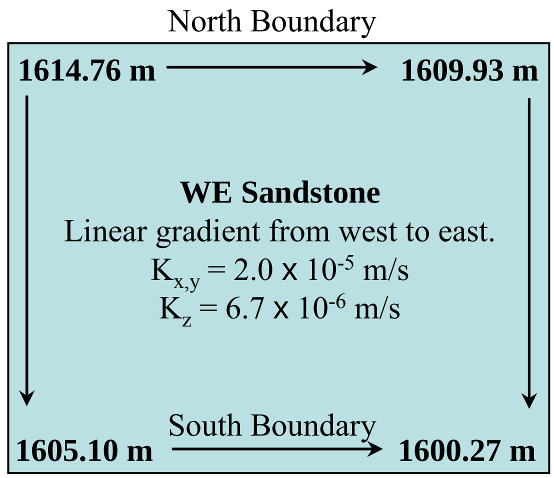

(E)

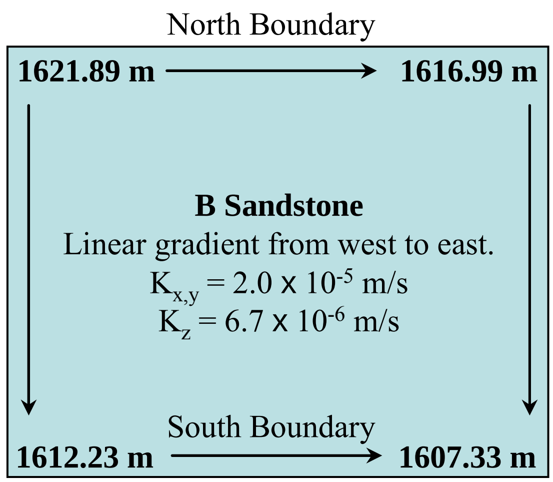

Figure 5-5. Plan view of constant head boundary conditions and hydraulic conductivity used in local model: The Upper Laramie Formation (A), Lower Laramie Formation (B), Upper Fox Hills Formations including the A_2 Sandstone (C) and the WE Sandstone (D), and the Lower Fox Hills Formation B Sandstone (E).

The purpose of the local model is to understand drawdown effects from mining, tracer transport during mining, and flow direction in areas in and surrounding the mining zone. Once natural flow regimes were established through steady state simulation, a pumping regime was imposed on the system. Drawdown was computed by steady state flow solutions. Once well field drawdown was modeled, steady state pumping conditions were simulated in conjunction with a transient tracer simulation. MODFLOW solved for steady state flow and MT3D solved for transient tracer concentration under generic pumping systems.

In the hypothetical scenario presented in this local model, six injection wells surrounded one central pump well and were separated from each other by 30 meters (approximately 100 feet). Two adjacent pump systems were screened in the A_2 sandstone, making 12 wells in total (Fig. 5-1). Injection simulation included a tracer concentration of 200 mg/L at a flow rate of 54.51 m^3/d (10 gpm).

Central pumping wells flowed at a rate of 275.22 m^3/d. Total pumping rate exceeded total injection rate by 1% in order to maintain a cone of depression around the central pump well. Typically, pumping exceeds injection by 1-3%. By sustaining a low-pressure zone around the pump well, local groundwater was forced to flow inward toward the pump well rather than outward. Effects of in-situ recovery on drawdown and tracer transport are shown for steady state pumping and injection.

5.3 Model Results

Based on physical flow parameters set forth in this study, mining solutions are unlikely to 1) be transported through low-permeability shale units that bound the mining zone or 2) travel laterally within the A_2 Sandstone to a distance outside of the proposed mining zone boundary. Figure 5-6 through 5-9 represent natural flow conditions and advective and dispersive transport of mining fluids during mining. Figure 5-6 shows model results for hydraulic head in the Lower Laramie Formation sandstone, A_2 Sandstone, and B Sandstone (Lower Fox Hills Formation) under natural conditions. Hydraulic connection between sandstones is limited given that large hydraulic head differences between layers are maintained. The model achieved a correlation coefficient of 0.96 between modeled and observed hydraulic head.

Figure 5-7 shows model results for steady state injection and pumping in the 7-spot well configuration. Pumping and injection wells are screened in the A_2 Sandstone. The effects of drawdown caused by pumping is limited to a small area surrounding the well field. Decreased hydraulic head occuring at the central pumping wells are called cones of depression. They extend radially from the pumping well and are seen at the two pumping wells in the A_2 Sandstone under the steady state pumping regime. Drawdown radially extends ~80 meters around the imposed well field in the model.

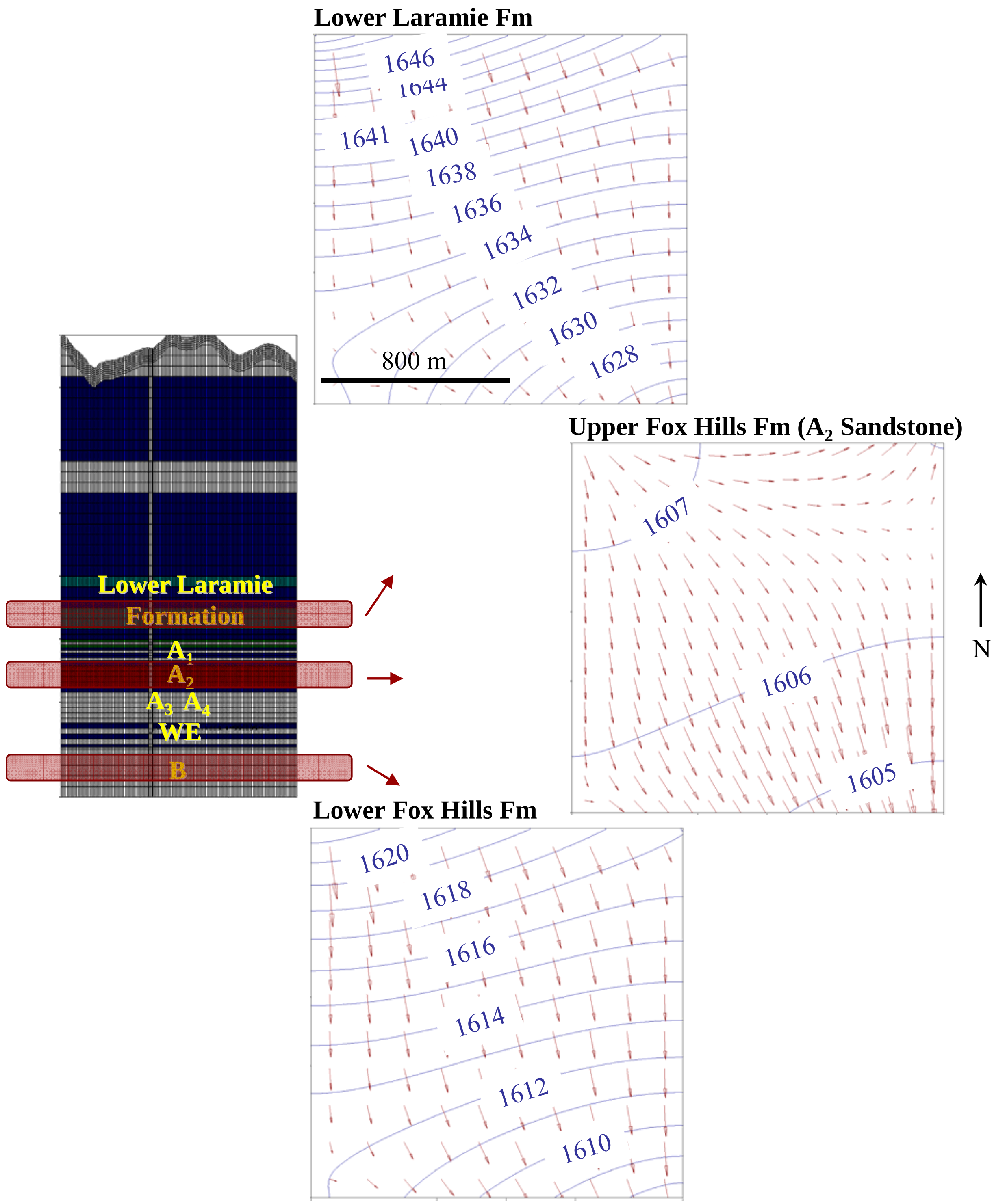

Figure 5-6. Local model simulation of hydraulic head in the Lower Laramie Formation sandstone, A_2 Sandstone, and B Sandstone under natural conditions. Contour interval is 1 meter. Horizontal lines in cross section view represent lithologic layering of sandstones, shale, and coal.

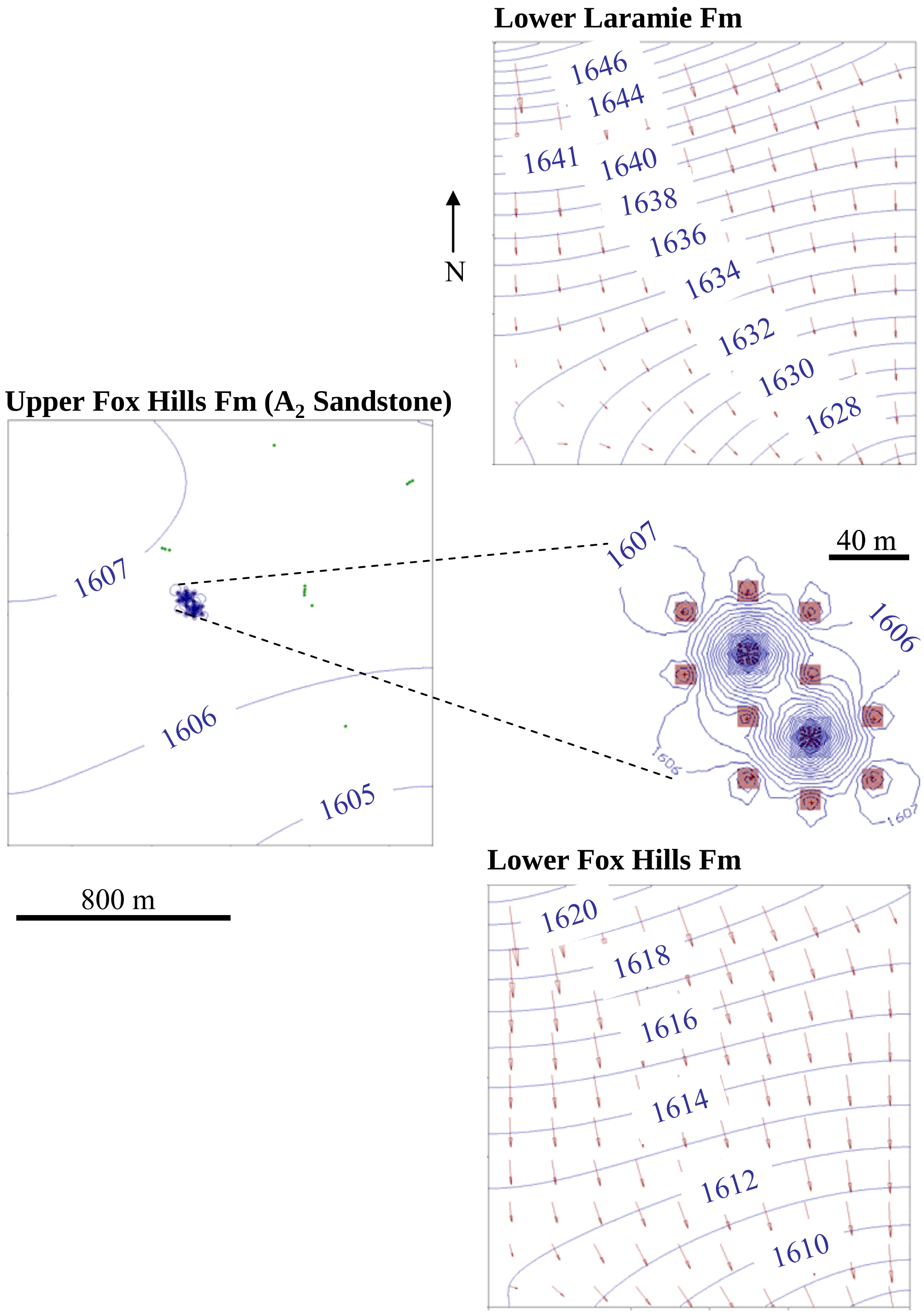

Figure 5-7. Influence of drawdown induced by steady state pumping shown in plan view. Hydraulic head in the Lower Laramie Formation, the A_2 Sandstone (with a zoom-in on contours near the well field), and B Sandstone are shown. Hydraulic head contour interval is 1 meter.

Model results for advection and dispersion of tracer concentration injected into the A_2 Sandstone showed a limited area affected by the injection (Fig 5-8). This is due to the cone of depression seen in Figure 5-7 that draws flow toward the pumping wells. Because of the low hydraulic head gradient in the sandstones, high pumping rates may not be necessary to contain flow. Plan view results for tracer concentrations in overlying and underlying units are not shown because no effect was observed. Similarly, Figure 5-9 shows a north-south cross section during pumping. Solute concentrations were confined by low-permeability shale units to the Upper Fox Hills Formation.

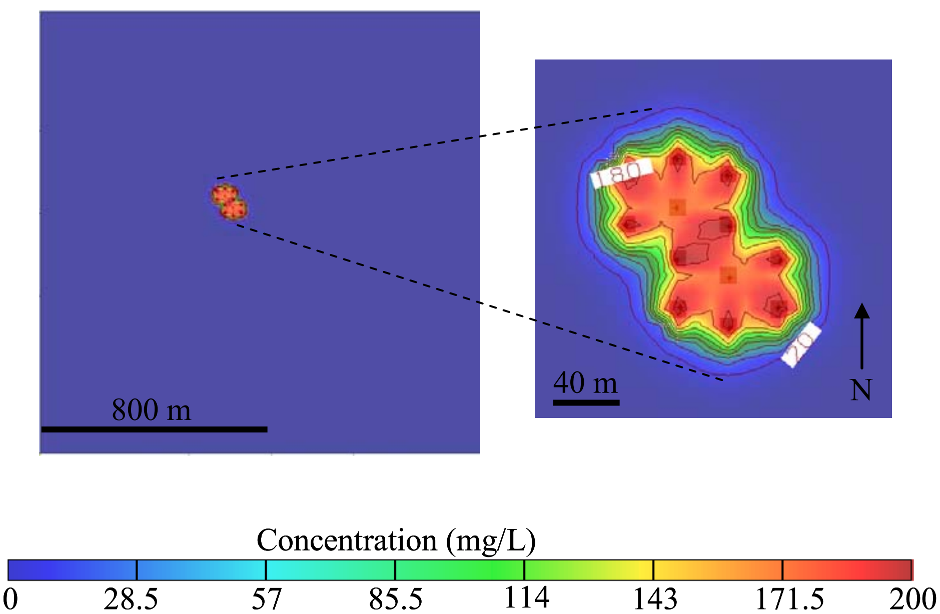

Figure 5-8. Model simulation of tracer distribution in A_2 Sandstone well field during steady state pumping conditions, shown in plan view.

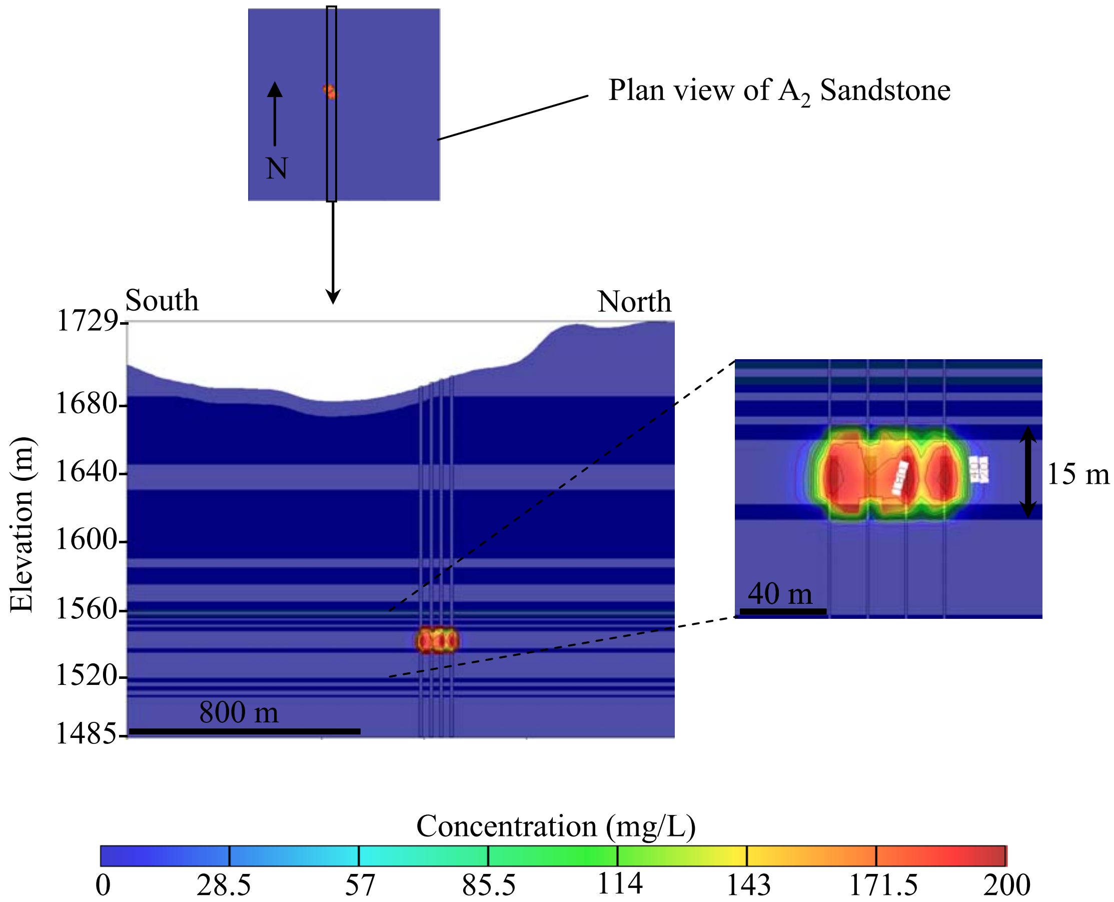

Figure 5-9. North-south cross section of model area showing tracer distribution at injection wells during steady state pumping conditions.

Based on these results, which are dependant on a suite of assumptions about mining practices discussed in the next section, physical groundwater conditions at the Centennial Project site limit the vertical and lateral transport of mining fluids associated with in-situ recovery. This is seen under the specified modeling conditions in this study where low-permeability shale layers bound the mining zone. As they have been interpreted from well logs, the shale layers help to not only restrict groundwater flow into neighboring aquifer zones, but also help to maintain relatively low hydraulic head observed in the Upper Fox Hills Formation.

5.4 Sensitivity Analysis

The extent of in-situ recovery effects on physical flow primarily depend on the vertical hydraulic conductivity of bounding shale units and the horizontal hydraulic conductivity of the mined sandstone. Sensitivity analyses were conducted to explore the model sensitivity to changes in these parameters. Vertical hydraulic conductivity was increased up to three orders of magnitude to simulate the possibility of vertical fractures and/or lateral discontinuities in shale layers. Hydraulic conductivity of the mined sandstone in the model was increased to explore the affect of hydraulic conductivity on the radial extent of mining-induced drawdown.

Results of the first sensitivity study are presented in vertical cross sections from south to north of the Lower Laramie Formation, the Upper Fox Hills Formation, and the Lower Fox Hills Formation (B Sandstone) with variable inputs for vertical hydraulic conductivity of shale units. For all simulations, horizontal hydraulic conductivity was equal to 1×10^{-8} m/s, a conservative value for shales. Hydraulic head contour lines show sharp bends at the contacts between different lithologic units (sandstones, shales, and coals). At some of these contacts, hydraulic head also changes drastically. This observation is in agreement with observed hydraulic head variation throughout the vertical column (Fig. 5-3).

The scenario with the best calibration was one in which vertical hydraulic conductivity (K_z) was equal to 1×10^{-10} m/s in shale units (Fig. 5-10). A correlation coefficient of 0.96 was achieved between calculated hydraulic head and hydraulic heads shown in Table 5-2. As vertical conductivity increased, the model calibration to observed values decreased. This result suggests that shale layers bounding the proposed mining zone significantly limit vertical groundwater flow within the study area of the local model.

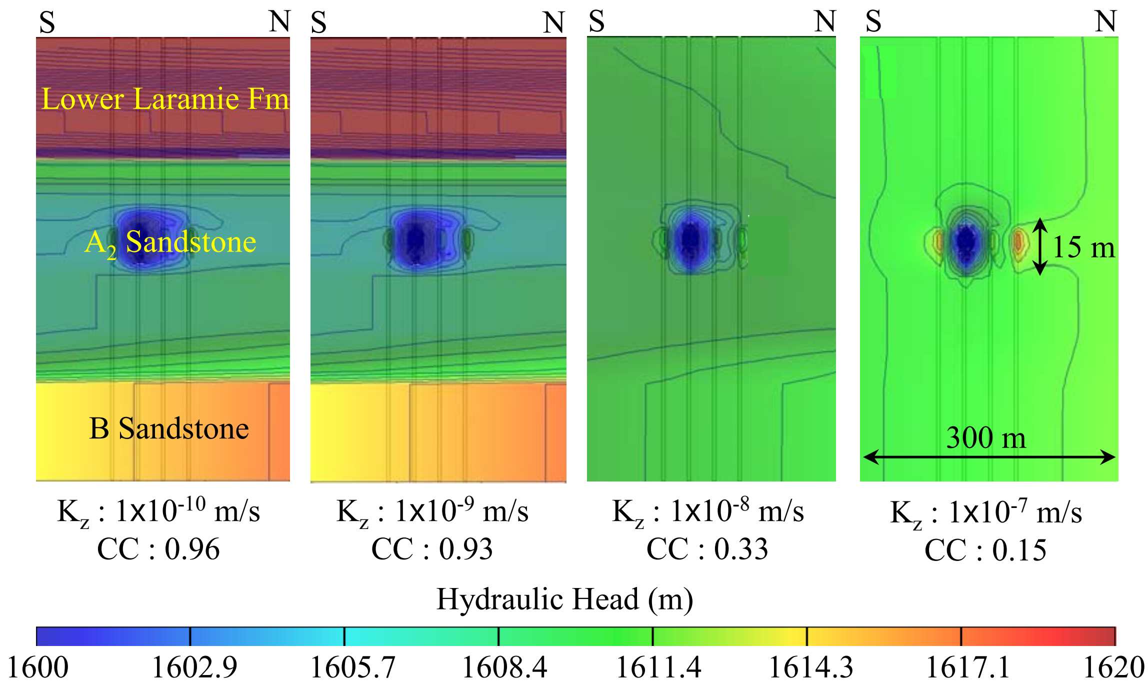

Figure 5-10. Vertical hydraulic head profiles under variable vertical hydraulic conductivity (K_z) scenarios during steady state pumping. Hydraulic head contour interval is 1 meter. Cross section is from south to north and includes the Lower Laramie Formation, the Upper Fox Hills Formation (A_1, A_2, A_3, A_4, WE Sandstones), and the Lower Fox Hills Formation (B Sandstone). Horizontal hydraulic conductivity for all simulations is 1 x 10^{-8} m/s. The correlation coefficient (CC) of the model hydraulic head to observed hydraulic head values is shown.

Hydraulic conductivity within the proposed mining zone was simulated for values higher than that which was observed from the aquifer pumping test conducted by Powertech in 2008. Their analysis yielded a hydraulic conductivity of 7.2 x 10^{-6} m/s (Chapter 3.2). Anisotropy from the regional model was applied in the local simulation, where vertical hydraulic conductivity was three times less than horizontal hydraulic conductivity. The radial extent of drawdown was approximately 80 meters. When hydraulic conductivity in the model was increased by one order of magnitude (10x), the radial extent of drawdown reached approximately 100 meters (Fig. 5-11). The slope of the cone of depression in the first case was more steep than that of the second.

In both simulations, the extent of impact on groundwater flow was limited to an area within the study domain.

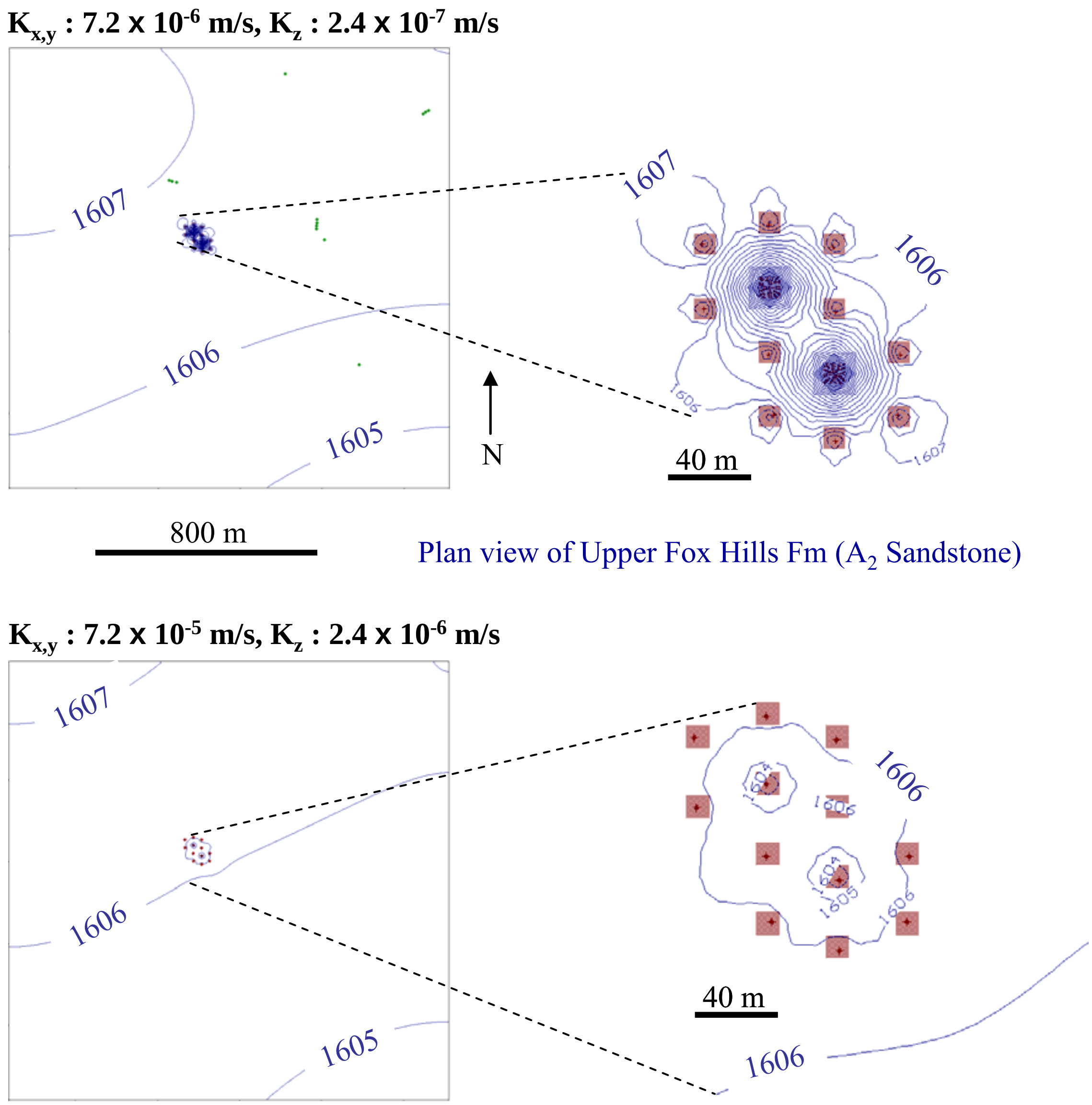

Figure 5-11. Plan view of the A_2 Sandstone under steady state pumping conditions with variable hydraulic conductivity. Anisotropy (3:1) is consistent between simulations. The slope of the induced cone of depression by is different between simulations. Hydraulic head contour interval is 1 meter.

5.5 Limitations

The local model presented in this chapter is limited in many ways. While it provides a conceptual understanding of flow in a local area, it should not be used as a method to determine the fate of uranium or even mining fluids in the system. This model seeks to represent the most likely aquifer conditions but, like regional modeling presented in Chapter 4, the solution is non-unique. Further adjustments of hydraulic conductivity and boundary conditions may yield slightly different results.

The addition of a tracer at injection wells to simulate advection and dispersion is limited to physical flow processes, excluding likely scenarios in which uranium reacts with groundwater or dissolved constituents. The model suggests that where mining fluids are injected, uranium will mobilize. This may not be the case if, for instance, uranium does not exist directly at the injection well. In fact, injection well placement is likely to be on either side of the uranium ore deposit. Furthermore, advection and dispersion are defined using typical relationships between horizontal and vertical transport, and therefore they are not specific to the Centennial Project aquifer conditions. Initial tracer concentration was chosen at a concentration high enough in order to be easily tracked over the time scale of the simulation, but does not represent a real world value (such as an actual concentration of chloride tracer).

Geologic dip was assumed to be minimal and therefore was not accounted for in the local model. Geologic formations were assigned horizontally, but as seen in the regional model, in fact they gently dip to the east (1.6 to 10 degrees). Laterally discontinuous sandstones and shales in the model area were not accounted for, as the model focus was on the hydrogeologic structure. Pumping and injection rates are based on reasonable estimation and do not represent rates suggested by Powertech.

Water level data was limited to a few wells in each sandstone. For instance, while the A_2 sandstone of the Upper Fox Hills Formation is hydrologically characterized by more than 5 wells, the WE sandstone of the same formation is only characterized by one. In addition, the calculated north-south and east-west hydraulic gradients between wells are sensitive to water level measurements. Sensitivity is the result of naturally low hydraulic gradients in the various sandstones, in which small changes in water level may have a great affect on the calculated gradient. The model is not calibrated against other wells in surrounding areas, resulting in great uncertainty in the forward modeling approach used in this study.

CHAPTER 6: SUMMARY AND CONCLUSIONS

Proposed in-situ recovery of uranium within the Laramie-Fox Hills aquifer has raised concern with privately owned wells located within the Laramie Formation and Fox Hills Formation. This study represents a first step in understanding the potential impact of in-situ recovery on groundwater by characterizing groundwater flow velocity and direction within and between major sedimentary formations. The lithology and dipping of the sedimentary units in the region are a result of the depositional environment of the primary geologic formations and Cretaceous Laramide Uplift, both of which modify the groundwater flow.

Newly constructed groundwater level maps presented in this study used available well data to show hydraulic head variability throughout the study domain. This variability likely results from diverse hydraulic properties of the Pierre Shale, the Fox Hills Formation, and the Laramie Formation. The composite water level map of the Laramie-Fox Hills aquifer shows that groundwater flows primarily south and trends east in the southern most portion of the study domain. Groundwater flow direction is roughly governed by topography in the area.

Slug and bail tests conducted in the low sandstones of the Laramie Formation yielded a hydraulic conductivity range between 3.2×10^{-7} m/s to 2.0×10^{-6} m/s. A multi-well aquifer pumping test conducted by Powertech in the Upper Fox Hills Formation (A_2 Sandstone) yielded a hydraulic conductivity of 7.2×10^{-6} m/s and may be representative of a larger area as compared to slug and bail tests. Uncertainties beyond the tested area could extend the hydraulic conductivity as much as one order of magnitude above or below these values. These field data were used to constrain hydraulic conductivity values used in regional and local modeling.

A numerical model for groundwater flow of the Laramie-Fox Hills aquifer in the northern Denver Basin was created. The model domain covered a land surface area of approximately 650 square kilometers. At this regional scale, groundwater flow within the model domain indicated that topography is the controlling parameter on groundwater flow direction. The southern most portion of the study domain was also influenced by the dipping of the Pierre Shale to the east. Groundwater flows south and slightly east at an estimated rate between 3.2×10^{-7} m/s and 2.5×10^{-5} m/s in conductive sandstone units. The agreement of calculated hydraulic heads with current water level data (1990-2010) was reasonable. The model achieved a correlation coefficient of 0.86, suggesting the model was reasonably representative of well data. This study used physically reasonable parameters that were constrained by field test data. The model yielded reasonable calibration results, lending confidence to the modeling results for hydraulic head and groundwater flow direction and velocity.

Groundwater modeling results in general are non-unique, therefore a model sensitivity study was conducted to gauge how model results change with different input parameters. Because the Laramie Formation includes more shale units than the Fox Hills Formation, higher hydraulic head gradients are expected within the Laramie Formation. Boundary conditions were adjusted to examine model sensitivity to lower gradients in the Fox Hills Formation. Model results for the given scenario yielded an overprediction of water levels overall, yet showed reasonable model calibration with a correlation coefficient of 0.87. Model overprediction may have been a result of an increase in groundwater usage over the time frame water level data was collected (1990-2010). The sensitivity analysis demonstrated that while the original model calibrated well, the differences in hydraulic head gradients between the Laramie and Fox Hills

Formation may be significant to modeling groundwater flow. The hydraulic head gradients represented in the current model may be the average of high gradients in the Laramie Formation and low gradients in the Fox Hills Formation.

The local scale groundwater flow model offered an illustration of a relatively well-characterized hydrogeologic system within the northern section of the proposed mining zone. Vertical hydraulic head profiles suggest that there are effective confining units separating the proposed mining zone (Upper Fox Hills Formation) from the overlying and underlying sandstones given large disparities in hydraulic head. Two adjacent 7-spot pumping and injection well configurations were used to examine water level drawdown in the area in response to long term pumping. Steady state pumping was simulated by pumping at a rate of 275.22 m^3/d at two central wells and injecting at a rate of 54.5 m^3/d (10 gpm) at ten surrounding wells. Given these rates, the total pumping rate exceeded the total injection rate by 1%. The purpose for the disparity between pumping and injection rates was to maintain a cone of depression around central extraction wells, as is typical during in-situ recovery operations. The cone of depression helps to force groundwater to flow toward low pressure zones at the pumping wells rather than traveling away from the well field. In this study drawdown effects were limited to a ~80 meter radius surrounding the well field within the A_2 Sandstone of the Upper Fox Hills Formation. Effects on the overlying Lower Laramie Formation and underlying Lower Fox Hills Formation were not observed.

MT3D, a three-dimensional advection and dispersion transport model, was used for simulating solute transport around the pumping and injection well field. Modeling results suggest that solute concentrations are generally confined to the proposed mining zone (A_2 Sandstone) by bounding low-permeability shale layers. Impacts of in-situ uranium mining on groundwater did not extend past the immediate vicinity of the well field under the imposed pumping and injection scenarios used in this study. However, caution should be exercised when interpreting these results given various model assumptions. The impact on groundwater flow in areas overlying, underlying and downgradient of the Upper Fox Hills Formation can be minimized given further understanding of the hydrogeologic conditions surrounding the site.

Although this modeling study did not account for assorted geochemical and microbiological reactions taking place in groundwater, and considered simplified lithology, it offers a conceptual understanding of local groundwater flow in the northern portion of the project area. By depicting groundwater flow conditions in the mining zone and surrounding units, flow modeling similar to the local scale model presented in this study can help define areas of potential transport of mining fluids during in-situ recovery.

REFERENCES

Abdelouas,A., Lutze, W., and Nuttall, H.E., 1998, Chemical reactions of uranium in groundwater at a mill tailings site, *Journal of Contaminant Hydrology*, 34: 343-361.

Allison, G.B., Gee, G.W., and Tyler, S.W., 1994, A review of vadose-zone techniques for estimating groundwater recharge in arid and semiarid regions, *Soil Science Society of America Journal*, 58: 63-72.

Anderson, R.T. and Lovely, D.R., 2002, Microbial redox interactions with uranium: an environmental perspective *in* Interactions of Microorganisms with Radionuclides, Ed. Keith-Roach, M.J. and Livens, F.R. Elsevier Science Ltd.

Arnold, Larry R., 2010, Hydrogeology and steady-state numerical simulation of groundwater flow in the Lost Creek designated ground water basin, Weld, Adam, and Arapahoe Counties, Colorado, *Scientific Investigations Report* 10-5082.

Babcock, H.M., *and* Bjorklund, L.J., 1956, Ground-water geology of parts of Laramie and Albany Counties, Wyoming, and Weld County, Colorado, *U.S. Geological Survey, Water-Supply Paper 1367*, 61 p., 1 plate.

Barkmann, P.E., 2004, Vertical hydraulic conductivity measurements in the Denver Basin, Colorado, *The Mountain Geologist*, 41(4): 169-183.

Braddock, W.A. and Cole, J.C., 1978, Preliminary geologic map of the Greeley 1º x 2º quadrangle, Colorado and Wyoming, *U.S. Geological Survey Open-File Report 78-532.*

Butler, J.J., 1998, The Design, Performance, and Analysis of Slug Tests, Lewis Publishers, Boca Raton, 252 p.

Chang, Y., Peacock, A.D., Long, P.E., Stephen, J.R., McKinley, J.P., Macnaughton, S.J., Anwar Hussain, A.K.M., Saxton, A.M. and White, D.C., 2001, Diversity and characterization of sulfate-reducing bacteria in groundwater at a uranium mill tailings site, *Applied and Environmental Microbiology,* 67(7): 3149-3160.

Charbeneau, R.J., 1984, Groundwater Contamination. Groundwater restoration with in situ uranium leach mining National Research Council, Washington, DC, 147-155 p.

Chirlin, G.R., 1989, A critique of the Hvorslev method for slug test analysis: the fully penetrating well, *GWMR*, 1-9 p.

Colorado Division of Reclamation Mining and Safety website, 2010, (*http://mining.state.co.us*), Accessed June 15, 2010.

Colorado Division of Water Resources, Office of the State Engineer website, 2010 *(http://www.dwr.state.co.us/WellPermitSearch/default.aspx)*, Accessed June 15, 2010.

Davis, J.A. and Curtis, G.P., 2006, Consideration of Geochemical Issues in Groundwater Restoration at Uranium In-Situ Leach Mining Facilities: *Report NUREG CR-6870, U. S. Nuclear Regulatory Commission*, Rockville, MD, 111 p.

Davis, J.A., 1969, Uranium deposits of the Powder River Basin, *Union Pacific Railroad Company*, Natural Resources Division, Laramie, Wyoming, 82070.

Ellis, D.V. and Singer, J.M., 2007, Well Logging for Earth Scientists, Second Edition, Springer, Dordrecht, Netherlands.

Ethridge, F.G. and others, 1979, The uranium-bearing Fox Hills and Laramie aquifers, Cheyenne Basin, Colorado: structure, depositional systems, and groundwater; Part I, and interim report: Colorado State University, Department of Earth Resources, 40 p.

Fetter, C.W., 1994, Applied Hydrogeology-Fourth Edition: Macmillan College Publishing, New York, New York, 598 p.

Figueroa, L.A., Honeyman, B.D., Ranville, J.F., 2006, Coupled microbial and chemical reactions in uranium bioremediation *in* Uranium in the Environment: Mining Impact and Consequences. Springer Berlin Heidelberg.

Finneran, K.T., Anderson, R.T., Nevin, K.P., and Lovely, D.R., 2002, Potential for bioremediation of uranium-contaminated aquifers with microbial U(VI) reduction, *Soil and Sediment Contamination*, 11(3):339-357.

Francis, A., 2006, Biotransformation of uranium complexed with organic ligands *in* Uranium in the Environment: Mining Impact and Consequences, Springer Berlin Heidelberg.

Freeze, R.A., and Cherry, J.A., 1979, Groundwater: Prentice Hall, Englewood Cliffs, New Jersey, 604 p.

Green, G.N., 1992, The digital geologic map of Colorado in ARC/INFO format. *U.S. Geological Survey Open-File Report 92-0507*, http://pubs.usgs.gov/of/1992/ofr-92-0507/, Accessed Sep. 13, 2010.

Gu, B., Yan, H., Zhou, P., Watson, D.B., 2005a, Natural humics impact uranium bioreduction and oxidation, *Environmental Science and Technology,* 39: 5268-5275.

Gu, B., Wu, W., Ginder-Vogel, M., Yan, H., Fields, M.W., Zhou, J., Fendore, S., Criddle, C.S., and Jardine, P.M., 2005b, Bioreduction of uranium in a contaminated soil column, *Environmental Science and Technology,* 39: 4841-4847.

Hall, S., 2009, Groundwater restoration at uranium in-situ recovery mines, South Texas coastal plain, *U.S. Geological Survey Open-File Report 2009-1143*, 36 p.

Hershey, L. A. and J. Paul A. Schneider, 1972, Geologic Map of the Cache la Poudre River Basin, North-central Colorado, *U.S. Geological Survey.*

HydroSOLVE, Inc., 1996, *AQTESOLV v.3.50*, Reston, Virginia, *www.aqtesolv.com.*

Hvorslev, M.J., 1951, Time lag and soil permeability in ground-water observations, Bull. No. 36, *Waterways Exper. Sta. Corps of Engrs, U.S. Army,* Vicksburg, Mississippi, 1-50 p.

Istok, J.D., Senko, J.M., Krumholz, L.R., Watson, D., Bogle, M.A., Peacock, A., Chang, Y.J., and White, D.C., 2004, In situ bioreduction of technitium and uranium in a nitrate-contaminated aquifer, *Environmental Science and Technology,* 38: 468-475.

Kirkham, R.M., O'Leary, W., and Warner, J.W., 1980, Hydrogeologic and stratigraphic data pertinent to uranium mining, Cheyenne Basin, Colorado, *Colorado Geological Survey, Department of Natural Resources, Information Series 12*, 31 p.

Liu, C., Zachara, J.M., Zhong, L., Kukkadupa, R., and Kennedy, D.W., 2005, Influence of sediment bioreduction and reoxidation of uranium sorption, *Environmental Science and Technology,* 39: 4125-4133.

McDonald, M.G. and Harbaugh, A.W., 1988, A modular three-dimensional finite-difference ground-water flow model, *Techniques of Water-Resources Investigations of the U.S. Geological Survey*, *06-A1.*

Min, M., Fang, C., and Fayek, M., 2005, Petrography and genetic history of coffinite and uraninite from the Liueryiqu granite-hosted uranium deposit, SE China, *Ore Geology Reviews*, 26: 187-197.

Papadopolus, S.S., Bredehoft, J.D., and Cooper, Jr., H.H., 1973, *Water Resources Research* 9: 1087-89.

Pollack, D.W., 1994, User's guide for MODPATH/MODPATH-PLOT, Version 3: A particle tracking post-processing package for MODFLOW, the U.S. Geological Survey finite-difference ground-water flow model, *U.S. Geological Survey Open-File Report 94-494.*

Powertech (USA), Inc., 2008, Powertech 2008 NOI, Attachment B to *Division of Reclamation, Mining, and Safety September 16, 2008,* http://drmsweblink.state.co.us/drmsweblink/.

Powertech (USA), Inc., 2009, *Response to Division of Reclamation, Mining, and Safety September 25, 2009, Letter*, http://drmsweblink.state.co.us/drmsweblink/.

Rehm, B.W., Groenewald, G.H., Morin, K.A., 1980, Hydraulic properties of coal and related materials, Northern Great Plains, *Ground Water*, 18(6): 551-561.

Robson, S.G., 1983, Hydraulic characteristics of the principal bedrock aquifers in the Denver Basin, Colorado, *U.S. Geological Survey Hydrologic Investigations Atlas, Report HA-0659.*

Robson, S.G. and Banta, E.R., 1987, Geology and hydrology of deep bedrock aquifers in eastern Colorado, *U.S. Geological Survey Water-Resources Investigations Report 85-4240.*

Robson, S.G. and Banta, E.R., 1995, Ground Water Atlas of the United States, Segment 2-Arizona, Colorado, New Mexico, Utah, *U.S. Geological Survey Hydrologic Investigations Atlas HA-730-C.*

Schlumberger Water Services, 2009, *Visual MODFLOW v.9.1*, Waterloo, Ontario, Canada, *www.swstechnology.com.*

Sherman, H., Lamm, R.D., Kiuper, C.J., 1978, Ground water resources of the bedrock aquifers of the Denver Basin, Colorado: A Summary. N. Resources, *Denver, State of Colorado Division of Water Resources***,** 28 p.

Spear, J.R., Figueroa, L.A., and Honeyman, B.D., 1999, Modeling the removal of uranium U(VI) from aqueous solutions in the presence of sulfate reducing bacteria, *Environmental Science and Technology*, 33: 2667-2675.

Spencer, F.D., 1986, Coal geology and coal, oil, and gas resources of the Erie and Frederick Quadrangles, Boulder and Weld Counties, Colorado, *U.S. Geological Survey Bulletin 1619,* Washington, DC, pp. 1-37.

Stevenson, F.J., 1982, Humus Chemistry: Genesis, Composition, Reactions. Wiley, New York.

Suzuki, Y., Kelly, S.D., Kemner, K.M., Banfield, J.F., 2002, Nanometre-size products of uranium bioreduction, *Nature,* 41.

Topper, R., Spray, K.L., Bellis, W.H., Hamilton, J.L., Barkmann, P.E., 2003, Ground Water Atlas of Colorado: Denver, Colorado, *Division of Natural Resources, Colorado Geological Survey, Division of Minerals and Geology*.

Toth, 1963, A theoretical analysis of groundwater flow in small drainage basins, *Journal of Geophysical Research*, 68(16): 4795-4812.

U.S. Environmental Protection Agency, 2007, Monitored natural attenuation of inorganic contaminants in ground water, volume 1: Technical basis for assessment, *EPA/600/R-07/139*, *Office of Research and Development*, Cincinatti, OH.

U.S. Geological Survey, 1972, Carr SW Quadrangle Colorado 7.5 Minute Series (Topographic), V877, *Denver, U.S. Geological Survey.*

U.S.Geological Survey, 2010, Online resource, Seamless Data Warehouse, URL: http://seamless.usgs.gov/ned1.php. Last accessed 08/30/2010.

Voss, W. C. and D. E. Gorski, 2007, Report on the Centennial Project Weld County, Colorado, Vancouver, BC, *Powertech Uranium Corporation***:** 1-46.

Wall, J.D. and Krumholz, L.R., 2006, Uranium Reduction, *Annual Reviews Microbiology*, 60: 149-66.

Delaney, P.G. and Loveys, J., 2000, Visual MODFLOW Student Version Tutorial Guide, *Waterloo Hydrogeologic, Inc.*

Weber, K.A., Achenbach, L.A. and Coates, J.D., 2006, Microorganisms pumping iron: anaerobic microbial oxidation and reduction, *Nature Reviews Microbiology,* 4: 752–764, doi:10.1038/nrmicro1490.

Wu, W., Carley, J., Lou, J., Ginder-Vogel, M.A., Cardenas, E., Leigh, M.B., Hwang, C., Kelly, S.D., Ruan, C., Wu, L., Van Nostrand, J., Gentry, T., Lowe, K., Mehlhorn, T., Carroll, S., Luo, W., Fields, M.W., Gu, B, Watson, D., Kemner, K.M., Marsh, T., Tiedje, J., Zhou, J., Fendorf, S., Kitanidis, P.K., Jardine, P.M., and Criddle, C.S., 2007, In situ bioreduction of uranium (VI) to submicromolar levels and reoxidation by dissolved oxygen, *Environmental Science and Technology*, 41: 5714-5723.

Zheng, C., 1990, MT3D, A modular three-dimensional transport model for simulation of advection, dispersion and chemical reaction of contaminants in groundwater systems, *Report to the U.S. Environmental Protection Agency*, 170 p.

Zielinski, R.A., 1975, Trace element evaluation of a suite of rocks from Reunion Island, Indian Ocean, *Geochimica et Cosmochimica Acta*, 39: 713-734.

APPENDIX 1:
NORTH CENTENNIAL PROJECT

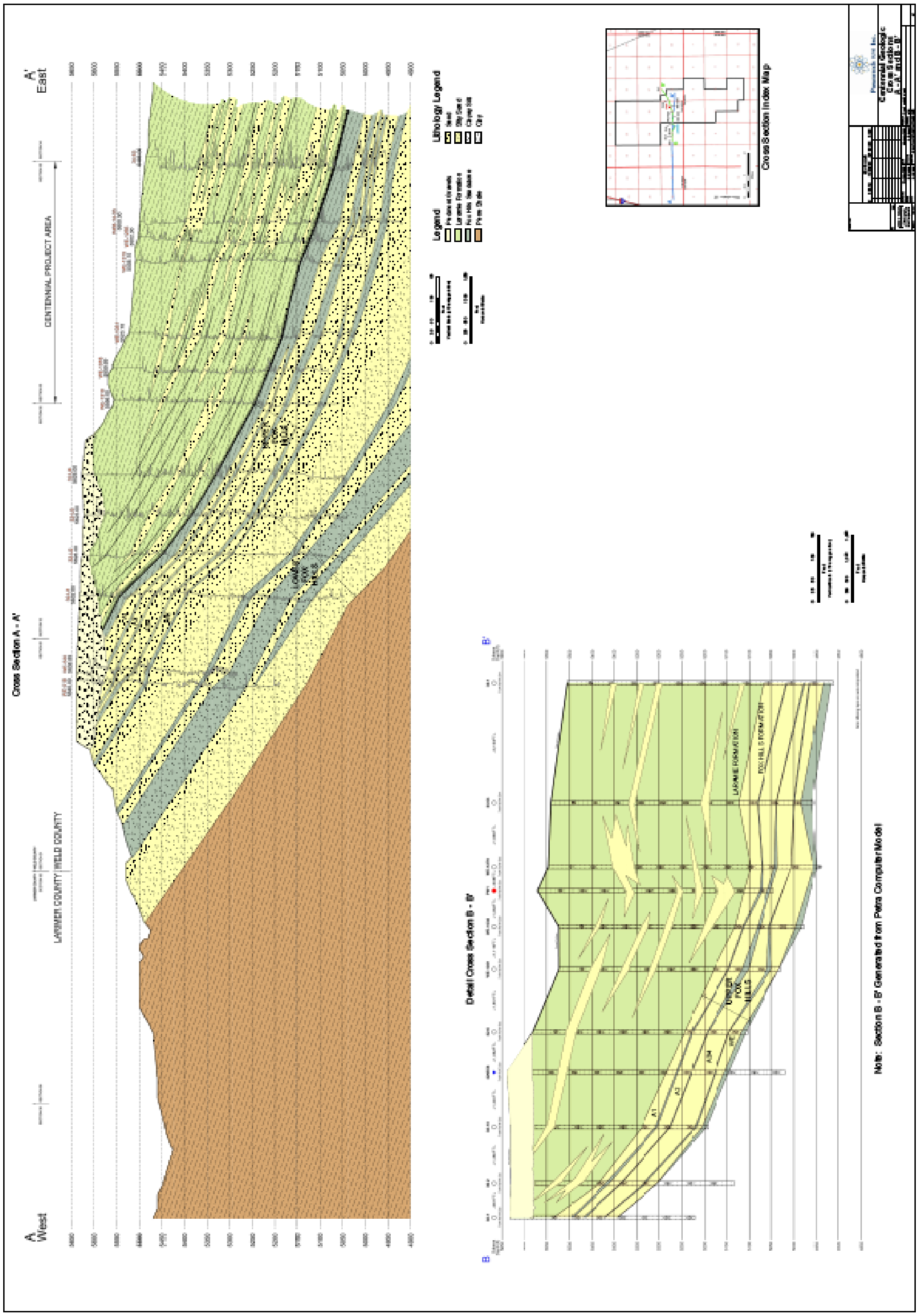

APPENDIX II: POST-MINING CONDITIONS AND BIOREDUCTION

After mining is ended, the remaining uranium in groundwater is present as either dissolved U(VI) or as solid phase uranous minerals. Eventually the pre-mining groundwater flow trend resumes and groundwater chemistry depends primarily on the oxidation and pH of the aquifer. The reducing capacity of the natural system, or natural attenuation capacity, affects the oxidation state of the system. Uranium is removed from groundwater if uranous minerals precipitate by reductants in either groundwater or minerals. Therefore, restoration and/or bioremediation of groundwater relies heavily on the reduction of uranium. Reduction of uranium can occur during restoration or by the natural attenuation of the host rock. Both abiotic and microbial processes are at work in sandstone-hosted uranium deposits.

II.1 Natural Attenuation

It has been documented that natural attenuation may be part of the remedy for inorganic contaminant plumes in groundwater (U.S. Environmental Protection Agency, 2007). The natural capacity of groundwater and rock to decrease uranium concentration depends on the redox characteristics of the system. If a groundwater-rock system is in equilibrium, the oxidizing capacity is reflective of the oxidants and reductants in the groundwater. Reactive oxidants and reductants are briefly listed below.

Oxidants (Electron acceptors)	Reductants (Electron donors)
O_2	S^0
Fe(III)-oxides	Fe(II), FeS_2
NO_3^-	UO_2
Mn^{4+}	CH_4
U^{6+}	Organic matter
CO_2	H_2
SO_4^{2-}	NH_4^+

Table II-1. Common oxidants and reductants at a sandstone redox boundary.

In abiotic reactions, oxidation potentials of redox pairs can be compared easily in a redox tower, shown in Figure II-1. Based on redox relationships it can be assumed that oxygen, iron (Fe) oxides, nitrates, and manganese are more thermodynamically favorable for reduction than U(VI). For instance, since Fe(III) is more energetically favorable, it will be reduced before U(VI). In other words, these components will compete with uranium for reduction in the groundwater. Given that the potentials are very close, however, this competition will depend upon site-specific environmental conditions.

In natural systems the order of reduction reactions often does not follow the simple relationships presented in the redox tower. For example, it has been found that uranium can coprecipitate with iron oxides when U(VI) is mobile in solution (Liu and others, 2005). When it is in the groundwater, U(VI) is more readily available to microorganisms (bioavailable) than oxidized iron precipitates (Finneran, 2002). The presence of additional groundwater constituents such as manganese oxides, nitrates, phosphates, aluminum, and nickel can affect the transformation of U(VI), but have a secondary impact on uranium redox reactions.

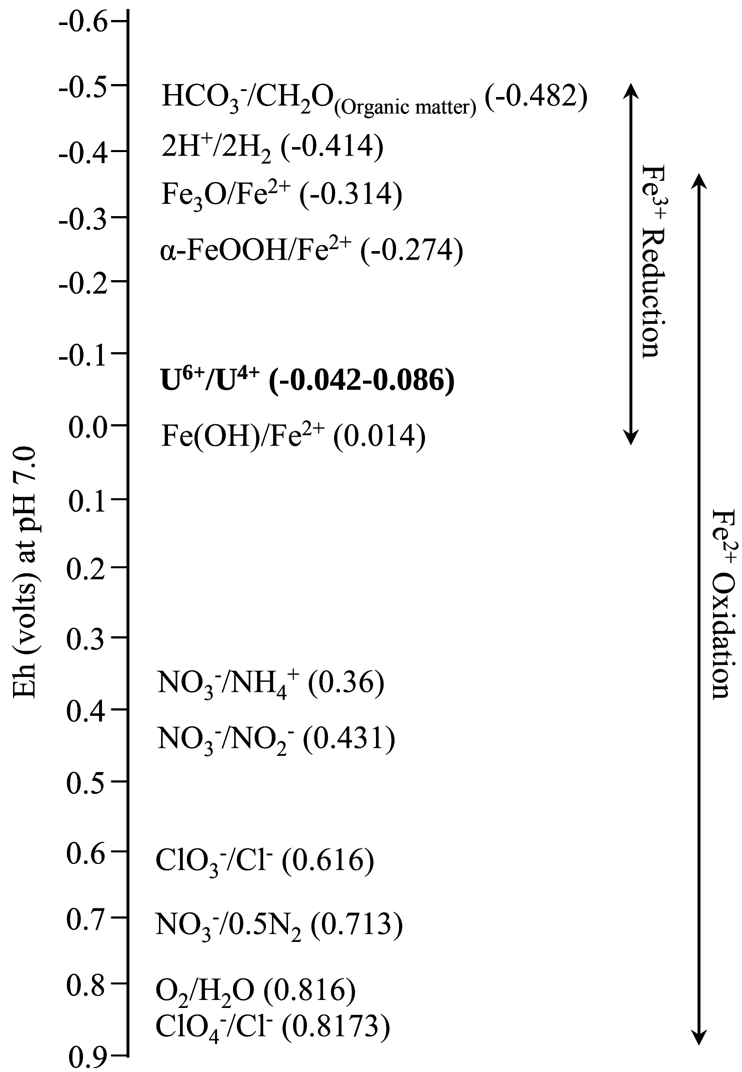

Figure II-1. Redox tower modified from Weber and others (2006). Uranium redox pair values from Flippov and Kanevskii (2005).

Abiotic reduction of U(VI) by sulfide is very slow, and while reduction by aqueous ferrous iron [Fe(II)] is also slow, it can be accelerated if U(VI) and the Fe(II) are sorbed onto Fe-oxides (Finneran, 2002). Since pyrite (FeS_2) is highly reactive, it is often the culprit for U(VI) reduction at redox boundaries. This happens by coupled reduction-oxidation reactions, whereby U(VI) is reduced when pyrite is oxidized into ferrous iron and sulfate. Biological effects enter in the next step, where ferrous iron is then available to be oxidized by iron-oxidizing bacteria (i.e. *Acidithiobacillus*) and facilitate the reduction of U(VI) until all the pyrite is depleted at the boundary (Finneran, 2002). However, computer models have shown one case where Fe(II) is not a universal reductant for U(VI) when biological effects are taken into account. Gu et al. (2005b) found this at the Oak Ridge site in Tennessee based on both ferrihydrite- and goethite-based surface complexation modeling in the presence of bacteria (*Shewanella, Geobacter metallireducens, Geobactereae).* For this reason, it is essential to describe microbial affects on the reduction of uranium in natural systems. They may enhance the natural attenuation capacity of aquifers.

II.2 Microorganisms in Bioreduction

Microbial processes involving the reduction of uranium are important to understanding, and perhaps even controlling, the transport and fate of uranium in groundwater. Microorganisms may directly affect the speciation, complexation, sorption, and mobility of uranium in natural waters that interact with host rock minerals. When microorganisms cause a shift from oxidized uranium, U(VI), to reduced uranium, U(IV), it is called bioreduction. This section highlights key points of bioreduction processes, the precipitation of both U(IV) crystals and U(IV)-complexed forms, and their stability during reoxidation of groundwater.

In reference to uranium, bioremediation is a general term that refers to processes by which microorganisms are used to reduce aqueous U(VI) cations to insoluble U(IV) minerals (bioprecipitation), or remove U(VI) from solution by adsorption to the cell wall (biosorption). Because uraninite (UO_2), a common secondary uranium mineral, is highly insoluble, its formation is often the desired result in bioremediation. Applications of bioremediation to contaminated sites are becoming increasingly common even though results are varied (Hall, 2009).

The role of microorganisms in uranium mineral precipitation within the sandstone is not fully understood. For example, U(VI) can be abiotically reduced by sulfide, H_2, organic matter, or pyrite as well as by bacteria. It is clear that microbial activity is necessary to oxidize organic matter to produce bicarbonate (HCO_3^-), a component which complexes with aqueous U(VI) to allow for transport with groundwater. In addition, microbial activity accelerates the reactivity and dissolution of pyrite, revealing the connection between biotic and abiotic development of uranium mineral formation. In a myriad of avenues, the concept of bioreduction can be applied effectively to uranium mineral precipitation.

Iron oxides and natural organic matter are abundant in the Fox Hills aquifer since hematite, fossils, and trace fossils can be found in outcrops. Because both iron oxides and natural organic matter can sorb to mineral surfaces, with and without uranium, and form aqueous complexes with metals, they factor into uranium dynamics. Their multifaceted influence on the complexation, sorption, reduction, and oxidation of uranium makes them important in understanding groundwater chemistry in this aquifer.

Many species of bacteria are used in laboratory and field experiments for uranium bioreduction, particularly iron- and sulfate-reducing bacteria. Although uranium is not part of any enzyme or biological structure, it may be used for respiration and growth (Wall and Krumholz, 2006), depending on the microorganism. For a complete list of microorganisms documented to reduce U(VI) see Table II-2. Generally, microbial processes are electron donor limited in oxic environments (Anderson and Lovely, 2002).

Anaeromyxobacter dehalogenans strain 2 CP-C	*Desulfosporosinus* spp. P3	*Psuedomonas* sp. CRB5
Cellulomunos flaigena ATCC 482	*Desulfovibrio baarsii* DSM 2075	*Pyrobaculum islandicum*
Cellulomunos sp. WS01	*Desulfovibrio desulfuricans* ATCC 29577	*Salmonella subterranean* sp. nov. strain FRC1
Cellulomunos sp. WS18	*Desulfovibrio desulfuricans* strain G20	*Shewanella alga* BrY
Cellulomunos sp. ES5	*Desulfovibrio* sp. UFZ B 490	*Shewanella oneidensis* MR-1
Clostridium sp.	*Desulfovibrio sulfodismutans* DSM 3696	*Shewanella putrefaciens* strain 20
Clostridium sphenoides ATCC 19403	*Desulfovibrio vulgaris* Hildenborough ATCC 29579	*Veillonella alcalescens*
Deinococcus radiodurans R1	*Geobacter metallireducens* GS-15	*Thermoanaerobacter* sp.
Desulfotomicrobium norvegicum DSM 1741	*Geobacter sulfurreducens*	*Thermos scotoductus*
Desulfotomaculum reducens	*Psuedomonas putida*	*Thermoterrabacterim ferrireducens*
Desulfosporosinus orientis DSM 765	*Psuedomonas* sp.	

Table II-2. Bacteria shown to reduce U(VI) to U(IV) (Wall and Krumholz, 2006).

Iron is one of the most abundant elements on Earth and serves key functions in microbial processes. Fe(II) can donate electrons in both anoxic and oxic environments at circumnuetral pH, and Fe(III) can serve as a terminal electron acceptor for iron-reducing bacteria (Weber et al., 2006). The influence of microbial iron oxidation and reduction on the environment can be seen where redox-sensitive constituents are altered in the system. Of particular importance is the anoxic oxidation of organic matter and H_2 to form carbonate species and H^+. Because carbonates will complex with U(VI) in groundwater at redox boundaries, the presence of Fe(III), typically in the form of Fe(III) oxides and Fe(III) sulfides, can result in carbonate complexation with U(VI) rather than reduction on the oxidized region of the redox boundary. On the other hand, reduced iron minerals such as siderite ($FeCO_3$) will abiotically react quickly with U(VI).

Iron-reducing bacteria *Geobacter* have been widely studied because they can out-compete sulfate-reducing bacteria for electron donors when sufficient iron oxides are available (Finneran, 2002). This is due to the fact that they maintain electron donor concentrations too low for sulfate-reducing bacteria to survive. One example of the use of *Geobacteraceae* for bioreduction is the Shiprock aquifer in New Mexico, where bacteria were successfully stimulated by a simple electron donor, quinones, to reduce U(VI) (Chang et al., 2001). At one point, *Geobacteraceae* was the only known iron-reducing organism to couple growth to the reduction of U(VI) in this manner (Finneran, 2002). The effectiveness of humic material (i.e. quinones) as an electron donor is discussed later in this chapter.

Dissimilatory metal-reducing bacteria can also manufacture magnetite (Fe_3O_4) which contains both Fe(II) and Fe(III). One laboratory study found that the addition of magnetite increases uranium bioreduction as well as abiotic reduction (Behrends, 2005). This may be due to the fact that magnetite can serve as a binding site for high reduction-oxidation activity. This suggests that uranium may be more quickly reduced or oxidized if magnetite is present in the system.

Sulfate-reducing bacteria are also increasingly studied because of their ubiquity in anoxic and oxic environments and their ability to survive over large pH and salt range (Chang et al., 2001). In addition to facilitating sulfate and iron reduction, sulfate-reducing bacteria such as *Shewanella* (also an iron reducing bacterium) are able to reduce and accumulate various metals including U(VI). More specifically, they can generate insoluble uranium-sulfides with H_2S. Interestingly, a tolerance for highly toxic elements allows sulfate reducing bacteria to retain their motility upon exposure to high levels of U(VI), making sulfate reducing bacteria redox reactions kinetically favorable over iron reducing bacteria under highly toxic conditions (Spear et al., 1999).

Each bacterial species has benefits for bioreduction. For example *Geobacter metallireducens, Thermoterrabacterium ferrireducens, Shewanella putrefaciens,* and *Desulfotomaculum reducens* can gain energy for growth from U(VI) respiration, demonstrating the versatility of bacteria in bioreduction applications (Wall and Krumholz, 2006). *Desulfovibrio vulgaris* oxidizes H_2 or lactate to reduce U(VI) by electron transport via a C3-type cytochrome. However, it cannot use uranium for growth, and laboratory experiments have shown that it reduces Fe(III) before sulfate when stimulated with lactate. It was initially studied because of its tolerance or resistance to Zn, Cu, Ni, and Co.

The most direct bacterium for bioreduction of uranium is *Desulfotomaculum,* which can grow with U(VI) as its sole electron acceptor and has a high tolerance for U. However, because it produces toxic H_2S by oxidizing of existing H_2 in the aquifer, it may be best to suppress it and allow Fe(III) reducers to reduce U(VI) instead (Chang et al., 2001).

Organic electron donors such as acetate, glucose, ethanol, lactate, and others can be added to a system to stimulate microbial activity which in turn helps to create anaerobic conditions that enhance metal-reducing conditions (Istok et al., 2004). Laboratory experiments have shown that under anoxic conditions, bacterial species have selective tastes for organic matter which serve as electron donors. For example, *Geobacter* bacteria are best stimulated by acetate and glucose, and *Desulfovibrio* bacteria are stimulated by similar monodentate ligands (acetate) (Finneran et al., 2002). However, sulfate reducing bacteria *Shewanella* respond best to polydentate ligands such as malonate, oxalate, and citrate (Anderson and Lovely, 2002).

Laboratory studies have also shown that the behavior of *Desulfovibrio vulgaris* changes when the electron donor is replaced. For example, when abiotic H_2 was the reductant instead of lactate, reduction of U(VI) was concurrent with sulfate reduction instead of prior to sulfate reduction. Theories to explain dynamics between specific sulfate reducing bacteria, iron reducing bacteria, and assortments of organic matter are still in development as each combination appears unique. Complexity is added to the system as organic ligands, colloids, and particles have dual functions: they may reduce U(VI), or complex with it, rendering U(VI) unavailable for bioreduction or removal by biosorption.

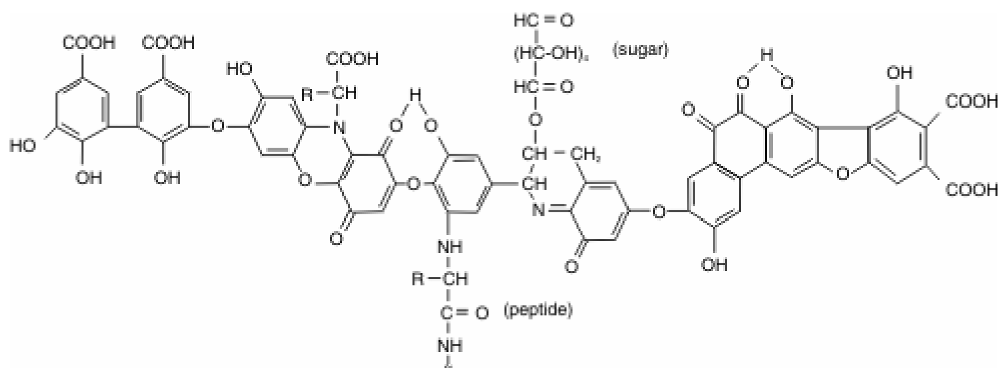

Figure II-2. Model structure of humic acid (Stevenson, 1982).

Humic material is complex, microbially-degraded organic material (ie. lignite and black shale) and exists in groundwater as humic acid (Fig. 1-2), fulvic acid, and humin, depending on pH and solubility. The addition of humic material to a system can alleviate the toxicity of metals such as Ni^{2+} on microorganisms (Gu et al., 2005a). Furthermore, if a system is strongly anaerobic, humic materials can increase U(VI) reduction (Gu et al., 2005b). More specifically, humics such as anthraquinone-2,6-disulfonate (AQDS) and anthrahydroquinone-2,6-disulfonate (AHQDS) can be used as electron shuttles to enhance U(VI) reduction. Reduced humics appear to be more competent than oxidized material in transforming U(VI) (Finnerman and others, 2002). One study by Finneran and others (2002) showed that the addition of organic matter without an electron shuttle (humic material) has little to no effect, but the addition of an electron donor can augment bacterial reduction of U(VI). Experimental studies such as this suggest that an assortment of processes and techniques (all of which are not entirely evident thus far) are necessary for the bioreduction of U(VI).

II.3 Reoxidation

Typically, it is assumed that if a mineral is precipitated, it is removed from solution and limited in its bioavailability to microorganisms. However, when reduced U(IV) is complexed with ligands and thus it can be mobile. In addition, one study showed that because uraninite crystals can be minuscule, averaging about 1.5 nanometers, the U(IV) in pure crystal form was still mobile in the groundwater (Suzuki et al., 2002). If U(IV) is precipitated but still transportable in solution, it implies that nanocrystals may still be accessible for microbial or abiotic oxidation even after bioreduction. This undermines the common assumption that mineral precipitation removes uranium from solution. Furthermore, uranium cycling in the groundwater after reduction may amplify uncertainty in interpretations that attempt to measure the reductive capacity of sandstones.

Figueroa and others (2006) summarizes the availability of U(VI) for bioreduction given ligand complexation. Even though microorganisms can reduce U(VI) while it is complexed with ligands, the molecule is unavailable for precipitation. Indeed, a study by Francis (2006) revealed that anaerobic bacteria were able to reduce U(VI) to U(IV) with little precipitation of uranium. This may be a common occurrence in which bioreduction does not remove uranium from the groundwater.

In addition to small particle size, uraninite crystals may become trapped inside the cell wall and precipitate upon cell death, or they may be sorbed onto cell surfaces (where reduction took place) and travel with cells in solution (Spear and others, 1999). Suzuki and others (2002) found the latter to be the true in laboratory studies using *Desulfosporosinus* spp. In this case U(IV) would likely be vulnerable to reoxidation.

Other studies show that uranium reductases reside between the cell wall and the cytoplasmic membrane and enlist the help of several proteins for reduction. They contributed to optimal U(VI) reduction that led to UO_2 precipitation inside the periplasm of *S. oneidensis* and even within the cytoplasm of *Desulfovibrio* (Wall and Krumholz, 2006). Not all of the proteins were necessary for U(VI) reduction, but bacteria that possess all proteins will yield rapid uranium reduction and resist oxidation, given that U(IV) would no longer be exposed to oxidizing groundwater zones. In addition to these speculations, Wall and Krumholz (2006) suggest that U(VI) does not generally have access to intracellular proteins, and therefore will more readily reduce, precipitate, and adsorb onto cells which possess enzymes exposed to their exterior. For this reason, bacteria with enzymes (electron-carriers) in the periplasm and on the outer wall will be best candidates for reducing U(VI).

As oxidizing fronts can shift with time, one pertinent question for bioremediation studies is: How well do uranium precipitates resist reoxidation? Resistance to oxidation depends on the oxidizing capacity of the groundwater and its constituents, and the ability of sulfate reducing bacteria and iron reducing bacteria to directly and indirectly consume dissolved oxygen. In addition, the nature and strength of the uranium mineral and uranium complexation bonds will have an effect. For instance, if U(IV) has complexed with humic material, it is easily re-oxidized upon contact with O_2 (Gu, 2005). Aside from this, the question of reoxidation tendencies has not been widely addressed in the literature. Wu et al. (2007) conducted a field study of U(IV) reoxidation capacity of a contaminated sandstone and found the results to be spatially varied rather than microbially defined. Further research in field studies is needed to better understand these dynamics.

Interestingly, mackinawite (FeS) may precipitate with uraninite in the presence of sulfate reducing bacteria and can shield U(IV) from future oxidative dissolution (Abdelouas and others, 1999). Therefore the addition of FeS (or iron that will react with H_2S) to aquifers containing indigenous sulfate reducing bacteria may be a viable option for sustaining reduction of U(VI) over time. While there is an immense amount of literature detailing specific interactions of bacterial species in laboratories and field studies, a comprehensive understanding of the geochemical relationship between microorganisms and uranium is yet to be seen. It is clear that microbial activity has enormous influence on the redox chemistry of uranium in groundwater.

APPENDIX III:
STATE RECORDS: GROUNDWATER DATA

Table III-1. Relevant well data compiled from the Colorado Division of Water Resources, Office of the State Engineer online database (*http://www.dwr.state.co.us*).

Permit Number (Well Name)	Easting (NAD 83)	Northing (NAD 83)	Aquifer Name	Date Well Constructed	Date Well Plugged	Well Depth (ft)	Top of Screen (ft)	Bottom of Screen (ft)	Screen Length (ft)	Static Water Level (ft)
12	528520	4494775	QUATERNARY ALLUVIUM	8/6/2008		37	25	35	10	27
19	520442.9	4493239	QUATERNARY ALLUVIUM	9/4/2008		44	32	42	10	14
19	528611	4486775	ALL UNNAMED AQUIFERS	4/26/2006		41	21	41	20	19
59	528929.5	4494730.8	ALL UNNAMED AQUIFERS	3/28/2003		39	19	39	20	17
116	501536.5	4490602.6	ALL UNNAMED AQUIFERS	7/29/1992		58	43	58	15	13
325	526510.6	4500356.9	ALL UNNAMED AQUIFERS	2/21/1996		40	26	36	10	9
328	498332.3	4497023.2	ALL UNNAMED AQUIFERS	12/11/1991		38	28	38	10	21
1473	520384.1	4494576.3	ALL UNNAMED AQUIFERS	12/15/1993		66	24	66	42	15
1547	524807.1	4486694.7	ALL UNNAMED AQUIFERS	2/11/1998		66	40	66	26	22
1547	524734.9	4486644	ALL UNNAMED AQUIFERS	6/15/2003		73	43	73	30	28
1556	501655.9	4490648	ALL UNNAMED AQUIFERS	10/3/2006		58	45	55	10	10
1577	524943.8	4492515	ALL UNNAMED AQUIFERS	8/29/2009		57	29	49	20	35
1633	522757.3	4489220.2	ALL UNNAMED AQUIFERS	4/9/1990		58	28	58	30	26
2531	524330	4492448.8	ALL UNNAMED AQUIFERS	3/9/1993		84	61	81	20	49
3121	496084	4515720	QUATERNARY ALLUVIUM	4/1/2005		43	23	43	20	24
4148	523248.4	4495509.8	ALL UNNAMED AQUIFERS	3/24/2000		35	25	35	10	15
4184	528920.1	4486411.2	ALL UNNAMED AQUIFERS	6/9/1999		35	20	35	15	8
4554	528125.6	4497168.9	ALL UNNAMED AQUIFERS	3/28/2003		37	27	37	10	13
6350	529332.1	4494080.8	ALL UNNAMED AQUIFERS	5/2/2003		40	20	40	20	18
6350	529332.1	4494080.8	ALL UNNAMED AQUIFERS	5/2/2003		40	20	40	20	18
6357	497853	4498715.3	ALL UNNAMED AQUIFERS	8/15/1990		95	45	95	50	38
6410	529204.2	4487627.2	ALL UNNAMED AQUIFERS	6/28/1995		40	20	40	20	10
6930	521424.6	4495647.8	ALL UNNAMED AQUIFERS	1/26/1991		58	36	56	20	33
8332	521276.1	4492359.8	ALL UNNAMED AQUIFERS	8/6/1993		58	38	58	20	39
8869	519860.2	4494044.8	ALL UNNAMED AQUIFERS	10/18/1990		42	22	42	20	18
10130	500754.4	4492137.1	ALL UNNAMED AQUIFERS	5/4/2002		69	49	69	20	18
10220	516784.5	4487900.5	QUATERNARY ALLUVIUM	8/30/2007		60	20	40	20	21
10398	499564	4499490	ALL UNNAMED AQUIFERS	7/29/2006		45	28	38	10	26
10398	499620.4	4499457.8	ALL UNNAMED AQUIFERS	3/14/2000	8/3/2006	43	30	40	10	12
10526	515770.7	4532087.2	ALL UNNAMED AQUIFERS	4/25/2002		51	20	51	31	23
10604	502171.2	4487391.5	ALL UNNAMED AQUIFERS	4/18/1994		38	28	38	10	7
10605	501421.7	4487390.5	ALL UNNAMED AQUIFERS	9/30/1994	3/26/1997	33	21	31	10	6
10605	501463.8	4487390	ALL UNNAMED AQUIFERS	3/18/1997		43	30	40	10	8
10995	499966	4502132	ALL UNNAMED AQUIFERS	8/30/2005		45	25	45	20	25

Permit Number (Well Name)	Easting (NAD 83)	Northing (NAD 83)	Aquifer Name	Date Well Constructed	Date Well Plugged	Well Depth (ft)	Top of Screen (ft)	Bottom of Screen (ft)	Screen Length (ft)	Static Water Level (ft)
11033	517533.1	4486685.5	QUATERNARY ALLUVIUM	5/8/2008		48	36	46	10	38
11037	528155.7	4486729.2	ALL UNNAMED AQUIFERS	12/11/2001		41	21	41	20	12
11305	512305.3	4489686.9	ALL UNNAMED AQUIFERS	6/27/2003		41	21	41	20	16
11315	521683.2	4491270.3	ALL UNNAMED AQUIFERS	5/24/2001		30	17	27	10	4
11323	521811.8	4488804.7	ALL UNNAMED AQUIFERS	12/21/1992		56	38	53	15	32
11574	529227.7	4492320.8	ALL UNNAMED AQUIFERS	5/12/1995		38	23	33	10	12
11682	521838.2	4493052.3	ALL UNNAMED AQUIFERS	10/28/1992		48	35	45	10	25
11776	502049	4488166	ALL UNNAMED AQUIFERS	6/18/1998		50	37	47	10	5
11888	496992.1	4497090.5	ALL UNNAMED AQUIFERS	10/26/2007		52	37	47	10	33
11889	497015.9	4497047	ALL UNNAMED AQUIFERS	10/27/2007		48	33	43	10	28
12070	500076.5	4505053	ALL UNNAMED AQUIFERS	5/28/1990		57	41	57	16	16
12723	529728	4493970.3	ALL UNNAMED AQUIFERS	5/22/2003		38	25	35	10	16
12746	519226.5	4502742	ALL UNNAMED AQUIFERS	4/4/1991		43	30	43	13	22
12840	500224	4505081.8	ALL UNNAMED AQUIFERS	4/19/1993		52	35	50	15	17
12904	530802	4495899	QUATERNARY ALLUVIUM	5/5/2010		19	14	19	5	5
12906	531057.7	4495894.8	ALL UNNAMED AQUIFERS	3/24/1997		20	10	20	10	10
12956	529728	4494008.8	ALL UNNAMED AQUIFERS	5/21/2003		38	26	36	10	16
13257	518006.2	4486707.7	ALL UNNAMED AQUIFERS	4/16/1991		52	42	52	10	32
13429	503011.4	4529556.9	ALL UNNAMED AQUIFERS	6/5/1993		51	33	48	15	26
13442	524468.2	4490837.3	ALL UNNAMED AQUIFERS	5/7/1992		62	42	62	20	31
13964	516853.8	4489149.8	ALL UNNAMED AQUIFERS	3/14/2003		30	20	30	10	11
13965	517054.6	4489149.8	ALL UNNAMED AQUIFERS	3/15/2003		28	18	28	10	8
14483	528750.2	4495567.8	ALL UNNAMED AQUIFERS	3/10/1993		33	20	30	10	9
14507	524038.1	4492091.8	ALL UNNAMED AQUIFERS	1/29/1990		91	66	87	21	50
14531	521774.3	4489130.5	ALL UNNAMED AQUIFERS	5/10/2005		47	34	44	10	18
14553	522411.6	4487498.5	ALL UNNAMED AQUIFERS	4/6/2004		62	38	62	24	38
14577	527740.4	4493126.3	ALL UNNAMED AQUIFERS	5/22/1995		26	13	23	10	8
15235	529218.1	4491653.5	ALL UNNAMED AQUIFERS	3/16/2006		37	23	33	10	11
16090	528985.1	4489240	ALL UNNAMED AQUIFERS	4/4/2007		35	23	35	12	12
16708	529977.6	4489206.7	ALL UNNAMED AQUIFERS	12/15/2002		23	10	20	10	7
17046	499773.1	4500491.3	ALL UNNAMED AQUIFERS	12/18/1990		39	25	35	10	21
17335	524873.6	4494866	ALL UNNAMED AQUIFERS	4/16/1991	11/18/1992	20	9	19	10	16
17565	516625.9	4504859.6	ALL UNNAMED AQUIFERS	5/23/1991		26	16	26	10	23
17566	512183	4503800.5	ALL UNNAMED AQUIFERS	5/23/1991	4/12/2005	30	20	30	10	29
18054	499484.6	4494780.7	ALL UNNAMED AQUIFERS	5/12/2000		36	20	30	10	9
18057	499401.7	4494778.2	ALL UNNAMED AQUIFERS	5/15/2000		40	25	35	10	9
18100	501761.2	4529377.4	ALL UNNAMED AQUIFERS	9/18/1991		55	25	55	30	36
18339	500184.7	4509066.4	ALL UNNAMED AQUIFERS	6/25/1997	9/19/2006	35	15	35	20	21
18339	500144.2	4509106.5	ALL UNNAMED AQUIFERS	8/7/2006		32	12	32	20	11
18448	527502.5	4489453.2	ALL UNNAMED AQUIFERS	11/27/1991		40	30	40	10	25

Permit Number (Well Name)	Easting (NAD 83)	Northing (NAD 83)	Aquifer Name	Date Well Constructed	Date Well Plugged	Well Depth (ft)	Top of Screen (ft)	Bottom of Screen (ft)	Screen Length (ft)	Static Water Level (ft)
18697	521019.3	4497453.9	ALL UNNAMED AQUIFERS	2/28/1992		47	27	47	20	27
18766	514666.5	4492736.4	ALL UNNAMED AQUIFERS	3/4/1992	5/17/1993	162	152	162	10	141
18767	514666.5	4492736.4	ALL UNNAMED AQUIFERS	2/11/1992	5/17/1993	138	128	138	10	125
19195	497527.6	4495457.2	ALL UNNAMED AQUIFERS	10/14/1994		80	50	80	30	27
19196	497562.1	4496101.7	ALL UNNAMED AQUIFERS	6/29/1990		59	39	59	20	15
19280	497629.2	4498294.5	ALL UNNAMED AQUIFERS	10/23/1996		86	63	83	20	26
19377	498512.8	4499362	ALL UNNAMED AQUIFERS	8/17/2006		82	60	80	20	46
19378	499526.7	4498671	ALL UNNAMED AQUIFERS	8/1/2007		44	32	42	10	29
19380	497525.8	4499607.8	ALL UNNAMED AQUIFERS	12/14/2001		70	50	70	20	10
19430	501959.2	4508172.4	ALL UNNAMED AQUIFERS	3/10/2003		36	26	36	10	20
19430	501938.6	4508309.9	ALL UNNAMED AQUIFERS	8/21/2001		34	18	28	10	11
19444	497383.9	4493723.2	ALL UNNAMED AQUIFERS	4/24/1991		54	31	54	23	18
19630	514666.5	4492736.4	ALL UNNAMED AQUIFERS	9/10/1992	5/17/1993	159	149	159	10	125
20913	522471.1	4492942.8	ALL UNNAMED AQUIFERS	4/1/2004		50	30	50	20	34
25080	531325.5	4497135.5	ALL UNNAMED AQUIFERS	12/11/2004	2/9/2005	30	10	30	20	14
25434	520919.4	4500359.9	ALL UNNAMED AQUIFERS	2/12/1996		45	32	42	10	23
25435	520997	4500357.4	ALL UNNAMED AQUIFERS	2/13/1996		45	31	41	10	23
25436	521047	4500364.4	ALL UNNAMED AQUIFERS	2/14/1996		45	32	42	10	23
27773	501697.5	4500131.2	ALL UNNAMED AQUIFERS	6/22/1996		44	24	44	20	15
34700	500171.8	4504447.8	ALL UNNAMED AQUIFERS	7/19/1990		20	14	20	6	14
35724	501446.5	4490588.1	ALL UNNAMED AQUIFERS	5/22/1990		65	45	65	20	22
36244	498247.8	4528446.9	ALL UNNAMED AQUIFERS	9/9/1994		40	20	40	20	21
36382	524228.2	4521183.3	ALL UNNAMED AQUIFERS	4/28/1997		75	55	75	20	36
36383	518377.3	4519545.4	ALL UNNAMED AQUIFERS	2/16/2004		100	60	100	40	47
36385	528726.6	4488466.2	ALL UNNAMED AQUIFERS	3/20/1990		44	24	44	20	9
36385	521673	4519542	ALL UNNAMED AQUIFERS	6/6/2008		200	135	195	60	90
37136	532003.3	4517101.2	ALL UNNAMED AQUIFERS	11/3/2003		300	220	280	60	134
37833	501393.5	4514539.5	ALL UNNAMED AQUIFERS	3/4/2000		400	330	390	60	24
38141	528648.1	4488145.7	ALL UNNAMED AQUIFERS	3/26/1991		40	20	40	20	12
38627	501140.1	4490245.1	ALL UNNAMED AQUIFERS	5/1/1991		70	50	70	20	20
38628	501049.1	4490276.1	ALL UNNAMED AQUIFERS	4/30/1991		65	45	65	20	25
38661	512016.3	4486457.3	ALL UNNAMED AQUIFERS	9/19/2000	1/23/2003	38	18	38	20	12
39360	531806.2	4492203.8	LARAMIE FOX HILLS	7/30/1999		445	365	425	60	175
40034	522436	4489721.7	ALL UNNAMED AQUIFERS	11/6/1991		66	46	66	20	27
40760	519342.5	4487361.2	ALL UNNAMED AQUIFERS	5/21/2002		42	32	42	10	16
40763	507195.1	4489684.5	ALL UNNAMED AQUIFERS	6/6/2002		22	12	22	10	6
40830	497844.1	4508274.4	ALL UNNAMED AQUIFERS	3/23/1992		98	75	95	20	22
41254	528614.4	4489044.7	ALL UNNAMED AQUIFERS	4/19/1992		45	32	42	10	14
41346	501330.9	4490305.1	ALL UNNAMED AQUIFERS	9/8/1992		60	40	60	20	18
42584	524109.6	4486114.7	ALL UNNAMED AQUIFERS	10/25/1993		89	74	84	10	27

Permit Number (Well Name)	Easting (NAD 83)	Northing (NAD 83)	Aquifer Name	Date Well Constructed	Date Well Plugged	Well Depth (ft)	Top of Screen (ft)	Bottom of Screen (ft)	Screen Length (ft)	Static Water Level (ft)
42585	523100.1	4486139.7	ALL UNNAMED AQUIFERS	10/13/1993		62	49	59	10	25
42610	529301.3	4491655.8	ALL UNNAMED AQUIFERS	7/28/1993		44	21	41	20	11
43116	498130.9	4492374.7	ALL UNNAMED AQUIFERS	10/21/1992		35	22	35	13	10
43546	498527.3	4488803.6	ALL UNNAMED AQUIFERS	6/15/1994		25	19	25	6	5
44972	529251.2	4492320.3	ALL UNNAMED AQUIFERS	5/12/1995		40	25	35	10	13
44973	529198.7	4492321.8	ALL UNNAMED AQUIFERS	5/11/1995		38	23	33	10	12
45148	498593.9	4491793.6	ALL UNNAMED AQUIFERS	1/2/1996		25	15	25	10	7
45150	498500.8	4491880.7	ALL UNNAMED AQUIFERS	12/28/1995		25	10	25	15	6
45151	498499.5	4491798.1	ALL UNNAMED AQUIFERS	1/2/1996		28	18	28	10	6
45152	498593.5	4491766.1	ALL UNNAMED AQUIFERS	5/7/1996		29	11	29	18	8
45155	498555.6	4491873.7	ALL UNNAMED AQUIFERS	1/12/1996		24	14	24	10	7
45157	498595.2	4491872.7	ALL UNNAMED AQUIFERS	1/10/1996		30	20	30	10	7
46182	528126.2	4490734.2	ALL UNNAMED AQUIFERS	4/3/1996		23	13	23	10	5
47200	510809	4508770	LARAMIE FOX HILLS	10/12/2007		283	250	280	30	230
47201	511165.2	4510681	LARAMIE FOX HILLS	8/17/2007		303	260	280	20	149
47202	509785.6	4510186	LARAMIE FOX HILLS	8/22/2007		95	80	90	10	62
47203	509578.3	4509948.5	LARAMIE FOX HILLS	8/15/2007		234	120	140	20	116
47204	509358	4512139.5	LARAMIE FOX HILLS	8/10/2008		494	419	459	40	402
47206	511370.2	4502205.5	LARAMIE FOX HILLS	8/7/2007		103	80	100	20	73
47211	510967.8	4514522	LARAMIE FOX HILLS	9/6/2007		520	485	505	20	245
47212	508069.4	4522736.5	LARAMIE FOX HILLS	8/31/2007		529	495	515	20	390
47213	509905.8	4514706	LARAMIE FOX HILLS	8/29/2007		190	155	185	30	138
47222	509378.4	4515724.5	LARAMIE FOX HILLS	9/7/2007		529	495	515	20	390
47225	509358	4512139.5	LARAMIE FOX HILLS	8/7/2007		547	527	547	20	425
47524	496238	4491530	ALL UNNAMED AQUIFERS	12/3/2007		25	15	25	10	13
47525	496194	4490455	ALL UNNAMED AQUIFERS	12/4/2007		17	7	17	10	6
47526	497112.9	4488306	ALL UNNAMED AQUIFERS	12/6/2007		20	10	20	10	15
47527	496290.9	4487377	ALL UNNAMED AQUIFERS	12/6/2007		20	10	20	10	10
47576	500105.9	4503156	ALL UNNAMED AQUIFERS	12/19/2007		25	10	25	15	12
47993	499720.3	4493169.2	ALL UNNAMED AQUIFERS	2/22/1998		25	10	25	15	7
48187	500224	4505081.8	ALL UNNAMED AQUIFERS	4/19/1993		52	35	50	15	17
48191	497383.9	4493726.2	ALL UNNAMED AQUIFERS	4/24/1991		51	31	51	20	18
48192	497116.6	4493528.7	ALL UNNAMED AQUIFERS	3/3/1998		60	30	60	30	10
50468	496164.7	4492291.2	ALL UNNAMED AQUIFERS	7/22/2004		60	10	60	50	18
51858	521214.5	4489187.7	ALL UNNAMED AQUIFERS	6/8/1999		60	47	57	10	35
52458	501628.5	4490403.1	ALL UNNAMED AQUIFERS	12/20/1999		57	37	57	20	11
52648	501537.8	4490566.1	ALL UNNAMED AQUIFERS	4/21/2000		57	37	57	20	20
52810	512099.6	4486114.3	ALL UNNAMED AQUIFERS	9/25/2000		23	20	23	3	4
52813	512031.1	4486603.8	ALL UNNAMED AQUIFERS	10/26/2000		40	16	40	24	11
52814	511991.4	4486600.4	ALL UNNAMED AQUIFERS	5/3/2000		40	20	40	20	22

Permit Number (Well Name)	Easting (NAD 83)	Northing (NAD 83)	Aquifer Name	Date Well Constructed	Date Well Plugged	Well Depth (ft)	Top of Screen (ft)	Bottom of Screen (ft)	Screen Length (ft)	Static Water Level (ft)
52820	512004.9	4486085.8	ALL UNNAMED AQUIFERS	5/4/2000		40	19	40	21	18
52822	512152.7	4485919.8	ALL UNNAMED AQUIFERS	5/2/2000		40	20	35	15	9
52823	512052	4485912.3	ALL UNNAMED AQUIFERS	10/9/2000		40	18	40	22	12
52862	499363.3	4494769.2	ALL UNNAMED AQUIFERS	5/16/2000		36	23	33	10	9
53731	528138.7	4490735	ALL UNNAMED AQUIFERS	9/29/2001	11/23/2005	21	4	21	17	8
54061	512111.1	4486357.8	ALL UNNAMED AQUIFERS	8/4/2000		36	16	36	20	12
54062	512121	4486443.5	ALL UNNAMED AQUIFERS	7/28/2000		40	20	40	20	10
54063	512128.8	4486617.3	ALL UNNAMED AQUIFERS	8/4/2000		40	20	40	20	11
54777	512032.7	4486450.3	ALL UNNAMED AQUIFERS	9/1/2002		25	14	24	10	13
55103	522154.7	4486764.2	ALL UNNAMED AQUIFERS	4/19/2001		51	36	46	10	25
55132	496854.3	4492022.2	ALL UNNAMED AQUIFERS	2/6/2001		25	10	25	15	10
55153	524499.1	4495734.3	ALL UNNAMED AQUIFERS	6/30/2006		40	20	40	20	18
55817	499245.7	4494789.7	ALL UNNAMED AQUIFERS	5/27/2003		55	19	39	20	4
57959	501620.9	4490200.5	ALL UNNAMED AQUIFERS	3/3/2003		60	40	60	20	10
58237	501750	4490305.6	ALL UNNAMED AQUIFERS	2/22/2003		60	20	40	20	7
58238	512028.9	4486371.3	ALL UNNAMED AQUIFERS	1/23/2003		41	21	41	20	14
58251	501840.2	4490045.6	ALL UNNAMED AQUIFERS	3/4/2003		60	10	30	20	8
58305	512068.4	4486525.3	ALL UNNAMED AQUIFERS	2/28/2003		30	20	30	10	8
58306	512058.9	4486320.8	ALL UNNAMED AQUIFERS	2/28/2003		30	20	30	10	8
58359	512204.8	4485949.3	ALL UNNAMED AQUIFERS	4/15/2003		30	20	30	10	6
58361	501743.7	4490602.6	ALL UNNAMED AQUIFERS	2/21/2003		60	6	26	20	8
58362	501742.8	4490389.1	ALL UNNAMED AQUIFERS	2/24/2003		60	6	26	20	6
58363	501725.1	4490206.6	ALL UNNAMED AQUIFERS	2/26/2003		60	40	60	20	8
58364	501655.3	4490586.1	ALL UNNAMED AQUIFERS	3/13/2003		60	40	60	20	10
58412	501611.5	4490017.1	ALL UNNAMED AQUIFERS	3/14/2003		60	40	60	20	17
58442	501818.1	4490213.6	ALL UNNAMED AQUIFERS	3/1/2003		60	28	60	32	8
58555	501847.3	4489938.6	ALL UNNAMED AQUIFERS	3/31/2003		60	10	40	30	7
58722	501571.6	4490291.6	ALL UNNAMED AQUIFERS	3/7/2003		60	40	60	20	11
58723	501552.3	4490410.6	ALL UNNAMED AQUIFERS	3/10/2003		60	40	60	20	12
58724	501566.4	4490488.1	ALL UNNAMED AQUIFERS	3/11/2003		60	40	60	20	11
58725	501635.7	4490315.1	ALL UNNAMED AQUIFERS	3/6/2003		60	40	60	20	8
59262	528952.9	4493908.5	ALL UNNAMED AQUIFERS	3/16/2005		40	20	40	20	18
59263	529055.9	4493927.8	ALL UNNAMED AQUIFERS	5/16/2003		40	20	40	20	18
59264	529016.3	4493921.8	ALL UNNAMED AQUIFERS	5/3/2003		40	20	40	20	18
59530	501069.5	4490457	QUATERNARY ALLUVIUM	5/1/2007		40	26	40	14	13
59531	501442.7	4490149.5	ALL UNNAMED AQUIFERS	8/19/2008		45	25	45	20	12
60462	528938	4493468.5	ALL UNNAMED AQUIFERS	3/17/2005		40	2	40	38	18
61413	499261.1	4505437.5	ALL UNNAMED AQUIFERS	8/4/2004		78	68	78	10	33
63104	499120.8	4504381	ALL UNNAMED AQUIFERS	5/10/2006		45	25	45	20	26
63906	523758.5	4486352	ALL UNNAMED AQUIFERS	5/2/2006		75	59	69	10	33

Permit Number (Well Name)	Easting (NAD 83)	Northing (NAD 83)	Aquifer Name	Date Well Constructed	Date Well Plugged	Well Depth (ft)	Top of Screen (ft)	Bottom of Screen (ft)	Screen Length (ft)	Static Water Level (ft)
64048	528632.6	4486724	ALL UNNAMED AQUIFERS	4/27/2006		42	20	42	22	19
64049	528601.3	4486725	ALL UNNAMED AQUIFERS	4/28/2006		42	20	42	22	19
66354	528946.2	4495966	QUATERNARY ALLUVIUM	2/18/2008		39	26	36	10	16
67137	496726.1	4495122.5	QUATERNARY ALLUVIUM	7/15/2008		60	32	42	10	26
68786	528975.6	4489747.5	ALL UNNAMED AQUIFERS	12/18/2009		27	17	27	10	7
78834	510555.2	4526924.7	LARAMIE FOX HILLS	2/2/1995		168	150	168	18	51
85476	495921.4	4508138.9	ALL UNNAMED AQUIFERS	12/13/2002		50	20	50	30	34
90811	501981.9	4520973	ALL UNNAMED AQUIFERS	8/6/2007		400	360	400	40	150
91385	531610.4	4494726.8	ALL UNNAMED AQUIFERS	8/27/1991		320	260	320	60	110
92985	522583.6	4492914	ALL UNNAMED AQUIFERS	6/15/2006		40	20	40	20	30
101249	522613.8	4492277.8	ALL UNNAMED AQUIFERS	5/30/2002		43	23	43	20	30
106097	531100	4498591.5	ALL UNNAMED AQUIFERS	6/18/1990		33	23	33	10	15
112978	533718.6	4488932.2	LARAMIE FOX HILLS	8/20/1990		342	282	342	60	164
129076	502021.7	4487770	ALL UNNAMED AQUIFERS	10/18/1991		45	25	45	20	12
139265	520680.2	4497644.5	QUATERNARY ALLUVIUM	9/5/2008		40	20	40	20	28
149818	515065.9	4509875.2	ALL UNNAMED AQUIFERS	1/16/1998		48	28	48	20	21
151317	515349.4	4488363.3	ALL UNNAMED AQUIFERS	2/7/1990		45	35	45	10	36
156336	502754.9	4495243.6	ALL UNNAMED AQUIFERS	5/22/1990		35	15	35	20	10
156974	518264	4498778.9	ALL UNNAMED AQUIFERS	5/25/1990		36	27	32	5	16
156974	518264	4498778.9	ALL UNNAMED AQUIFERS			36	27	32	5	16
157149	502664.9	4495228.7	ALL UNNAMED AQUIFERS	6/30/1990	7/19/1996	36	20	36	16	18
157149	502664.7	4495213.6	ALL UNNAMED AQUIFERS	3/23/1996		58	18	38	20	16
157384	519229.5	4503495.5	ALL UNNAMED AQUIFERS	5/15/1990		50	30	50	20	20
157669	498794.8	4490886.1	ALL UNNAMED AQUIFERS	6/12/1990		35	20	35	15	8
158279	504123.8	4527800.8	ALL UNNAMED AQUIFERS	6/19/1991		41	18	38	20	16
158680	502294.3	4487095	ALL UNNAMED AQUIFERS	11/2/1990		41	19	39	20	5
158923	519166.3	4505771	ALL UNNAMED AQUIFERS	3/29/1991		36	26	36	10	16
158972	495946.9	4521082.2	ALL UNNAMED AQUIFERS	10/15/1997		560	490	550	60	71
159014	495179.7	4488004.6	ALL UNNAMED AQUIFERS	12/18/1990		48	28	48	20	14
159014	495179.7	4488004.6	ALL UNNAMED AQUIFERS	12/18/1990		48	28	48	20	14
159167	526785	4494062.3	ALL UNNAMED AQUIFERS	3/18/1992		30	19	30	11	3
160256	528910.5	4503600	ALL UNNAMED AQUIFERS	7/11/1991		140	100	140	40	60
160408	524279.5	4486515.7	ALL UNNAMED AQUIFERS	7/5/1991		72	51	71	20	30
160445	514150.1	4487426.3	ALL UNNAMED AQUIFERS	7/11/1991		55	45	55	10	20
161181	517242.2	4532666.7	ALL UNNAMED AQUIFERS	12/14/1991		320	300	320	20	190
161529	501463.6	4508224.4	ALL UNNAMED AQUIFERS	9/23/1991		60	40	60	20	20
161530	501346.8	4507874.9	ALL UNNAMED AQUIFERS	8/25/1994		30	19	30	11	6
161865	529458.5	4500299.4	LARAMIE FOX HILLS	10/10/1991		450	415	450	35	132
162033	531610.4	4494726.8	LARAMIE FOX HILLS	8/27/1991		320	260	320	60	110
165031	502002.1	4508481.9	ALL UNNAMED AQUIFERS	8/27/1992		30	11	30	19	10

Permit Number (Well Name)	Easting (NAD 83)	Northing (NAD 83)	Aquifer Name	Date Well Constructed	Date Well Plugged	Well Depth (ft)	Top of Screen (ft)	Bottom of Screen (ft)	Screen Length (ft)	Static Water Level (ft)
165267	500344	4514735.5	ALL UNNAMED AQUIFERS	8/20/1992		32	13	32	19	10
165323	519201.3	4505183	ALL UNNAMED AQUIFERS	4/24/1993		47	27	47	20	23
166963	507869.3	4522784.1	ALL UNNAMED AQUIFERS	4/14/1993		25	5	25	20	6
167522	516071.7	4521982.5	LARAMIE	9/14/1992		240	200	240	40	135
167632	531610.4	4494726.8	ALL UNNAMED AQUIFERS	8/27/1991		320	260	320	60	110
169203	495817.9	4495109.7	ALL UNNAMED AQUIFERS	6/16/1993		28	13	23	10	13
170390	529855.6	4489356.2	ALL UNNAMED AQUIFERS	10/20/1993		35	15	35	20	6
170715	515076.9	4509848.7	ALL UNNAMED AQUIFERS	8/24/1993		44	22	40	18	23
171177	501756.5	4508177.9	ALL UNNAMED AQUIFERS	9/23/1993		40	20	40	20	22
171364	502076.3	4488970.6	ALL UNNAMED AQUIFERS	3/31/1994		56	46	51	5	11
174163	496655.3	4490177.6	ALL UNNAMED AQUIFERS	2/24/1992	4/9/1996	28	17	28	11	24
174164	496636.9	4490031.1	ALL UNNAMED AQUIFERS	2/24/1992	4/9/1996	28	17	28	11	22
174165	496396.8	4490076.6	ALL UNNAMED AQUIFERS	2/25/1992	4/8/1996	28	17	26	9	24
174166	496446.5	4490133.6	ALL UNNAMED AQUIFERS	2/25/1992	4/9/1996	27	17	27	10	24
174167	496480.6	4490160.6	ALL UNNAMED AQUIFERS	2/26/1992	4/9/1996	28	18	28	10	25
174168	496518.7	4490099.6	ALL UNNAMED AQUIFERS	2/26/1992	4/8/1996	28	18	28	10	23
174169	496507.4	4490107.1	ALL UNNAMED AQUIFERS	5/4/1992	6/30/1995	30	19	30	11	22
174170	496537.9	4490008.1	ALL UNNAMED AQUIFERS	5/4/1992	4/8/1996	30	20	30	10	23
174814	503429.5	4529049.4	ALL UNNAMED AQUIFERS	1/20/1994		50	30	50	20	22
174865	500495.3	4490065.6	ALL UNNAMED AQUIFERS	8/31/1995		38	28	33	5	8
175485	520590.7	4497221.4	ALL UNNAMED AQUIFERS	8/17/1993		42	22	42	20	25
176717	515856.6	4499674.5	LARAMIE FOX HILLS	4/1/1994		200	140	200	60	39
178200	500360.5	4514604.5	ALL UNNAMED AQUIFERS	5/20/1996		35	15	35	20	9
179048	504148.1	4529077.9	ALL UNNAMED AQUIFERS	2/22/1995		41	24	41	17	31
179820	520190	4498590.9	ALL UNNAMED AQUIFERS	8/28/1999		36	26	36	10	21
182683	510193.6	4527092.2	ALL UNNAMED AQUIFERS	12/20/1994		275	215	275	60	28
183016	500187.7	4505151	ALL UNNAMED AQUIFERS	7/10/1995		60	40	60	20	18
183716	498478.5	4499869.8	ALL UNNAMED AQUIFERS	2/10/1995		82	42	82	40	18
183900	502323.5	4487463.5	ALL UNNAMED AQUIFERS	3/1/1995		45	30	45	15	12
186294	497540.6	4508241.4	ALL UNNAMED AQUIFERS	7/25/1995		27	17	27	10	10
186577	520318.1	4498780.4	ALL UNNAMED AQUIFERS	1/19/1998		39	31	36	5	25
187641	504605.2	4529015.9	ALL UNNAMED AQUIFERS	7/8/1995		100	70	90	20	32
190310	500530.3	4517375.6	ALL UNNAMED AQUIFERS	10/28/1995		21	10	21	11	9
192619	510208.8	4526768.2	LARAMIE FOX HILLS	4/11/1996		120	80	120	40	26
192620	510226.2	4526765.2	LARAMIE FOX HILLS	4/5/1996		120	80	120	40	26
192675	528043.4	4490836	ALL UNNAMED AQUIFERS	5/31/2005		40	16	40	24	17
192947	500329.5	4514665.5	ALL UNNAMED AQUIFERS	5/16/1996		33	13	33	20	9
193154	506145.7	4506547.3	ALL UNNAMED AQUIFERS	5/8/1996		400	340	400	60	215
193738	510149.3	4526878.7	ALL UNNAMED AQUIFERS	4/16/1996		120	80	120	40	25
193850	502647.2	4494199.1	ALL UNNAMED AQUIFERS	5/6/1996		36	16	36	20	6

Permit Number (Well Name)	Easting (NAD 823	Northing (NAD 83)	Aquifer Name	Date Well Constructed	Date Well Plugged	Well Depth (ft)	Top of Screen (ft)	Bottom of Screen (ft)	Screen Length (ft)	Static Water Level (ft)
194173	506990.3	4506422	ALL UNNAMED AQUIFERS	5/1/1996		370	300	360	60	212
194907	497913.2	4500498.3	ALL UNNAMED AQUIFERS	7/1/1996		58	38	58	20	8
195444	518645.6	4507101.6	ALL UNNAMED AQUIFERS	9/29/1999		340	270	330	60	40
196167	498793.6	4513250.5	ALL UNNAMED AQUIFERS	8/30/1996		30	16	30	14	15
196516	505952.4	4513732.4	ALL UNNAMED AQUIFERS	10/28/1996		550	490	550	60	258
196630	504519.2	4529223.4	LARAMIE FOX HILLS	8/20/1996		120	80	110	30	29
197028	509904.7	4527344.2	LARAMIE FOX HILLS	8/23/1996		120	80	120	40	30
198793	510166.9	4527010.2	ALL UNNAMED AQUIFERS	2/24/1997		120	80	120	40	19
199434	499933	4513120	ALL UNNAMED AQUIFERS	11/11/1996		30	15	30	15	15
203323	516022.1	4487433.3	ALL UNNAMED AQUIFERS	5/20/1998		60	40	60	20	18
203772	510259.1	4493969	ALL UNNAMED AQUIFERS	9/3/1997		340	310	340	30	10
203832	507883.5	4509086.3	ALL UNNAMED AQUIFERS	5/26/2004		700	600	660	60	248
204472	502301.8	4520973.7	ALL UNNAMED AQUIFERS	8/29/1997		360	310	360	50	100
204702	509706.5	4495016	ALL UNNAMED AQUIFERS	9/23/1997		360	290	350	60	18
205529	502857.5	4514821	ALL UNNAMED AQUIFERS	2/1/1998		340	270	330	60	68
205576	507473.1	4508397.8	ALL UNNAMED AQUIFERS	12/13/1998		600	530	590	60	130
205577	507477.8	4508800.3	ALL UNNAMED AQUIFERS	8/10/1999		620	550	610	60	128
206553	502719.5	4521059.7	ALL UNNAMED AQUIFERS	12/29/1997		400	340	400	60	85
206554	502505.5	4520902.2	ALL UNNAMED AQUIFERS	1/2/1998		450	390	450	60	130
206786	525707.1	4505913.5	ALL UNNAMED AQUIFERS	1/16/1998		640	600	640	40	183
206925	495236.4	4511719	ALL UNNAMED AQUIFERS	4/26/2000		220	170	210	40	32
208150	512715.1	4515404.9	ALL UNNAMED AQUIFERS	3/26/1998		46	26	46	20	20
208572	511443	4514813.9	ALL UNNAMED AQUIFERS	5/20/1998		618	538	598	60	242
209595	505166.3	4508465.3	ALL UNNAMED AQUIFERS	12/20/1998		450	390	450	60	170
209650	506477.3	4510037.3	ALL UNNAMED AQUIFERS	12/9/1998		600	540	600	60	270
211256	515852.2	4500240.5	LARAMIE FOX HILLS	8/3/1998		680	620	660	40	100
212329	529652.9	4489227.2	ALL UNNAMED AQUIFERS	8/6/2000		220	170	210	40	70
213351	495631.7	4499729.3	ALL UNNAMED AQUIFERS	7/15/1998		22	12	22	10	16
213759	503105.4	4485830	ALL UNNAMED AQUIFERS	2/8/1999		30	20	30	10	12
213910	515078.8	4501862	ALL UNNAMED AQUIFERS	1/23/2008		160	115	160	45	73
214263	528920.9	4529385.5	ALL UNNAMED AQUIFERS	8/23/1998		228	218	228	10	160
214811	530562.3	4496420.8	ALL UNNAMED AQUIFERS	2/23/1999		30	10	30	20	6
215381	512740.1	4515002.8	ALL UNNAMED AQUIFERS	5/24/1999		31	20	31	11	24
215382	512740.5	4514813.3	ALL UNNAMED AQUIFERS	12/27/1999		42	22	42	20	20
216364	515844	4513287	ALL UNNAMED AQUIFERS	12/19/2003		560	420	480	60	112
216491	529879.5	4485923.2	LARAMIE FOX HILLS	4/12/1999		300	220	280	60	93
216802	510205.6	4526781.7	ALL UNNAMED AQUIFERS	8/27/1999		120	60	120	60	16
216862	521689.1	4511410.1	ALL UNNAMED AQUIFERS	5/26/1999		323	223	283	60	28
217217	510172.6	4527059.2	ALL UNNAMED AQUIFERS	8/25/1999		117	57	117	60	31
217536	499116.7	4521060.7	ALL UNNAMED AQUIFERS	7/10/1999		540	420	480	60	20

Permit Number (Well Name)	Easting (NAD 83)	Northing (NAD 83)	Aquifer Name	Date Well Constructed	Date Well Plugged	Well Depth (ft)	Top of Screen (ft)	Bottom of Screen (ft)	Screen Length (ft)	Static Water Level (ft)
218126	498711.3	4492297.7	ALL UNNAMED AQUIFERS	7/2/1999	7/14/2007	42	27	42	15	7
218126	498719	4492299	QUATERNARY ALLUVIUM	6/24/2007		47	30	47	17	12
218290	509449.5	4502766.7	ALL UNNAMED AQUIFERS	12/6/2000		740	660	720	60	260
218483	498426.5	4501102.3	ALL UNNAMED AQUIFERS	9/23/1999		50	30	50	20	13
218509	499879.4	4506118.4	ALL UNNAMED AQUIFERS	12/1/1998		23	8	23	15	15
218510	499889.7	4506118.4	ALL UNNAMED AQUIFERS	1/5/1999	3/5/2008	24	9	24	15	14
218511	499871.2	4506126.4	ALL UNNAMED AQUIFERS	12/2/1998	3/5/2008	24	9	15	6	15
218512	499890.1	4506131.9	ALL UNNAMED AQUIFERS	12/2/1998	3/5/2008	23	8	23	15	15
218831	520899.9	4506951	ALL UNNAMED AQUIFERS	1/21/2000		460	390	450	60	185
219124	509198.6	4498732.6	ALL UNNAMED AQUIFERS	12/22/1999		565	485	545	60	90
219275	513111.6	4521218.5	ALL UNNAMED AQUIFERS	11/13/1999		200	130	190	60	93
219455	506899.9	4493061.5	ALL UNNAMED AQUIFERS	7/30/2002		60	40	60	20	30
219458	511077.9	4520859.5	ALL UNNAMED AQUIFERS	4/28/2001		200	150	190	40	90
219459	510513.5	4521090	ALL UNNAMED AQUIFERS	4/27/2001		220	170	210	40	72
220182	521124.4	4517031.3	ALL UNNAMED AQUIFERS	7/9/2001		390	290	330	40	105
220186	512274.6	4516403.4	ALL UNNAMED AQUIFERS	12/29/1999		200	150	190	40	10
220787	512677	4516398.4	ALL UNNAMED AQUIFERS	12/29/1999		42	22	42	20	20
220796	529580.8	4492334.8	ALL UNNAMED AQUIFERS	7/19/2002		40	20	40	20	17
221110	530464.2	4499224.9	ALL UNNAMED AQUIFERS	5/20/2000		284	240	280	40	79
222491	510099.9	4526846.7	ALL UNNAMED AQUIFERS	1/25/2000		100	40	100	60	17
222657	511446.7	4516847.4	ALL UNNAMED AQUIFERS	2/7/2000		40	11	31	20	12
222812	515889	4486765.3	ALL UNNAMED AQUIFERS	7/25/2000		270	210	250	40	12
222960	527450.3	4519730.3	LARAMIE	4/17/2000		145	112	132	20	42
223323	509396.4	4502202.2	ALL UNNAMED AQUIFERS	2/18/2000		700	640	700	60	230
223852	496596.7	4507678.4	ALL UNNAMED AQUIFERS	9/20/2000		43	23	43	20	23
223985	506463.3	4515404.5	ALL UNNAMED AQUIFERS	1/24/2001		560	350	410	60	200
223986	506559.4	4514917.4	ALL UNNAMED AQUIFERS	1/26/2001		400	360	390	30	200
224111	507814.5	4509706.3	ALL UNNAMED AQUIFERS	4/25/2000		700	640	700	60	233
224131	514636.4	4513761.3	ALL UNNAMED AQUIFERS	6/28/2000		632	552	612	60	226
224133	512293	4508207.2	ALL UNNAMED AQUIFERS	3/20/2000		700	640	700	60	149
224157	500003	4511070.9	ALL UNNAMED AQUIFERS	8/29/2001		33	19	29	10	12
224288	507307	4509308.8	ALL UNNAMED AQUIFERS	4/15/2000		700	640	700	60	228
224847	498671.1	4520417	ALL UNNAMED AQUIFERS	6/26/2005		880	800	860	60	59
224847	498668	4520417.2	ALL UNNAMED AQUIFERS	10/12/2000		660	570	630	60	415
225223	520152.6	4506597.5	ALL UNNAMED AQUIFERS	6/4/2001		560	500	560	60	81
225224	520353.7	4506595.5	ALL UNNAMED AQUIFERS	2/19/2001		360	270	330	60	200
225290	522864.6	4486113.2	ALL UNNAMED AQUIFERS	5/29/2000		50	30	50	20	25
225373	508271.8	4508238.8	ALL UNNAMED AQUIFERS	10/15/2000		720	660	720	60	234
225470	525513.7	4504644	ALL UNNAMED AQUIFERS	7/6/2000		635	575	615	40	215
225499	509842.5	4494859	ALL UNNAMED AQUIFERS	5/21/2000		360	290	350	60	9

Permit Number (Well Name)	Easting (NAD 83)	Northing (NAD 83)	Aquifer Name	Date Well Constructed	Date Well Plugged	Well Depth (ft)	Top of Screen (ft)	Bottom of Screen (ft)	Screen Length (ft)	Static Water Level (ft)
225823	508746.6	4502117.2	ALL UNNAMED AQUIFERS	6/13/2000		700	630	690	60	72
225944	498182	4519516	ALL UNNAMED AQUIFERS	9/27/2001		440	380	440	60	17
225967	505455.5	4505143.3	ALL UNNAMED AQUIFERS	6/20/2000		360	300	360	60	200
226364	520539.7	4506594	ALL UNNAMED AQUIFERS	5/19/2001		440	380	440	60	86
226366	520742.6	4506333	ALL UNNAMED AQUIFERS	12/14/2000		200	150	190	40	80
226525	505041.6	4500332.7	ALL UNNAMED AQUIFERS	9/15/2000		340	290	330	40	60
226579	498180	4519177.7	ALL UNNAMED AQUIFERS	7/19/2000		440	380	440	60	230
226595	510047.2	4526938.2	ALL UNNAMED AQUIFERS	7/11/2000		100	40	100	60	18
226629	506129.3	4508396.3	ALL UNNAMED AQUIFERS	10/6/2000		700	640	700	60	255
227069	507351.1	4500337.7	ALL UNNAMED AQUIFERS	10/12/2000		740	680	740	60	255
227081	512508.4	4516714.4	ALL UNNAMED AQUIFERS	7/31/2000		200	150	190	40	60
227518	517520.8	4498705.5	ALL UNNAMED AQUIFERS	8/23/2000		200	130	190	60	0
227585	516263.4	4495980.9	ALL UNNAMED AQUIFERS	9/14/2000		420	360	420	60	90
228537	510144.7	4526938.7	ALL UNNAMED AQUIFERS	10/20/2000		100	40	100	60	20
228634	507333.9	4503807.7	ALL UNNAMED AQUIFERS	10/6/2000		400	350	390	40	165
228634	507333.8	4503813.7	ALL UNNAMED AQUIFERS	12/11/2000		600	540	600	60	86
228946	515915.8	4512564.5	ALL UNNAMED AQUIFERS	5/17/2001		620	560	620	60	197
228967	504553.7	4521317.2	ALL UNNAMED AQUIFERS	11/19/2000		580	520	580	60	400
229036	498272.5	4498651.8	ALL UNNAMED AQUIFERS	6/20/2001		78	58	78	20	24
229052	510488.3	4527062.7	ALL UNNAMED AQUIFERS	5/23/2000		100	100	80	20	20
229183	532051.3	4495533.8	ALL UNNAMED AQUIFERS	12/16/2002		400	320	380	60	123
229184	532084.3	4497027.5	ALL UNNAMED AQUIFERS	10/8/2007		360	310	360	50	140
229375	503936.6	4521402.2	ALL UNNAMED AQUIFERS	10/31/2000		420	370	410	40	95
229378	504363.2	4521739.2	ALL UNNAMED AQUIFERS	1/19/2001		580	510	570	60	380
229510	502380.4	4508457.9	ALL UNNAMED AQUIFERS	12/21/2000		32	18	32	14	17
229556	507754	4515309.9	ALL UNNAMED AQUIFERS	7/12/2001		620	520	560	40	360
229864	510065.2	4527303.7	ALL UNNAMED AQUIFERS	3/30/2001		140	100	140	40	30
229865	509999.6	4527303.7	ALL UNNAMED AQUIFERS	1/17/2001		60	20	60	40	25
229869	510420.3	4526966.2	ALL UNNAMED AQUIFERS	12/19/2002		100	60	100	40	33
230098	514827.9	4498304.5	ALL UNNAMED AQUIFERS	12/3/2001		620	560	620	60	70
230559	512565.9	4507263.7	ALL UNNAMED AQUIFERS	2/1/2001		600	540	600	60	85
231113	518670.4	4506815.5	ALL UNNAMED AQUIFERS	3/1/2001		360	280	340	60	50
231772	516379.2	4495160.4	ALL UNNAMED AQUIFERS	3/21/2001		500	430	490	60	120
231773	516650.7	4495043.4	ALL UNNAMED AQUIFERS	3/22/2001		420	350	410	60	60
231929	508998.5	4505141.2	ALL UNNAMED AQUIFERS	3/14/2001		740	690	730	40	218
232419	522826.3	4490847.5	ALL UNNAMED AQUIFERS	6/1/2007		240	200	240	40	135
232626	516695.7	4486088	ALL UNNAMED AQUIFERS	1/21/2005		850	770	810	40	20
232631	520889.2	4507404	LARAMIE FOX HILLS	5/24/2001		680	620	680	60	147
232661	516072.2	4502842.1	LARAMIE FOX HILLS	5/30/2001		400	380	440	60	78
232676	508255.6	4506575.2	ALL UNNAMED AQUIFERS	8/26/2002		700	640	700	60	220

Permit Number (Well Name)	Easting (NAD 83)	Northing (NAD 83)	Aquifer Name	Date Well Constructed	Date Well Plugged	Well Depth (ft)	Top of Screen (ft)	Bottom of Screen (ft)	Screen Length (ft)	Static Water Level (ft)
232677	508456.7	4506572.2	ALL UNNAMED AQUIFERS	12/24/2001		700	620	680	60	230
232773	505598.2	4511514.4	ALL UNNAMED AQUIFERS	7/4/2001		620	540	580	40	280
233026	511056.9	4519463	ALL UNNAMED AQUIFERS	10/18/2002		240	190	230	40	59
233033	519330.3	4507144.1	ALL UNNAMED AQUIFERS	9/19/2001		640	580	640	60	90
233034	519323.5	4507345.1	ALL UNNAMED AQUIFERS	8/28/2002		700	640	700	60	190
233322	501996.2	4508803.4	ALL UNNAMED AQUIFERS	11/21/2002		30	15	30	15	14
234337	510461.4	4527383.7	ALL UNNAMED AQUIFERS	7/20/2001		90	50	90	40	25
234411	505541.2	4511827	ALL UNNAMED AQUIFERS	1/12/2005		840	740	800	60	260
234434	520763.9	4506790	ALL UNNAMED AQUIFERS	3/20/2002		680	620	680	60	160
234752	516063.2	4503302.6	LARAMIE FOX HILLS	9/25/2001		300	200	260	60	60
234866	511276.6	4520609	ALL UNNAMED AQUIFERS	8/30/2002		200	150	190	40	22
235642	511075.9	4493970.5	ALL UNNAMED AQUIFERS	9/12/2001		400	330	390	60	0
235957	509307.1	4503525	ALL UNNAMED AQUIFERS	5/6/2008		420	360	410	50	180
236307	515895.4	4511784.2	LARAMIE FOX HILLS	11/19/2001		540	480	540	60	232
236313	513335.4	4519237.4	ALL UNNAMED AQUIFERS	1/5/2002		200	150	190	40	68
236687	498887.8	4521040.7	ALL UNNAMED AQUIFERS	11/7/2001		500	430	490	60	35
236710	508991.2	4505600.2	ALL UNNAMED AQUIFERS	11/14/2001		760	700	760	60	210
237321	512872.1	4508691.2	ALL UNNAMED AQUIFERS	1/29/2002		500	440	500	60	125
237436	510352.1	4526767.7	ALL UNNAMED AQUIFERS	10/24/2003		120	85	105	20	18
237437	510306.3	4526767.7	LARAMIE	7/8/2003		12	90	110	20	20
237438	510296.8	4526813.2	ALL UNNAMED AQUIFERS	7/30/2003		125	105	125	20	25
237717	514435.1	4499457	LARAMIE FOX HILLS	5/10/2002		710	630	690	60	154
238266	497370.2	4520131.2	ALL UNNAMED AQUIFERS	1/22/2002		440	380	440	60	25
238403	527878.6	4485971.2	ALL UNNAMED AQUIFERS	4/10/2002		65	38	65	27	17
238799	511443	4514813.9	ALL UNNAMED AQUIFERS	5/20/1998		618	538	598	60	242
238897	506545.2	4509748.5	ALL UNNAMED AQUIFERS	2/4/2005		640	560	620	60	400
238942	507693.8	4510858.3	LARAMIE FOX HILLS	11/24/2003		780	700	760	60	259
239166	507351.1	4500337.7	ALL UNNAMED AQUIFERS	10/12/2000		740	680	740	60	255
239457	496969.6	4520943.2	ALL UNNAMED AQUIFERS	6/4/2002		500	380	440	60	200
239625	507333.9	4503807.7	ALL UNNAMED AQUIFERS	12/11/2000		600	540	600	60	86
239626	507912	4503865.7	ALL UNNAMED AQUIFERS	6/20/2002		660	600	660	60	114
240014	521890.3	4506875.5	ALL UNNAMED AQUIFERS	1/27/2004		660	580	640	60	70
240243	521668.4	4506952	ALL UNNAMED AQUIFERS	4/23/2005		625	585	625	40	180
240309	514278.5	4508340.2	ALL UNNAMED AQUIFERS	8/27/2002		440	140	200	60	61
240310	514276.1	4508742.7	ALL UNNAMED AQUIFERS	12/11/2002		400	180	240	60	81
240426	511966.8	4508166.2	ALL UNNAMED AQUIFERS	3/20/2000		700	640	700	60	150
240658	497456.4	4520876.7	ALL UNNAMED AQUIFERS	6/10/2002		560	460	520	60	54
240809	507714.9	4509268.3	ALL UNNAMED AQUIFERS	4/15/2000		700	640	700	60	228
240810	507368.3	4509339.3	ALL UNNAMED AQUIFERS	4/1/2003		760	660	720	60	180
240867	521331.1	4505174	ALL UNNAMED AQUIFERS	11/1/2002		700	620	680	60	201

Permit Number (Well Name)	Easting (NAD 83)	Northing (NAD 83)	Aquifer Name	Date Well Constructed	Date Well Plugged	Well Depth (ft)	Top of Screen (ft)	Bottom of Screen (ft)	Screen Length (ft)	Static Water Level (ft)
241445	501432	4486652.5	ALL UNNAMED AQUIFERS	6/10/2002		100	40	100	60	20
242025	504853.5	4508982.5	ALL UNNAMED AQUIFERS	7/30/2004		860	800	860	60	167
242032	507878.4	4504138.2	ALL UNNAMED AQUIFERS	9/17/2002		660	600	660	60	125
242473	506258.2	4509032.3	ALL UNNAMED AQUIFERS	11/22/2002		460	410	450	40	62
242477	510470.9	4526940	ALL UNNAMED AQUIFERS	10/29/2003		125	105	125	20	19
242735	520903	4506496	ALL UNNAMED AQUIFERS	1/23/2003		680	620	680	60	185
242759	521619.1	4506524.5	ALL UNNAMED AQUIFERS	10/30/2003		660	580	640	60	194
243392	521710.1	4506594	ALL UNNAMED AQUIFERS	3/24/2004		660	600	660	60	200
243405	496069	4514427.5	ALL UNNAMED AQUIFERS	7/15/2003		950	890	950	60	140
243910	501346.8	4507874.9	ALL UNNAMED AQUIFERS	8/25/1994		30	19	30	11	6
244816	520334.8	4506702.5	ALL UNNAMED AQUIFERS	12/30/2003		550	470	530	60	47
244845	519334.4	4495227.9	ALL UNNAMED AQUIFERS	9/23/2003		40	21	40	19	17
244892	507237.4	4504229.7	ALL UNNAMED AQUIFERS	1/28/2003		660	440	500	60	62
244996	501942.9	4508573.5	ALL UNNAMED AQUIFERS	8/23/2004		38	13	38	25	8
245550	522907.8	4504971	ALL UNNAMED AQUIFERS	9/4/2004		680	620	680	60	140
245553	523358.8	4504989	ALL UNNAMED AQUIFERS	5/27/2004		680	620	680	60	73
245852	504056.3	4528864.9	ALL UNNAMED AQUIFERS	1/16/2003		48	33	48	15	28
245910	519417.1	4487420.7	ALL UNNAMED AQUIFERS	5/21/2002		42	32	42	10	16
245912	507659	4489121	ALL UNNAMED AQUIFERS	6/6/2002		22	12	22	10	6
245945	502458.8	4516454	ALL UNNAMED AQUIFERS	2/15/2003		16	8	16	8	12
245951	508456.7	4506572.2	ALL UNNAMED AQUIFERS	12/24/2001		680	620	680	60	230
245993	510747.9	4527099.7	ALL UNNAMED AQUIFERS	6/20/2003		97	67	87	20	35
246684	496416.1	4494060.7	ALL UNNAMED AQUIFERS	4/2/2003		30	20	30	10	10
247352	520822.5	4499640.5	ALL UNNAMED AQUIFERS	11/16/2004		34	24	34	10	26
247353	522350.4	4499650.5	ALL UNNAMED AQUIFERS	11/18/2003		30	20	30	10	22
248237	529760	4498814.4	ALL UNNAMED AQUIFERS	6/23/2003		30	10	30	20	12
248259	526048	4498130.9	ALL UNNAMED AQUIFERS	4/16/2003		440	380	440	60	155
248658	500778.1	4501933	ALL UNNAMED AQUIFERS	2/24/2005		40	20	40	20	19
249026	515286.9	4501796.5	ALL UNNAMED AQUIFERS	12/17/2004		440	320	380	60	96
249114	507644.6	4506827.5	ALL UNNAMED AQUIFERS	6/24/2004		700	600	660	60	235
249204	510144.6	4526964	ALL UNNAMED AQUIFERS	10/25/2003		170	145	165	20	22
251484	520704.4	4503635.5	ALL UNNAMED AQUIFERS	7/18/2006		510	480	510	30	200
251657	500778.5	4502024.5	ALL UNNAMED AQUIFERS	2/25/2005		38	20	38	18	19
251706	504711.8	4529647.9	ALL UNNAMED AQUIFERS	3/12/2004		240	185	220	35	67
251927	517435.6	4488459.8	ALL UNNAMED AQUIFERS	11/18/2003		30	5	30	25	1
251945	510748.7	4527316	ALL UNNAMED AQUIFERS	11/11/2003		100	80	100	20	27
252350	509391.4	4506211.2	ALL UNNAMED AQUIFERS	11/4/2003		490	710	770	60	195
252704	509434.9	4507741.2	ALL UNNAMED AQUIFERS	11/18/2003		780	720	780	60	210
252716	514402.4	4515572.5	ALL UNNAMED AQUIFERS	5/1/2006		400	220	280	60	68
252831	530999.7	4492149.8	ALL UNNAMED AQUIFERS	9/15/2003		41	21	41	20	15

Permit Number (Well Name)	Easting (NAD 83)	Northing (NAD 83)	Aquifer Name	Date Well Constructed	Date Well Plugged	Well Depth (ft)	Top of Screen (ft)	Bottom of Screen (ft)	Screen Length (ft)	Static Water Level (ft)
253118	511056.6	4508779.5	ALL UNNAMED AQUIFERS	9/16/2005		400	350	400	50	180
253214	530184.6	4493815.5	ALL UNNAMED AQUIFERS	8/18/2004		40	8	28	20	8
253308	508680.1	4506329.7	ALL UNNAMED AQUIFERS	1/21/2004		740	660	720	60	196
253334	518116.9	4522386.4	ALL UNNAMED AQUIFERS	11/26/2003		150	90	150	60	40
253434	518935.8	4502664	ALL UNNAMED AQUIFERS	8/30/2006		42	22	42	20	30
253895	516181.5	4511385.5	ALL UNNAMED AQUIFERS	6/11/2006		520	480	520	40	220
253897	516684.5	4511389	ALL UNNAMED AQUIFERS	12/13/2008		520	480	520	40	92
254000	508520.3	4506513.2	ALL UNNAMED AQUIFERS	2/25/2004		740	660	720	60	211
254064	510083.9	4526822.2	ALL UNNAMED AQUIFERS	12/19/2003		150	130	150	20	33
254224	508513.8	4506696.2	LARAMIE FOX HILLS	1/26/2004		740	640	700	60	216
254477	498976.4	4519675.5	ALL UNNAMED AQUIFERS	2/7/2004		760	640	700	60	69
254740	515308.5	4514880.5	ALL UNNAMED AQUIFERS	5/22/2004		429	329	369	40	85
255097	508706.2	4506510.2	LARAMIE FOX HILLS	2/19/2004		740	660	720	60	203
255269	510067.4	4527060.2	ALL UNNAMED AQUIFERS	5/16/2004		200	160	180	20	36
255305	498831.5	4520243.5	ALL UNNAMED AQUIFERS	3/17/2004		840	760	820	60	60
255311	519894.1	4501977	ALL UNNAMED AQUIFERS	4/9/2004		48	28	48	20	22
256117	501890.9	4519098.5	ALL UNNAMED AQUIFERS	1/18/2005		720	560	620	60	117
256209	511057.7	4509049	ALL UNNAMED AQUIFERS	10/29/2004		700	560	620	60	247
256245	530760.8	4531380.1	ALL UNNAMED AQUIFERS	6/25/2004		400	360	400	40	197
256400	515893.5	4486471.5	ALL UNNAMED AQUIFERS	8/15/2004		700	640	680	40	21
256558	520761.1	4507186.5	ALL UNNAMED AQUIFERS	6/16/2004		680	620	680	60	157
256711	501932.3	4519253.5	ALL UNNAMED AQUIFERS	12/15/2004		720	640	700	60	90
256920	524048.9	4490110.2	ALL UNNAMED AQUIFERS	5/17/2004		60	38	60	22	30
258315	500711.7	4518274	ALL UNNAMED AQUIFERS	8/31/2004		800	720	780	60	29
258346	520262.8	4502032.5	ALL UNNAMED AQUIFERS	10/5/2004		40	20	40	20	24
258347	524288.3	4505543.5	ALL UNNAMED AQUIFERS	3/18/2005		660	520	580	60	174
258348	524273.7	4505284.5	ALL UNNAMED AQUIFERS	3/16/2005		660	600	660	60	177
258776	507197.4	4506680.5	ALL UNNAMED AQUIFERS	2/15/2005		660	560	620	60	256
258795	510119.3	4527223.5	ALL UNNAMED AQUIFERS	3/8/2005		250	210	250	40	20
258898	510382.9	4527062.2	ALL UNNAMED AQUIFERS	8/1/2007		120	100	120	20	30
259516	508699.7	4506693.5	LARAMIE FOX HILLS	2/11/2005		780	660	720	60	205
259521	528652.7	4487710.5	ALL UNNAMED AQUIFERS	2/21/2005		43	23	43	20	21
260337	528349.3	4498824	ALL UNNAMED AQUIFERS	11/23/2004		35	10	30	20	11
260488	508199.4	4512093.5	ALL UNNAMED AQUIFERS	12/30/2004		720	620	680	60	249
260636	506937	4514646	ALL UNNAMED AQUIFERS	4/5/2006		820	720	780	60	160
260750	520249.6	4505204	ALL UNNAMED AQUIFERS	11/22/2006		28	11	28	17	14
260808	510387.5	4526159	ALL UNNAMED AQUIFERS	3/10/2005		150	90	150	60	20
261616	525031	4526676.5	ALL UNNAMED AQUIFERS	2/3/2005		100	70	90	20	22
261884	516120.1	4519433.5	ALL UNNAMED AQUIFERS	1/24/2008		340	300	340	40	123
262391	510114.5	4526818.5	ALL UNNAMED AQUIFERS	7/5/2005		225	115	135	20	30

Permit Number (Well Name)	Easting (NAD 83)	Northing (NAD 83)	Aquifer Name	Date Well Constructed	Date Well Plugged	Well Depth (ft)	Top of Screen (ft)	Bottom of Screen (ft)	Screen Length (ft)	Static Water Level (ft)
262719	530930	4487702	ALL UNNAMED AQUIFERS	5/25/2005		55	25	55	30	12
262745	511222	4520147	ALL UNNAMED AQUIFERS	5/12/2005		280	180	240	60	30
262800	510402.9	4493357	ALL UNNAMED AQUIFERS	8/15/2005		420	350	410	60	0
263014	517548.5	4506132.5	ALL UNNAMED AQUIFERS	12/14/2007		460	430	460	30	165
263344	512706.3	4503697	ALL UNNAMED AQUIFERS	9/30/2005		600	540	600	60	116
263480	518673.6	4506724.5	ALL UNNAMED AQUIFERS	3/1/2001		340	280	340	60	50
263658	498589	4520141	ALL UNNAMED AQUIFERS	6/29/2006		800	700	760	60	60
264169	512606.1	4504093	ALL UNNAMED AQUIFERS	6/2/2009		220	180	220	40	145
264172	501160.2	4532016	ALL UNNAMED AQUIFERS	8/20/2005		48	28	48	20	32
264303	515986.1	4505013	ALL UNNAMED AQUIFERS	9/30/2005		360	275	335	60	20
264565	511103.5	4510274.5	ALL UNNAMED AQUIFERS	8/5/2005		400	340	380	40	75
266280	518638	4506876	ALL UNNAMED AQUIFERS	9/16/2008		580	520	580	60	185
266442	510650.5	4510781.5	ALL UNNAMED AQUIFERS	5/16/2006		425	365	425	60	200
266443	511078.3	4511025.5	ALL UNNAMED AQUIFERS	1/28/2006		370	330	370	40	210
266777	508059.8	4505969	ALL UNNAMED AQUIFERS	4/11/2006		800	740	800	60	186
267138	511107	4512124.5	ALL UNNAMED AQUIFERS	5/11/2006		385	345	385	40	185
267139	511106.5	4512254.5	ALL UNNAMED AQUIFERS	1/23/2006		415	375	415	40	230
267296	500205.5	4490360	ALL UNNAMED AQUIFERS	5/2/2006		40	30	40	10	10
267403	501682.3	4518147.5	ALL UNNAMED AQUIFERS	2/15/2006		760	510	570	60	110
267404	520883.8	4509928	ALL UNNAMED AQUIFERS	2/6/2006		200	160	200	40	100
267405	520893.4	4510211.5	ALL UNNAMED AQUIFERS	2/4/2006		160	100	160	60	20
267561	520867.4	4511237	ALL UNNAMED AQUIFERS	3/7/2006		475	415	475	60	55
268002	519558	4510390	ALL UNNAMED AQUIFERS	11/23/2007		420	300	340	40	170
268143	497268.4	4505602.5	ALL UNNAMED AQUIFERS	10/31/2006		80	40	60	20	42
269051	508435.9	4511971	ALL UNNAMED AQUIFERS	7/14/2006		545	495	545	50	340
269199	511082.8	4511911.5	ALL UNNAMED AQUIFERS	6/28/2006		420	360	420	60	220
269264	505807.7	4513685	ALL UNNAMED AQUIFERS	9/20/2006		660	520	580	60	287
270048	501672.3	4488538.5	ALL UNNAMED AQUIFERS	9/6/2006		50	35	50	15	7
270201	502174	4520113	ALL UNNAMED AQUIFERS	9/15/2006		240	180	240	60	99
271415	522382.1	4487433.5	ALL UNNAMED AQUIFERS	5/7/2007		55	35	55	20	41
271727	516761.5	4513177.5	ALL UNNAMED AQUIFERS	1/18/2007		440	380	440	60	216
271955	510770.9	4510406	ALL UNNAMED AQUIFERS	1/24/2007		400	360	400	40	215
271956	510969.8	4510575.5	ALL UNNAMED AQUIFERS	1/22/2007		420	370	420	50	240
272023	501542	4519497	ALL UNNAMED AQUIFERS	3/31/2007		800	720	780	60	70
272556	517586.7	4506086.5	ALL UNNAMED AQUIFERS	2/17/2006		465	420	465	45	200
272728	501840	4520271	LARAMIE FOX HILLS	4/5/2007		560	500	560	60	100
272817	512784.6	4519509	ALL UNNAMED AQUIFERS	5/14/2007		160	110	150	40	62
273375	499938.6	4512295	ALL UNNAMED AQUIFERS	4/30/2007		27	20	27	7	18
274130	520765.1	4496347.5	ALL UNNAMED AQUIFERS	7/19/2007		50	30	50	20	26
274642	528096.8	4495278	ALL UNNAMED AQUIFERS	4/30/2008		60	25	45	20	20
274994	504544.1	4490125	ALL UNNAMED AQUIFERS	10/24/2007		40	20	40	20	6

Permit Number (Well Name)	Easting (NAD 83)	Northing (NAD 83)	Aquifer Name	Date Well Constructed	Date Well Plugged	Well Depth (ft)	Top of Screen (ft)	Bottom of Screen (ft)	Screen Length (ft)	Static Water Level (ft)
275288	529902.4	4492480.5	ALL UNNAMED AQUIFERS	9/28/2007		37	17	37	20	17
275648	521874.5	4490048.5	QUATERNARY ALLUVIUM	11/5/2007		62	42	62	20	28
275778	517826.9	4512655	ALL UNNAMED AQUIFERS	11/8/2007		132	110	132	22	72
276026	511721	4514689	ALL UNNAMED AQUIFERS	1/18/2008		160	120	160	40	35
276317	515841.8	4488030	ALL UNNAMED AQUIFERS	1/9/2008		50	40	50	10	22
276445	525639.1	4500700	ALL UNNAMED AQUIFERS	1/30/2008		37	19	37	18	26
276546	522731.6	4492228.5	ALL UNNAMED AQUIFERS	11/22/2005		55	20	42	22	34
276547	522787.1	4492043.5	ALL UNNAMED AQUIFERS	12/22/2006		55	20	42	22	34
276548	522732.4	4492200	ALL UNNAMED AQUIFERS	11/22/2005		50	20	42	22	34
276549	522793.6	4492157	ALL UNNAMED AQUIFERS	12/22/2006		55	20	42	22	34
276550	522734.3	4492229.5	ALL UNNAMED AQUIFERS	11/22/2005		50	20	42	22	34
276551	522733.4	4492221.5	ALL UNNAMED AQUIFERS	11/22/2005		55	20	42	22	34
276552	522794.9	4492221	ALL UNNAMED AQUIFERS	12/22/2006		55	20	42	22	34
276553	522729.5	4492229.5	ALL UNNAMED AQUIFERS	12/22/2006		55	20	42	22	34
277023	515895.4	4511784.5	ALL UNNAMED AQUIFERS	11/19/2001		540	480	540	60	232
277056	508102.4	4500434	ALL UNNAMED AQUIFERS	4/10/2008		27	19	27	8	14
277661	526391.3	4495723.5	LARAMIE FOX HILLS	6/9/2008		340	275	335	60	135
278885	511399	4502105	ALL UNNAMED AQUIFERS	8/7/2007		103	80	100	20	73
278886	509136	4515554	ALL UNNAMED AQUIFERS	9/7/2007		495	465	495	30	275
278887	509131	4515554	ALL UNNAMED AQUIFERS	9/7/2007		250	230	250	20	124
278888	509145	4515554	LARAMIE FOX HILLS	9/12/2007		575	555	575	20	268
278889	509140.1	4515555.5	LARAMIE FOX HILLS	9/12/2007		495	465	495	30	275
278890	509137	4515558	ALL UNNAMED AQUIFERS	9/12/2007		495	465	495	30	276
278892	509389	4513118	ALL UNNAMED AQUIFERS	8/31/2007		529	495	515	20	390
278893	510837	4513142	ALL UNNAMED AQUIFERS	8/29/2007		190	155	185	30	138
278894	509392	4512214	ALL UNNAMED AQUIFERS	8/10/2007		494	419	459	40	402
278895	509400	4512217	ALL UNNAMED AQUIFERS	8/16/2007		251	231	251	20	246
278896	509385	4512216	LARAMIE FOX HILLS	8/7/2007		547	527	547	20	425
278897	509389	4512215	ALL UNNAMED AQUIFERS	8/22/2007		497	435	455	20	403
278898	509393	4512210	ALL UNNAMED AQUIFERS	8/24/2007		477	457	477	20	403
278899	511135	4511458	ALL UNNAMED AQUIFERS	8/15/2007		234	120	140	20	116
278900	511123.1	4510589	ALL UNNAMED AQUIFERS	8/22/2007		95	80	90	10	62
278901	509561	4511035	ALL UNNAMED AQUIFERS	8/17/2007		303	260	280	20	249
279493	496238	4491530	ALL UNNAMED AQUIFERS	12/3/2007		25	15	25	10	13
279494	496194	4490455	ALL UNNAMED AQUIFERS	12/4/2007		17	7	17	10	6
279498	497113	4488306	ALL UNNAMED AQUIFERS	12/6/2007		20	10	20	10	15
279499	496291	4487377	ALL UNNAMED AQUIFERS	12/6/2007		20	10	20	10	10
279503	500106	4503156	ALL UNNAMED AQUIFERS	12/19/2007		25	10	25	15	12
280088	520854.1	4496939.5	ALL UNNAMED AQUIFERS	3/24/2009		52	20	50	30	38
233474	541295.9	4530348.5	ALL UNNAMED AQUIFERS	6/4/2001		50	30	50	20	25
76346	536848.7	4506475	ALL UNNAMED AQUIFERS	1/26/2004		180	135	175	40	64

Permit Number (Well Name)	Easting (NAD 83)	Northing (NAD 83)	Aquifer Name	Date Well Constructed	Date Well Plugged	Well Depth (ft)	Top of Screen (ft)	Bottom of Screen (ft)	Screen Length (ft)	Static Water Level (ft)
242174	538075.9	4528965.5	ALL UNNAMED AQUIFERS	10/28/2002		240	160	200	40	60
201355	539968.8	4508436	ALL UNNAMED AQUIFERS	2/5/1997		285	220	260	40	88
97022	540000.1	4508428.5	ALL UNNAMED AQUIFERS	2/5/1997		285	220	260	40	88
268886	534049	4498787	LARAMIE FOX HILLS	9/30/2006		375	315	355	40	180
227017	534749.7	4498564.9	ALL UNNAMED AQUIFERS	3/10/2002		355	315	355	40	202
233124	540020.4	4501884.9	ALL UNNAMED AQUIFERS	2/14/2003		580	504	544	40	231
266186	538197.8	4506024.5	LARAMIE FOX HILLS	11/18/2005		160	115	160	45	20
266358	543347.6	4498136	ALL UNNAMED AQUIFERS	1/3/2006		260	215	260	45	150
270167	540621	4505862	ALL UNNAMED AQUIFERS	10/10/2006		150	80	140	60	46
199389	541858.3	4519292.7	ALL UNNAMED AQUIFERS	11/14/1996		140	80	140	60	55
258812	539002.5	4511495.5	ALL UNNAMED AQUIFERS	5/26/2005		180	110	170	60	100
261089	541721.2	4517639.5	ALL UNNAMED AQUIFERS	4/5/2005		265	205	265	60	105
267799	540400.3	4509244.5	ALL UNNAMED AQUIFERS	8/27/2007		380	320	380	60	67
266595	539575.9	4501261.5	LARAMIE FOX HILLS	3/2/2006		480	400	460	60	242

APPENDIX IV:
HYDRAULIC HEAD CONTOUR MAP OF STUDY AREA FOR ALL AQUIFERS

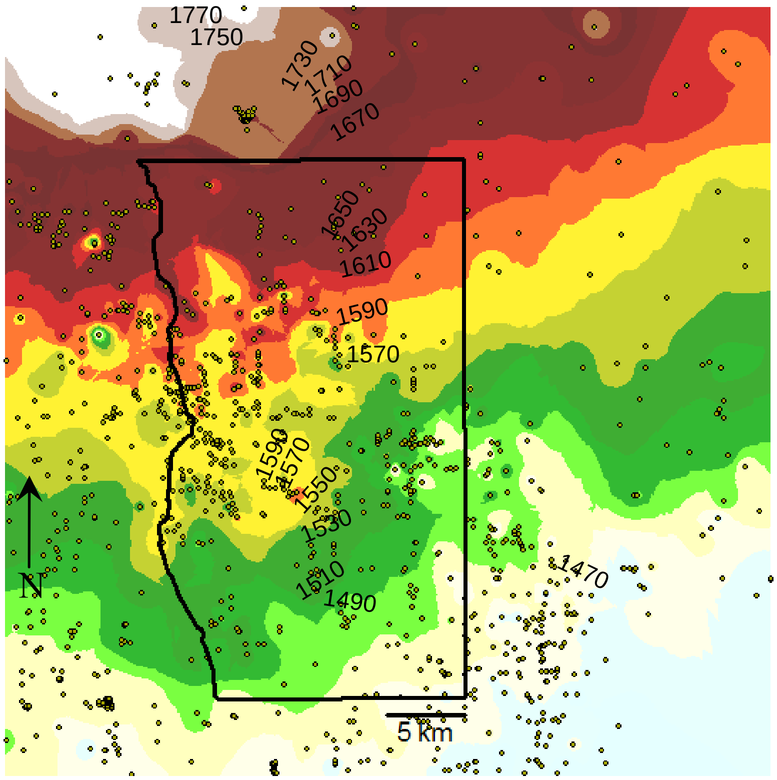

Figure 1-1. Colorado Division of Water Resources, Office of the Colorado State Engineer water level (hydraulic head) data 1990-2010, in meters above sea level. Contour interval is 20m. Includes wells described as existing in "All Aquifers."